KU LEUVEN

ARENBERG DOCTORAL SCHOOL
FACULTY OF SCIENCE

Matrix metalloproteinase-3: a prerequisite for structural and functional plasticity in the visual cortex of the mouse

Jeroen AERTS

Supervisor:
Prof. dr. L. Arckens
Co-supervisor:
Prof. dr. L. Moons

Dissertation presented in partial fulfilment of the requirements for the degree of PhD in Science

December 2014

MATRIX METALLOPROTEINASE-3: A PREREQUISITE FOR STRUCTURAL AND FUNCTIONAL PLASTICITY IN THE VISUAL CORTEX OF THE MOUSE

Jeroen AERTS

Supervisor:
Prof. dr. L. Arckens (KU Leuven)
Co-supervisor:
Prof. dr. L. Moons (KU Leuven)

Members of the Examination Committee:
Prof. dr. R. Huybrechts (KU Leuven)
dr. T.-T. Hu (ThromboGenics NV)
Prof. dr. C. Libert (VIB Inflammation Research Center, UGent)
Prof. dr. T. Pizzorusso (Institute of Neuroscience CNR, Pisa)
Prof. dr. P. Van Dijck (KU Leuven)

Dissertation presented in partial fulfillment of the requirements for the degree of PhD in Science

16 December 2014

Uitgegeven in eigen beheer, Jeroen Aerts, Zoölogisch instituut (ZI), Naamsestraat 59, B-3000 Leuven.

ISBN 978-90-8649-789-8
D/2014/10.705/97

Dankwoord

Wetenschappelijk onderzoek doen, het is iets speciaals: het ene experiment levert meer vragen op dan antwoorden, het andere experiment geeft helemaal geen antwoorden en de nieuwe vragen leiden je alsmaar verder weg. En dit gedurende vier jaar als onderdeel van een doctoraat. Hoe speel je dit klaar? Wel, u neemt een beetje boekenworm, een snuifje chirurg, een stukje techneut, een beetje verkoper en een schijfje wereldburger. Goed mengen en klaar! Veel lezen, muizen opereren, als het mis gaat: troubleshooten, je onderzoek in posterformaat adverteren en gepaard daarmee regelmatig op congres gaan en nieuwe mensen leren kennen. Dat laatste, het schijfje wereldburger, werd nog wat dikker toen ik in de laatste fase van mijn doctoraat de kans kreeg om onderzoek te doen aan de universiteit van Montréal. Doctoreren... het was een geweldige ervaring! Maar zonder de hulp van een hele hoop mensen had ik nooit de eindmeet gehaald en zij verdienen dan ook een woord van dank.

Eerst en vooral wil ik Prof. dr. Lut Arckens bedanken om me de kans te geven in haar labo te starten. Bedankt Lut voor je onvermoeibaar enthousiasme, het continu aanbrengen van nieuwe ideëen en je onfeilbare passie om ervoor te gaan. Sinds jouw intrigerende lessen over neurowetenschap tijdens mijn opleiding Biologie wist ik het: ik wou en zou onderzoek doen op hersenen en de keuze voor jouw labo was dan ook snel gemaakt. De veldslag naar het IWT toe, de spontane discussies in de gang, de MMP meetings en samen op congres: op elk moment inspireerde je me om nog net dat beetje extra te doen en je enthousiasme blijft nog steeds besmettelijk! Hierbij wil ik ook mijn co-promotor bedanken Prof. dr. Lieve Moons: bedankt voor alle input, in het bijzonder

tijdens de IWT voorbereidingen en bedankt om al mijn output grondig na te lezen.

Graag wil ik ook mijn juryleden Prof. dr. R. Huybrechts, Prof dr. P. Van Dijck, dr. T.T. Hu, Prof. dr. C. Libert en Prof. dr. T. Pizzorusso bedanken voor het nalezen van deze thesis, voor de nuttige suggesties en kritische opmerkingen. Door jullie is dit werk mede geworden tot wat het nu is, waarvoor mijn oprechte dank. Thank you Prof. dr. T. Pizzorusso for all your suggestions and valuable insights and the effort to travel to Belgium for this occasion. Ook wil ik graag Prof. dr. G. Opdenakker en Erik Martens bedanken voor de zymografie pilootstudie.

Een goede sfeer op het labo is goud waard en daarom wil ik alle collega's en ex-collega's bedanken. Bedankt Laurens, Tjing, Annelies, Leen, Katrien, Samme, Ellen, Isabelle en Marie-Eve. Extra dank gaat naar Tjing: jouw eeuwig positivisme heeft me door de moeilijkste periodes van mijn doctoraat geholpen. Ook onze vele discussies en jouw input waren voor mij enorm waardevol, bedankt! Natuurlijk ook dank aan Laurens: je hebt me alle "goede manieren" in het labo aangeleerd tijdens mijn thesisjaar en daarna stond je altijd garant voor knotsgekke avonden uit in Leuven. Katrien, Samme en Jeroen S: bedankt om samen aan de start als een team te werken naar het IWT toe, de sfeer toen zal ik nooit vergeten. Ook bedankt aan Ellen, Katrien en Samme voor de gezellige muzikale avonden. Een speciaal woord van dank gaat ook naar de onnoemlijk waardevolle en enthousiaste laboranten Ria en Lieve! Bedankt allebei voor jullie inzet, jullie gouden handen en de leuke babbels. Zonder jullie hulp had ik het zeker niet gehaald! Eline, bedankt voor de goede samenwerking! Dank ook aan al mijn thesisstudenten: Jessie, Lise en Sander, jullie waren top.

I also would like to thank Prof. dr. Christian Casanova and Prof. dr. Denis Boire to give me the opportunity to work in the lab in Montréal. Many thanks go to a bunch of great people that I was lucky to call colleagues for three months: Bruno and Jimmy, my dear Caballeros, our time together was much too short but I will see you on the battlefield! Sebastien aka "Clark Kent", thank you for one of the best work experiences I ever had. You are truly a Superman in disguise. Mathieu, aka "The Agarose Master", thanks for the great teamwork on the rabbit and the nice time in and outside the lab! Thank you Azadeh, Robyn,

Thomas, Reza, Kash, Ghazal for all the fantastic times and the afternoon coffee breaks which I already deeply miss.

Dank u ma en pa om me alle kansen te geven om mijn studies en doctoraat waar te maken. Zonder jullie onvoorwaardelijke steun en advies had ik dit nooit bereikt! Bedankt ook Dieter en Kristien om regelmatig vanuit Schiedam af te zakken voor een gezellig weekend in Lint of een leuke babbel in Leuven (soms een katerochtend weliswaar). Bomma en bompa, jullie liggen heel nauw aan mijn hart. Ook aan jullie heel erg bedankt voor de onvoorwaardelijke steun en de gezellige babbels bij jullie thuis. Ook bedankt aan de rest van mijn familie! Grety en Paul, bij jullie voelt het altijd als thuiskomen. Bedankt om mij in alles te steunen en Bourgondisch te verwennen tijdens de gezellige weekends in Aarschot. Ook de rest van jullie familie wil ik bedanken voor al hun steun!

Uiteraard bedank ik ook al mijn vrienden om me tijdens mijn doctoraat de nodige afleiding te bezorgen! Bedankt Jeroen, Max, William, Dimitri en anderen voor de leuke avonden uit met de nodige humor, muziek en "een druppeltje", want soms hebben we dat allemaal eens nodig hé :). Jeroen, Lancia-trips zijn een perfecte ontspanning, I want more! Max, onze festivaltrip naar de UK was onvergetelijk, lets do it again! William, ik hoop dat we nog vaak wat gerstennat samen nuttigen om net dat knotgek idee te krijgen om in onze muziek te stoppen! Ook aan Tom, Carmen, Frederik, Joost, Matthias, Mathias en Gust bedankt voor al het vertier in Leuven, Gent en Antwerpen. Jo, Pieter en Wieland, bedankt voor de zeer memorabele avonden uit en het weerzien in München. We moeten dit vaker doen! En natuurlijk ook dank aan "de biochemisten" waar ik me als bioloog helemaal thuisvoel. Bedankt voor de gezellige woensdagavonden en de memorabele snowboard-trips: ieeerséé́é! Moge er nog veel volgen!

Last but definitely not least: bedankt Julie om er altijd voor mij te zijn, me lief te hebben en op te peppen! Je bent mijn zielsverwant, mijn muze en de rijkdom in mijn leven. Van de eerste gesprekken in het labo tijdens mijn masterthesisjaar (dankuwel FWO!), tussen de verkeerd gedipte glaasjes door en alle excuses om langer op het werk te blijven om je te zien, tot de nachtelijke wetenschappelijke discussies (romantiek en wetenschap, het kan!), samen op congres gaan en onze prachtige tijd samen in Montréal: ik heb van elke seconde genoten! Samen zijn we meer dan 1 + 1 en ik kijk al uit naar onze toekomst!

"How can a three-pound mass of jelly that you can hold in your palm imagine angels, contemplate the meaning of infinity, and even question its own place in the cosmos? Especially awe inspiring is the fact that any single brain, including yours, is made up of atoms that were forged in the hearts of countless, far-flung stars billions of years ago. These particles drifted for eons and light-years until gravity and change brought them together here, now. These atoms now form a conglomerate - your brain - that can not only ponder the very stars that gave it birth but can also think about its own ability to think and wonder about its own ability to wonder. With the arrival of humans, it has been said, the universe has suddenly become conscious of itself. This, truly, it the greatest mystery of all."

V. S. Ramachandran (from The Tell-Tale Brain: A Neuroscientist's Quest for What Makes Us Human, 2011)

Contents

List of Abbreviations

^{33}P-dATP	radioactive deoxyadenosine 5' tri-phosphate
A	anterior (area)
ALS	amyolateral sclerosis
AMPA	alpha-amino-3-hydroxy-5-methyl-4-isoxazolepropionic acid
AMC	age-matched control
ANOVA	analysis of variance
AP-1	activator protein-1
APMA	4-aminophenylmercuric acetate
Arp2/3	actin-related protein 2/3 complex
Atg	autophagy-related protein
Au	auditory cortex
BDNF	brain derived neurotrophic factor
Bz	binocular zone
cdk5	cyclin-dependent-like kinase 5
cpd	cycles per degree
cpm	counts per minute
CSPG	chondroitin sulphate proteoglycan
CTGF	connective tissue growth factor
DJ-1	Parkinson disease protein 7
DNA	deoxyribonucleic acid
dLGN	dorsal lateral geniculate nucleus
Drp1	dynamin-related protein 1
EMMPRIN	extracellular matrix metalloproteinase inducer
Fis1	mitochondrial fission protein 1

GABA	gamma-aminobutyric acid
GPI	glycophosphatidyl inositol
GSK3β	glycogen synthase kinase 3 beta
IGF-1	insulin-like growth factor 1
IGFBP	insulin-like growth factor binding protein
IgGs	immunoglobulins G
ISH	*in situ* hybridization
Lmz	lateral monocular zone
LTD	long-term depression
LTP	long-term potentiation
m	monocular
MD	monocular deprivation
7wME	7 weeks post-ME
ME	monocular enucleation
Mfn	mitofusin
MMP	matrix metalloproteinase
MMPI	matrix metalloproteinase inhibitor
Mmz	medial monocular zone
Mz	monocular zone
mRNA	messenger RNA
NF	neurofilament protein
NF-66	alpha internexin
NF-H	high molecular weight neurofilament protein subunit
NF-L	low molecular weight neurofilament protein subunit
NF-M	medium molecular weight neurofilament protein subunit
NGF	nerve growth factor
NMDA	N-methyl-D-aspartate
NOS	reactive nitrogen species
OD	ocular dominance
OPA-1	optic atrophy 1
P	posterior (area) or postnatal day
P120	postnatal day 120
P45	postnatal day 45
P90	postnatal day 90

PBS	phosphate buffered saline
pNF	phosphorylated neurofilament protein
PNN	perineuronal net
Pro	pro-domain
PV	parvalbumin
PVDF	polyvinylidene fluoride
RGC	retinal ganglion cell
RNA	ribonucleic acid
ROCK	rho-associated protein kinase
ROS	reactive oxygen species
SC	superior colliculus
SEM	standard error of the mean
SDS	sodium dodecyl sulfate
TBS	tris buffered saline
TIMP	tissue inhibitor of metalloproteinase
TM	transmembrane
TNFα	tumor necrosis factor alpha
TPS	total protein stain
tRNA	transport RNA
V1	primary visual cortex
V1b	binocular V1
V1m	monocular V1
V2M	medial extrastriate visual cortex
V2Lb	binocular V2L
V2Lm	monocular V2L
VDCC	voltage-dependent calcium channel
w	week
WAVE1	Wiskott–Aldrich syndrome protein family verprolin homolog 1
WT	wildtype
Zn^{2+}	zinc ion
Zif268	zinc finger protein 268

List of Figures

List of Tables

Aim of the study

The mammalian brain is inherently plastic, meaning that it is capable of altering its structure and function in correspondence to changes in the environment. The visual cortex, the area in the brain that receives visual input, is undoubtedly one of the best and most studied areas of the brain for understanding cortical plasticity and development [96]. On top of unimodal plasticity also cross-modal changes can occur when input of one sensory modality is lost, for example in the case of blindness or deafness. Subsequently the deprived cortical neurons get recruited by the remaining modalities by functional and structural reorganization and in turn, the function of the remaining modalities strengthens to compensate for the sensory loss [17]. This type of plasticity has been extensively reported in several species after both partial deprivation or complete loss of sensory input [250, 17, 134, 283].

Recent work in our lab uncovered an age-dependent reactivation in the mouse visual cortex following irreversible sensory loss by removal of one eye, termed monocular enucleation (ME) [256, 334]. This extensive reactivation was only present in adults (P120) and consisted of an initial open-eye potentiation followed by cross-modally driven plasticity in the medial and lateral monocular zones starting from adjacent non-visual cortices around three weeks post-ME [334]. In contrast, adolescent (P45) mice did not display cross-modal reactivation at seven weeks post-ME [256]. The precise cellular mechanisms and key molecular players underlying these age-dependent processes still remain largely elusive. In that regard, matrix metalloproteinases (MMPs), Zn^{2+}-dependent endopeptidases that modulate extracellular matrix proteins, chemokines, cytokines, growth

factors, receptors and a range of intracellular substrates, have over the years been identified as major regulators of normal brain development and neuroplasticity [377, 97, 40, 205]. Interestingly, a recent study by Spolidoro et al. (2012) uncovered a role for MMPs in critical period plasticity of the visual cortex in monocular deprived rats. Infusion of a broad-spectrum MMP inhibitor prevented both the potentiation of the open-eye response and the increase in spine density on layer II-III pyramidal neurons after MD [309]. However, further studies concerning the role of MMPs in mediating the structure and function of the visual cortex, including uni- and cross-modal plasticity, are lacking. Moreover, the majority of MMP studies have focused on the gelatinases (MMP-2 and MMP-9) whereas MMP-3 is known to act upstream of MMP-9 [97, 338]. Therefore, the primary interest of this dissertation is to acquire knowledge specifically about the function of MMP-3 in the mouse visual cortex.

The objective of this study is two-fold: the first aim is to gain insight into the mechanistic properties of the MMP protease web by characterizing the structural and functional phenotype of the visual cortex of adult MMP-3 deficient (MMP-$3^{-/-}$) mice. The second aim is to establish a role for MMP-3 in age-dependent ME-induced cortical plasticity. Addressing both aims will lead to a better understanding of the MMP-3 biology in context of the structure and function of the visual cortex.

Chapter 1 provides an introduction and overview of the the general principles governing brain plasticity and MMP biology. In this dissertation we used the mouse visual system as a research model and therefore the visual pathways from the retina to the cortex are explained. Special emphasis is laid upon the structural and functional organization of the visual cortex, both primary and extrastriate areas. Different kinds of plasticity and regulators of plasticity in the visual cortex are discussed with a focus on ME-induced cortical plasticity which is one major research pillar in this dissertation. The last part of this chapter introduces the reader to the world of MMP biology with an overview of the structure, classification and regulatory mechanisms of MMPs. Finally, the role of MMPs in structural and functional plasticity and their potential as therapeutic targets is discussed.

The first research goal of this dissertation was to phenotypically characterize

the visual cortex of adult MMP-3$^{-/-}$ mice in order to gain insight into the MMP-3 protease web to guide further studies in visual cortex plasticity research. Therefore, as described in **chapter 2**, we performed a Golgi-Cox staining to compare the neuronal architecture of layer V pyramidal neurons in MMP-3$^{-/-}$ and WT mice. To corroborate these findings on a molecular level, we assessed the levels of neurofilament proteins in these mice. Apart from the structural phenotype we wanted to evaluate the potential for cross-modal plasticity of adult MMP-3$^{-/-}$ mice by assessing the ME-induced cortical activity profile with in situ hybridization for the neuronal activity marker *zif268*.

Chapter 3 further explores the molecular and cellular phenotype of the MMP-3$^{-/-}$ visual cortex to corroborate the findings of chapter 2. To evaluate the molecular processes underlying the cortical phenotype a proteomics approach revealed a set of differentially expressed proteins between MMP-3$^{-/-}$ and WT samples. A special interest was given to the family of collapsin response mediator proteins. In addition we explored cellular processes such as mitochondrial dynamics and autophagy to probe for a new avenue in MMP-related research.

The second aim of our research was to investigate the acute role of MMP-3 in age-dependent ME-induced cortical plasticity. In **chapter 4** we therefore evaluated the expression of MMP-3 in the visual cortex of P45 and P120 C57Bl/6J mice with different post-ME survival times to unmask a potential age-dependent regulating role of these enzymes in both cross-modal plasticity and open-eye potentiation. We expanded this line of research with MMP-2 and MMP-9, of which the function in neuroplasticity is well characterized. Condition-specific changes in MMP expression were evaluated with a combination of Western analysis and gelatin zymography. In addition, we describe the efforts made to optimize a fluorescent assay to measure the activity of MMP-3 in mouse brain samples.

The final chapter, **chapter 5**, is dedicated to discussing the obtained results in relation to the current state of knowledge in MMP biology and cortical plasticity. A theoretical molecular framework is proposed to explain the most prominent aspects of the MMP-3$^{-/-}$ cortical phenotype described in chapters 2 and 3. The second part of chapter 5 deals with the findings described in chapter 4 and discusses new avenues to overcome the problems faced when trying to measure

the activity of individual MMPs in vivo. Finally, several important remarks are made in light of future experiments to unravel a causal link between MMP activity and ME-induced cortical plasticity.

Chapter 1

General introduction

1.1 Neuroplasticity: a dynamic interplay between the world and the brain

The brain is able to change its functional and anatomical organization in response to environmental changes and this ability is termed neuroplasticity. This feature allows a person to, for example learn the fine motor skills necessary for playing a musical instrument or to combine different experimental findings to synthesize a thesis, which a person is able to read because they trained their brain to make sense of words. Acquiring and constantly improving these skills is dependent on adaptations in the organization and function of neural networks and this is why neuroplasticity is so fundamentally present in every aspect of our life. The term neuroplasticity was first coined in 1948 by the Polish neuroscientist Jerzy Konorski but it was not until the groundbreaking work of Hubel and Wiesel in 1962 that neuroplasticity research laid the foundation of our current understanding of the development and plasticity of the brain [362, 148, 149, 96]. The Nobel Prize laureates David Hubel and Torsten Wiesel started investigating the properties of the visual system of the cat with a main focus on the visual cortex [148]. In 1963, they described that occluding one eye during a brief period in early-life produced long-lasting changes in the functional

properties of the visual cortex and this gave birth to a model system to study cortical plasticity [362]. For this reason, the visual cortex is undoubtedly one of the best and most studied areas of the brain for understanding cortical plasticity and development [96].

1.2 The visual system of the mouse

For the large part of the 20th century, the visual system of the mouse was neglected in neuroscientific research compared to that of the cat or non-human primates like the macaque. This was mainly due to the fact that mice are nocturnal animals and are believed to rely more on tactile and olfactory information. In accordance, the visual acuity[1] of mice (0.5 cycles per degree (cpd)) is much lower than that of cats (6 cpd) or macaques (46 cpd) [282, 337]. However, in the last decades the mouse proved to be an invaluable model organism in the field of visual neuroscience, mainly because of transgenic and knockout technology which enables researchers to study the involvement of a specific gene product in the development, function and plasticity of the visual system. The commercial availability of a huge number of transgenic mouse lines and the establishment of several mouse consortiums and online databases contribute to the overall increase in use of mice in neuroscientific research [151]. In addition, the small size of their nervous system has the advantage to gather data simultaneously over a large spatial scale and the absence of gyri make stereotactic manipulations and in vivo imaging easier. Important to note is that mice are also safer, simpler and less expensive to maintain compared with cats or primates.

1.2.1 Perception: from retina to cortex

The first step to visual perception is light emitted or reflected by objects in the environment that hits the photoreceptors of the retina located in the back

[1] Visual acuity or the spatial resolving capacity of the visual system determines the sharpness of vision and is often measured as the maximum distinguishable cycles of a given stimulus per degree of visual angle (cycles per degree) [41].

of the eye. Different photoreceptors, termed cones and rods, transform the electromagnetic waves into electrical signals that are transmitted to the retinal ganglion cells (RGCs) which serve as the sole output neurons of the retina. RGC axons leave the eye and form the optic nerve. Axons in the optic nerve coming from the nasal retina cross over at the optic chiasm and target the contralateral part of the dorsolateral geniculate nucleus (dLGN), the primary relay station of visual information located in the thalamus [150, 18]. As a consequence, information from the left visual hemifield is projected to the right side of the brain and vice versa, with a central overlap of the two hemifields perceived by both eyes which is termed the binocular visual field. The binocular visual field of the mouse is very small compared to cats and primates and only comprises 1/3rd of the entire visual field due to the lateral positioning of the eyes [150]. The binocular part of the visual field is perceived by the temporal part of the retina and the corresponding RGCs project to the ipislateral dLGN. The dLGN relays information from both eyes to the primary visual cortex (V1) terminating in a monocular zone, which receives information of the contralateral eye, and a binocular zone receiving information from both eyes (figure 1.1) [150, 151].

A universal and beautiful feature of the visual system across all examined mammals [337] to date is that one point in visual space can be traced to a specific corresponding location along the entire visual system terminating in V1 and this feature is called retinotopy. More specifically, neighboring retinal ganglion cells project axons to neighboring neurons in the dLGN, which in turn project to neighboring neurons in V1. This allows the visual system to form a single map of the visual field in which adjacent neurons in V1 respond to adjacent locations in visual space [351, 302, 162, 96]. This form of organization allows the lateral part of the visual field to be represented in the medial visual cortex and the upper part of the visual field in the posterior visual cortex [84, 302].

1.2.2 Other retinorecipient brain regions

A recent study unveiled that the mouse retina projects to approximately 46 different brain regions, including the dLGN and the primary visual cortex

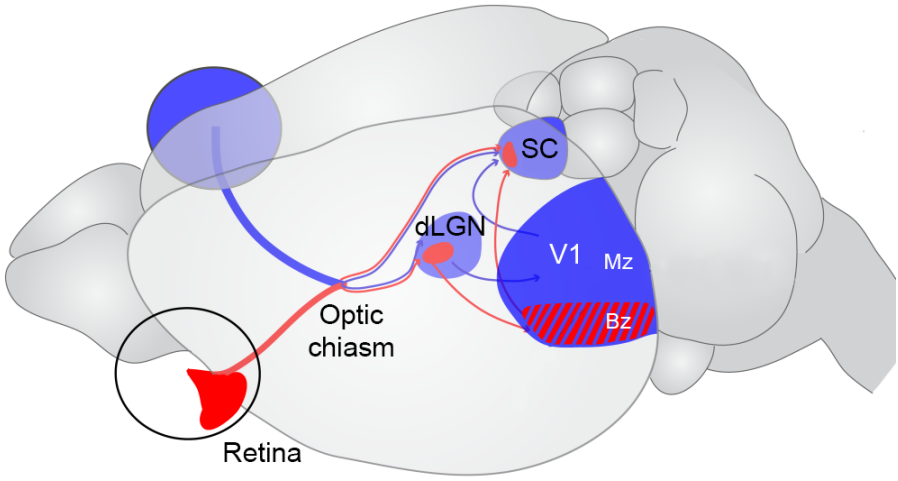

Figure 1.1: Dorsolateral schematic view of the mouse visual system.
Information from the ipsilateral (red) and contralateral (blue) retina partially segregate at the optic chiasm to project to the dorsolateral geniculate nucleus (dLGN) and the superior colliculus (SC). The dLGN targets the primary visual cortex (V1) which is composed of a monocular zone (Mz) which only receives input from the contralateral eye and the binocular zone (Bz) which receives information from both eyes. Adapted from [363].

which makes up the major image-forming pathway [234]. A subset of RGCs relays information through non-image-forming pathways and target regions such as the suprachiasmatic nuclei of the hypothalamus, the ventral LGN and the intergeniculate leaflet [132]. These retinofugal projections are involved in circadian rhythm and pupillary reflexes [132, 18, 41]. In mice and other nocturnal rodent species, nearly all RGCs leaving the optic chiasm also project to the superior colliculus (SC) (figure 1.1), whereas only a subpopulation targets the visual cortex via relays in the dLGN (figure 1.1) [41]. This is in sheer contrast with carnivores and primates in which the majority of RGCs project to the geniculocortical system and less than 10% targets the SC [18, 41]. The mouse SC is composed of seven distinct anatomical layers and receives visual information almost exclusively in the three superficial layers [313]. The deeper layers are characterized by multisensory neurons that receive input from the

superficial layers and respond to visual, auditory and somatosensory information [218, 313]. All this multisensory information is topographically mapped and integrated [313, 42], and together with cortical input a motor output is generated that regulates eye, head and body movements towards new stimuli [313, 41].

1.2.3 The primary visual cortex

The visual cortex, a cortical area common to all mammalian species, is responsible for complex integration and interpretation of information relayed from the eye to provide a rich visual sensory experience. Like the cortex of all mammals, the visual cortex of mice consists of six anatomically distinct layers numbered with Roman numerals (I to VI). Accross these layers, two neuron types are present: the majority are excitatory neurons with pyramidal or stellate morphology using glutamate as a neurotransmitter. The other class of neurons are inhibitory local-circuit interneurons with a non-pyramidal shape that release gamma-aminobutyric acid (GABA) as a neurotransmitter and comprise 20 to 30 % of all cortical neurons [18, 142]. The balance between excitatory and inhibitory signaling is crucial for normal cortical maturation, function and plasticity [138, 139, 130].

Layer I, also termed the molecular layer is devoid of cells and mostly consists of nerve endings. The upper layers II and III are jointly called the supragranular layer and are recognized for their abundant pyramidal neurons. Layer IV is known as the granular layer and includes stellate neurons. The deeper layers V an VI are denominated together as the infragranular layers and are also characterized by abundant pyramidal neurons [18].

1.2.3.1 Cortical processing within V1 and the role of pyramidal cells

To optimally process visual information, the different layers of V1 are tightly interconnected and send specific feedforward and feedback projections. The conventional model of cortical processing (figure 1.2a) formulates that layer IV neurons are the main target of the thalamus and make short-range connections to overlying layer II/III neurons which in turn send local and long-range

connections to neighboring layer II/III, layer V neurons and neurons in higher order (extrastriate) areas. Subsequently, layer V cells constitute short- and long-range connections with other cortical layer V neurons and to layers II/III and VI. In addition, layer V pyramidal neurons project to subcortical areas such as the SC, striatum, spinal cord and the pons. Finally, layer VI neurons send feedback signals to all cortical layers and subcortically to the LGN [324, 337]. Recent evidence from the lab of Constantinople and Bruno (2013) challenges this model by proving that the thalamocortical projection carrying sensory information not only targets layer IV but also layers V/VI and that layer V/VI sensory responses do not require layer IV [57]. Therefore they advocate a bistratified model of cortical processing where the thalamus copies sensory information to the upper stratum (layer II/III and IV) and the lower stratum (layers V/VI), allowing parallel processing of sensory information in distinct anatomical pathways (figure 1.2b) [57].

For the purpose of this dissertation, I will briefly focus on pyramidal neurons, because this cell type is crucial for integration of interlaminar and interareal synaptic information and computation [311]. Pyramidal cells are excitatory neurons characterized by a pyramidal soma and long apical dendrites (figure 1.2c). Oblique dendrites emanate from the main apical dendrite at various angles. In the cortex, they are located in layers II/III and layer V/VI and they receive and propagate information through the cortex as mentioned above [324, 337, 57]. Layer II/III pyramidal neurons have shorter apical dendrites and more obliques than layer V pyramidal cells [311]. Pyramidal neurons are often classified in two or three morphological groups based on the length of the apical dendrite and the appearance of the apical tuft: tall-tufted, tall-simple and short [186]. However, when taking more parameters into account, pyramidal neurons appear to have a continuous set of morphologies [183]. In addition, the extent of dendritic arborization of layer V pyramidal neurons is species-specific and differs based on the connections they have and the cortical area in which they reside [21, 183]. For example, in monkey, the complexity of the basal dendritic arbors of layer II/III pyramidal neurons increases with the hierarchical cortical level [94] and in the mouse visual cortex these arbors are simpler than in the somatosensory cortex [21]. In general, proximal dendrites

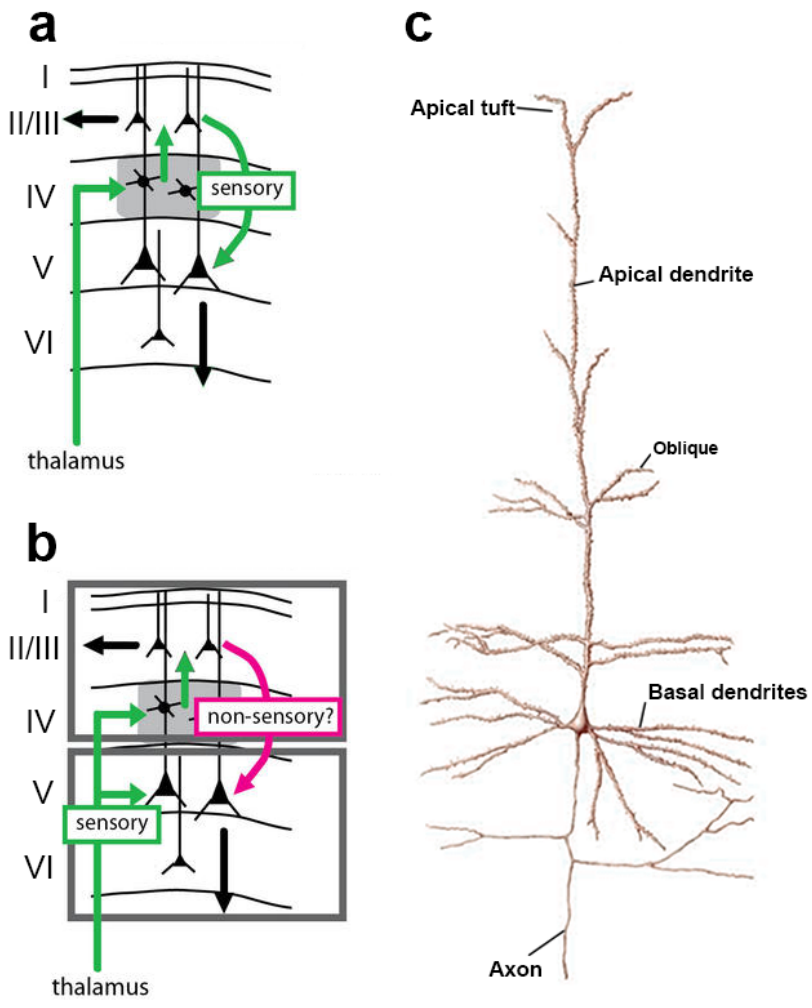

Figure 1.2: Cortical processing models and the general structure of a pyramidal neuron.

In the conventional model of cortical processing (a) sensory information coming from the thalamus is serially processed by the LIV-LII/III-LV loop along the densest axonal pathways (green). The bistratified model (b) proposes a parallel processing of sensory thalamic information (green) by the upper (LII/III and LIV) and deeper layers (LV/VI). This model also takes into account the minimal contribution of LII/III in propagating sensory information to the deeper layers (pink). An essential excitatory cell type in cortical processing is the pyramidal neuron with a typical layer V neuron depicted in (c). Adapted from [57, 18].

receive excitatory input from local sources, whereas the distal part of the apical dendrite receives input from more distant cortical and thalamic locations [311]. Pyramidal neurons integrate these different inputs to compute an output to the single and highly branched axon typically extending at the base of the soma [18, 311]. The synaptic and dendritic computation and summation to provide a final output signal is dependent on various factors, including the spatial and temporal input pattern and proximal and distal feedforward and feedback GABAergic inhibition [279, 311, 20, 142, 30]. Important to note is that layer II/III and V pyramidal neurons send long axons to the contralateral cortex through the corpus callosum [232]. In addition, a subset of layer II/III and layer V pyramidal neurons are also multisensory thereby integrating information from different modalities [52, 183].

A vastly studied and intriguing structure on the dendrites of pyramidal neurons is the dendritic spine, a small protrusion that constitutes the postsynaptic part of the excitatory glutamatergic synapse [18, 385]. Each pyramidal neuron is covered with thousands of dendritic spines that vary considerably in size and shape and are highly plastic [311, 385]. Spines are thought to increase the dendritic surface to allow more synaptic contacts per unit of dendritic length [385]. Alteratively, they could serve as distinct biochemical compartments to restrict the diffusion of important synaptic proteins [254]. Spines could also regulate synaptic currents resulting in altered dendritic integration and the function of neuronal circuits [254, 330]. However, their fundamental function remains highly enigmatic and dozens of different hypotheses have been proposed in literature [385, 204].

1.2.3.2 Extrastriate areas

Proper visual perception depends on additional processing of visual information by areas surrounding V1, called extrastriate areas, which are linked through feedforward and feedback connections in a hierarchical network [353, 41]. Neurons in these areas are sensitive to discrete aspects of visual information such as edge orientation, global motion or object motion [207]. Therefore, extrastriate areas are thought to transform visual information into meaningful information

about the external environment [41, 354, 253]. Similar to what is widely acknowledged in primates, recent analysis of cortico-cortical networks suggests the existence of two specialized visual information pathways in the mouse: a dorsal and a ventral stream [354, 355, 121]. The dorsal stream is responsible for the generation of spatial information about object location, motion detection and visuomotor planning, whereas the ventral stream mainly processes information to serve object recognition and form representation [294, 124, 18, 355].

Wang and Burkhalter (2007) provided the first complete map of extrastriate areas in the mouse through a combination of triple pathway tracing, receptive field recordings and callosal mapping and revealed nine higher areas beyond V1 (figure 1.3a) [353]. A recent study using intrinsic optical imaging even revealed eleven extrastriate areas [115] and each extrastriate area is typically characterized by a complete representation of the visual hemifield [353, 41]. Complementary to these studies, Van der Gucht and colleagues mapped seven different extrastriate areas using immunohistochemistry for non-phosphorylated neurofilament protein (NF), with a special emphasis on the medial part of the visual cortex (figure 1.3b) [336]. In addition to NF which is an excellent areal marker for cortical subdivisions, neuronal activity mapping with *zif268*[2] mRNA in combination with monocular and binocular enucleation, elegantly uncovered the borders between monocular zones, binocular zones and visual and non-visual cortex [333, 336].

In this dissertation, the extrastriate areas will be termed according to their eye-input specific functional subdivisions as referred to by Van der Gucht et al. (2007), Van Brussel et al. (2009) and Nys et al. (2014) [336, 333, 256].

[2]The gene *zif268* encodes for a transcription factor that belongs to the family of immediate early genes (IEG) that is considered as a reliable and accurate repoter gene for neuronal activity and has been extensively used to map neuronal activity in the visual cortex [367, 161, 9, 387, 336, 333, 256]. The gene is induced by neuronal activity without any *de novo* protein synthesis in the mammalian cortex [161, 177, 256]. One advantage of using *zif268* over other IEGs such as *c-fos* is that *zif268* has a high basal expression and is thus ideally suited for down-regulation studies [161].

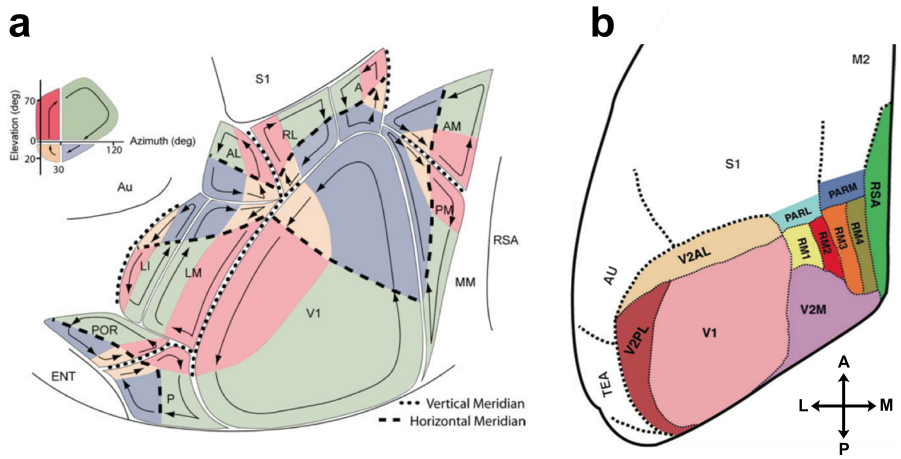

Figure 1.3: Topographic map of V1 and extrastriate areas.

A retinotopic map of V1 and extrastriate areas is visualized on a flat map of the left cortical hemisphere (a). The left inset represents the contralateral visual hemifield in spherical coordinates. Colors indicate different quadrants in respect to the horizontal median (azimuth) and vertical meridian (elevation) and the arrows indicate their orientation. The binocular field (upper: red; lower: yellow) is highly represented at the lateral border between LM and V1, whereas the monocular zones are depicted in green (upper) and blue (lower). All extrastriate areas contain a retinotopic visual hemifield and adjacent areas contain a topographic mirror-image. A cortical map based on cytoarchitectural data (b) shows a comparable organization with defined lateral, medial en anterior extrastriate areas (V2). Abbreviations: A, anterior area; AL, anterolateral area; AM, anteriomedial area; LI, laterointermediate area; LM, lateromedial area; PARL, lateral parasubiculum; PARM, medial parasubiculum; P, posterior area; PM, posteromedial area; POR, postrhinal area; RL, rostrolateral area; S1, primary somatosensory cortex; Au, auditory cortex; M2, medial motor cortex; MM, mediamedial area; ENT, entorhinal cortex; RSA, rentrosplenial agranular cortex; RM, rostromedial area; RSA, rostrosplenial area,; TEA, temporal association area; V2AL, anteriolateral extrastriate area; V2M, medial extrastriate area; V2PL, posterolateral extrastriate area. Adapted from [353, 336].

1.3 Experience-dependent plasticity

Various types of plasticity are present across different neuronal networks and they are able to work in parallel to employ changes both at the neuronal level as well as the network level [50]. One form of synaptic plasticity was characterized by Donald Hebb and is nicely summarized by the so-called Hebb's rule: "neurons that fire together, wire together" [18]. This rule explains that synchronized activation between a pre- and postsynaptic neuron increases the synaptic strength between those neurons and this is termed long-term potentiation (LTP). The opposing process also exists in which the synaptic efficacy decreases due to a de-correlated or lack of activation of two neurons and this process is called long-term depression (LTD). LTP is characterized by an increase in the number of glutamate sensitive AMPA (α-Amino-3-hydroxy-5-methyl-4-isoxazolepropionic acid) and NMDA (N-methyl-D-aspartate) receptors on the surface of the dendritic spine which enhances the membrane depolarization upon presynaptic glutamate release [50, 18]. Concomitant to the increase in synaptic efficacy, the dendritic spine head enlarges to accommodate more receptors and this is regulated by underlying cytoskeletal rearrangements (figure 1.5) [145].

Another important kind of synaptic plasticity, called homeostatic plasticity, maintains network homeostasis by balancing Hebbian plasticity and network activity to prevent unconstrained potentiation and depression [72, 331, 168]. A major form of homeostatic plasticity is comprised of synaptic scaling in which the strength of all synapses across a neuron is adjusted compensatory to the prolonged activity in the network [50]. When the activity in the network persistently increases, a compensatory decrease in excitatory synaptic strength will occur and vice versa. This adjustment in global synaptic strength depends on AMPA receptor trafficking [168] and is regulated by cell adhesion molecules, growth factors like brain derived neurotrophic factor (BDNF) [331] and signaling molecules like tumor necrosis factor-α (TNF-α) [164, 331]. Synaptic scaling in the visual cortex is observed after retinal lesions and accompanies changes in dendritic spine size on layer V pyramidal neurons [168]. Another form of homeostatic plasticity is metaplasticity, also called "the plasticity of synaptic plasticity" in which the prior history of synaptic plasticity for a given synapse

determines its future potential for plasticity. For example, a synapse that has undergone LTP is less likely to undergo it again because the treshold for inducing LTP increases and this process is NMDA receptor-dependent [1, 50].

1.3.1 Ocular dominance plasticity

A classical paradigm to measure plasticity in the visual cortex is by occluding one eye by means of lid suture or and eye patch and this is termed monocular deprivation (MD). The outcome of this disturbance in visual input can be determined in the binocular zone of the visual cortex, where the inputs from the two eyes first converge and compete for space [139, 96]. Neurons in the binocular zone respond in a different degree to visual stimuli presented to one eye or the other and this property is called ocular dominance (OD) [23, 139]. Performing MD causes visual cortical neurons to become dominated by the nondeprived eye and this OD plasticity is highest during a critical period in postnatal development which declines with age [22]. A complete OD shift underlies various forms of plasticity such as Hebbian and homeostatic plasticity, which act in concert [96]. Important to note is that the shift in OD occurs in V1 and not in earlier processing centers, which makes this paradigm ideal to study cortical plasticity mechanisms [96, 362]. The study of OD plasticity by means of MD can serve as a model to study vision disorders such as amblyopia or "lazy eye" where misaligned or unbalanced eye input disturbs OD [139]. Investigating age-dependent OD plasticity can open new avenues to treat this type of vision disorder later in life. In the last decade, considerable knowledge has been obtained about the factors regulating OD plasticity, including GABAergic intracortical inhibition, epigenetics, and Hebbian and homeostatic plasticity mechanisms [77, 310, 299, 130, 96].

1.3.1.1 Extracellular matrix and structural plasticity

The interstitial space between neurons is filled with a matrix of crosslinked molecules that are in turn bound with membrane molecules. This extracellular matrix (ECM) determines the mechanical and functional properties of neurons

and can influence intracellular signaling pathways. Key components of the brain ECM are chondroitin sulphate proteoglycans (CSPGs) which condense into lattice-like structures called perineuronal nets (PNN) [79]. In the visual cortex these PNN mostly surround fast-spiking inhibitory interneurons but also pyramidal neurons [7] and their formation coincides with the end of the critical period for OD plasticity [277, 23]. Degradation of CSPGs with the bacterial enzyme chondroitinase ABC reactivates OD plasticity in adult MD rats [277] and this implies that maturation of PNN restricts synaptic plasticity in the visual cortex [277, 166, 66]. In accordance, one of the functions of PNN is to compartmentalize AMPA receptors and restrict receptor mobility at the synapse [112, 166], hence regulating LTP and LTD mechanisms [166]. Concomitantly, the ECM is able to regulate structural plasticity by altering cytoskeletal dynamics and this aspect is recognized as an important regulator of critical period plasticity [263, 139, 221]. Regulation of cytoskeletal dynamics includes the rearrangement of the actin, tubulin and neurofilament framework to enable motility and plasticity of neurites and spines [131, 145, 383]. During the critical period, two days of MD elicits a transient increase in the level of the extracellular serine protease tissue plasminogen activator (tPA) [210] and tPA is necessary for the concomitant increase in dendritic spine motility on layer II/III and V pyramidal neurons contralateral to the deprived eye [263]. After four days of MD a reduction in spine density is observed on neurons serving the deprived eye and this is also reflected by a complete loss of functional response. This spine motility and pruning only occurs in the binocular zone, not the monocular zone, and serves as an anatomical substrate to re-establish the competitive balance between the two eyes [139].

1.3.2 Monocular enucleation-induced cross-modal plasticity

In contrast to MD, monocular enucleation (ME)[3] or the removal of one eye completely eliminates retinal input and can be considered as a model for irreversible unilateral deafferentiation to study both visual and cross-modal plasticity. Cross-modal plasticity entails that when the input of one sensory

[3]Whereas ME completely eliminates retinal input, spontaneous retinal activity still persists with MD and diffuse light can still hit the retina when applying MD by lid suture [2, 257].

modality disappears, the deprived cortical neurons get recruited by the remaining modalities by functional and structural reorganization and in turn, the function of the remaining modalities strengthens to compensate for the sensory loss [17]. It is indeed accepted that for example, when an individual loses vision, their somatosensory and auditory capabilities are altered. For the purpose of this manuscript I will focus on studies performed in our lab to address cross-modal plasticity in the mouse visual cortex using the ME paradigm.

Van Brussel et al. (2011) revealed that cortical reactivation after long-term ME has a partial non-visual component in adult mice of postnatal day (P) 120 [334]. Indeed, in contrast to short-term ME, which induces a marked reduction in neuronal activity in the contralateral visual cortex (figure 1.4a,b), P120 mice seven weeks after ME (7wME) displayed *zif268* expression levels comparable to those of age-matched control animals along the complete mediolateral extent of the visual cortex (figure 1.4a,c). In the first weeks post-ME, open-eye potentiation drives reactivation from the binocular zone outwards [101, 256] and from three weeks onwards cross-modally driven reactivation occurs in the adjacent lateral (V2L) and medial monocular (V1 and V2M) areas [334]. Two key experiments revealed that this latter reactivation process was indeed cross-modally driven. First, whisker stimulation in complete darkness in 7wME mice revealed *zif268* expression in V2M. Second, whisker trimming of 7wME mice abolished the observed *zif268* signal in all monocularly driven zones. A follow-up study by Nys et al. (2014) disclosed that this potential for cross-modal plasticity is age-dependent [256]. When performing ME on adolescent (P45) mice, an age characterized by the largest change in visually controlled genes post-ME [203], the cross-modal reactivation of the visual cortex appeared to be lacking 7w post-ME (figure 1.4d). Moreover, when comparing 7wME in P45, P90 and P120 there was a gradual increase in the reactivation along the full mediolateral extent of the visual cortex with only P120 7wME *zif268* expression reaching control levels. To conclude, ME in the mouse provides a valuable model to study age-dependent cross-modal plasticity.

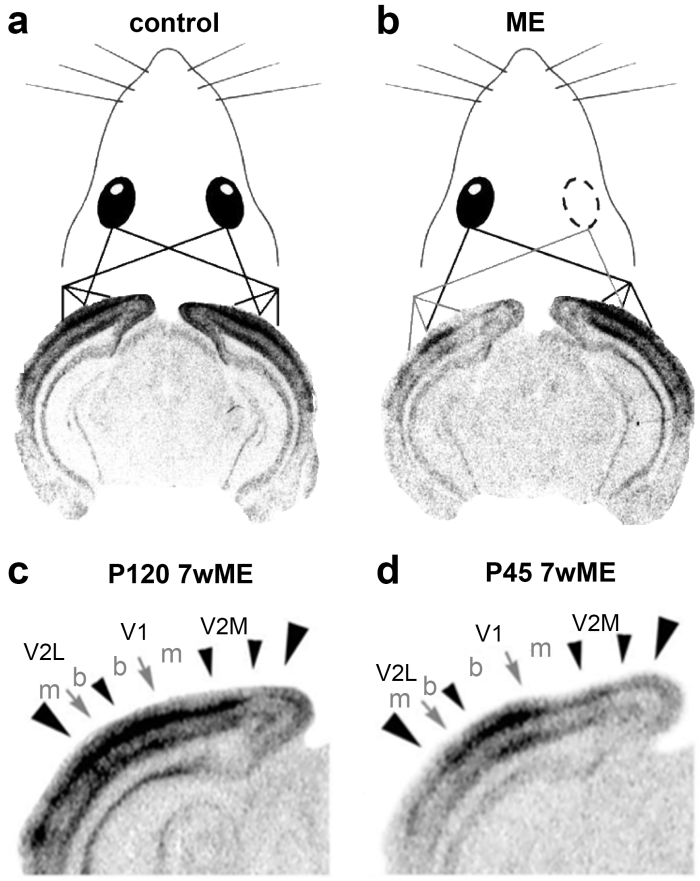

Figure 1.4: ME-induced cortical reactivation in P120 and P45 mice.

Radioactive in situ hybridization for the neuronal activity marker *zif268* enables the visualization of neural activity across all layers of the visual cortex with a darker signal representing higher *zif268* expression and thus higher neuronal activity. Mice with both eyes intact exhibit high *zif268* expression along the entire mediolateral extent of the visual cortex (a). Performing monocular enucleation (ME) or the removal of one eye induces a vast decrease in neuronal activity in the contralateral visual cortex with residual *zif268* expression in the binocular zone serving the remaining eye (b). Interestingly, in adult (P120) mice seven weeks post-ME (7wME) the contralateral visual cortex displays an extensive reactivation which is caused by both the potentiation of the remaining eye which drives reactivation from the binocular zone (letter b) outwards, and cross-modal plasticity which reactivates the medial and lateral monocular areas (letter m) (c). The potential for cross-modal plasticity is age-dependent since adolescent (P45) mice do not exhibit reactivation in the monocularly driven areas at 7wME (d). Abbreviations: V2L lateral extrastriate cortex; V2M, medial extrastriate cortex; V1, primary visual cortex. Adapted from [256].

1.3.3 Cytoskeletal dynamics in neuroplasticity

As briefly discussed in section 1.3.1.1, structural plasticity relies on the underlying dynamics of the cytoskeleton, composed of an interwoven network of actin filaments, microtubules and intermediate filaments (figure 1.5). Neurofilament proteins, a type of intermediate filaments, form a structural matrix that embeds microtubules, which transport cargo (e.g. proteins and organelles such as mitochondria) along the neurite and synapses [107]. Neurofilaments are composed of four subunits called heavy (NF-H), medium (NF-M) and light (NF-L) chains, and α-internexin (NF-66) [382]. A number of different roles have been identified for neurofilaments. In addition to maintaining neuronal structure, they are particularly abundant in axons and determine the axon diameter which is correlated with the axons conductivity [383]. Neurofilaments are also crucial for docking cellular constituents such as mitochondria [201]. Indeed, it has been shown that neurofilaments bind to mitochondria for proper allocation to energy-demanding synapses to modulate synaptic plasticity [350, 201]. Considerable attention has gone to the phosphorylation state of NF since this induces axonal radial growth and hyperphosphorylation of NF slows down their transport along microtubules, causing NF accumulation in the soma, which is a hallmark of neurodegenerative diseases such as amyothropic lateral sclerosis and Alzheimer's disease [67, 15]. Important to note is that the majority of phosphorylated NF is located in the axons, whereas dephosphorylated NF is primarily found in dendrites [383]. Finally, the stoichiometry of the different NF subunits is essential for proper functioning of the cytoskeleton since overexpression of NF-H and NF-M can induce NF aggregation whereas this is rescued by additionally overexpressing NF-L [179].

The main function of microtubules is to regulate long-range transport through interaction with the molecular motors dynein and kinesin that bind to cargo such as proteins, lipids, mitochondria and lysosomes [128]. However, both microtubules and actin filaments serve additional functions, especially in dendritic spines where they regulate spine stability and plasticity, receptor trafficking and docking of organelles [219, 145, 201]. The dynamics of actin cytoskeleton are well characterized in dendritic spines and are regulated by an

array of actin-binding proteins, such as the Arp2/3 complex, WAVE1, cortactin, profilin and cofilin (figure 1.5) [98]. The Arp2/3 complex promotes actin branching and regulates spine head growth, whereas WAVE1 and cortactin activate the Arp2/3 complex and influence spine density [98, 145]. Both profilin and the actin depolymerizing factor cofilin modulate spine head morphology and spine size during LTP [80, 145].

1.4 Mitochondrial dynamics and autophagy

Most of the energy consumed by the brain is generated by mitochondria in the form of ATP by processing oxygen and glucose-derived substrates. To effectively distribute this energy, mitochondria are continuously transported along the microtubule network to energy-demanding locations such as the pre- and post-synapse [280, 201]. Mitochondria are able to sequester cytoplasmatic calcium and therefore their location and abundance can modulate neuronal signaling and synaptic plasticity [49, 201]. In addition, mitochondria can control synaptic plasticity by the production of reactive oxygen species (ROS) that act as signaling molecules which are necessary for LTP and activation of NMDA receptor downstream targets [175]. To control number, morphology and size and to maintain their health, mitochondria continuously undergo fission and fusion which mixes mitochondrial DNA and metabolites [74, 201]. This process is regulated by dynamin-related protein 1 (Drp1) and fission protein 1 (Fis1) which mediate mitochondrial fission, whereas mitofusins (Mfn-1 and Mfn-2) and Optic Atrophy-1 (OPA-1) mediate mitochondrial fusion (figure 1.6) [74]. Numerous processes in the brain including dendritic growth and branching, spinogenesis, spine morphology and synaptic plasticity depend on proper mitochondrial dynamics and function [192, 49, 35].

Another way to control energy distribution in neurons is by mitophagy or the degradation of mitochondria by a process called autophagy. In fact, autophagy is an evolutionarily highly conserved cellular homeostatic process whereby cells control their cytoplasmic biomass, organellar abundance and distribution, and remove potentially harmful protein aggregates [70]. Several

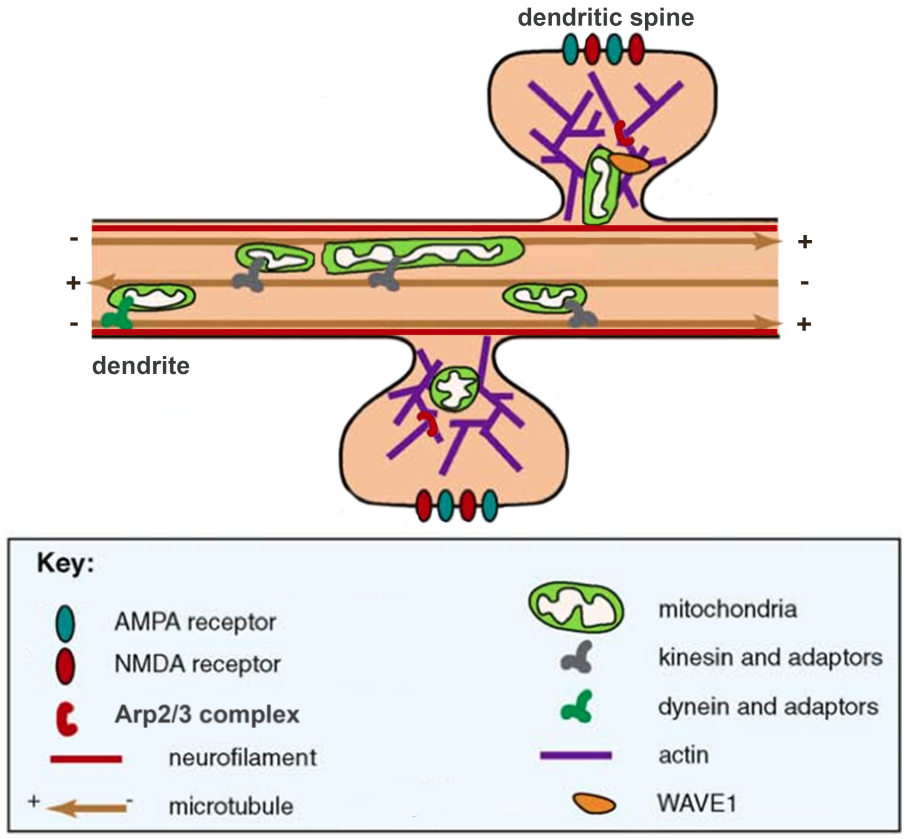

Figure 1.5: Cytoskeletal organization in dendrites.
Microtubules serve as railways for long-range transport via kinesin (anterograde transport, towards the plus-end) and dynein (retrograde transport, towards the minus-end) motors which attach cargo such as mitochondria through adaptor proteins. Neurofilament proteins shape the neuronal structure and regulate the docking of organelles at specific sites such as the dendritic spine. In the dendritic spine, the actin-based cytoskeleton can modulate rapid changes in growth and shape by branching and (de)polymerization, which is regulated by proteins such as the Arp2/3 complex and WAVE1. In addition, the actin cytoskeleton can facilitate docking and entry of organelles into the spine and it regulates the clustering and trafficking of membrane molecules such as AMPA and NMDA receptors. Adapted from [201].

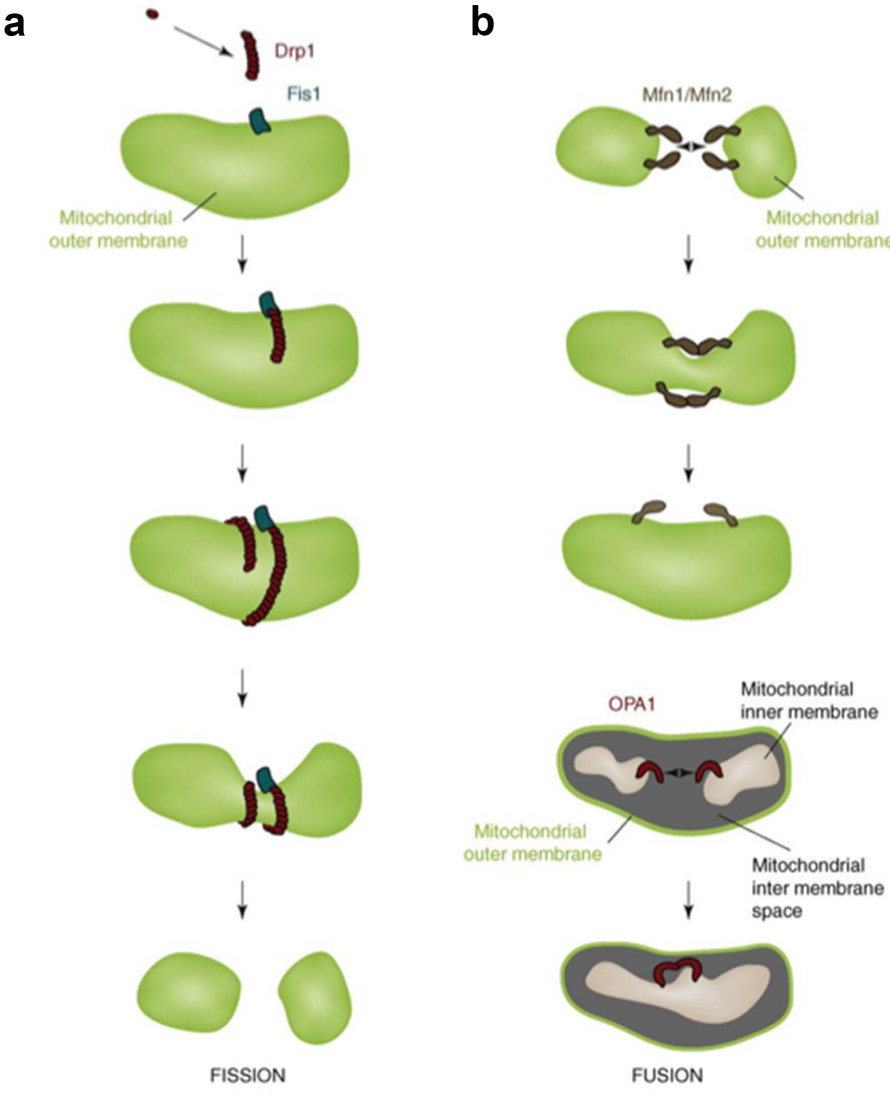

Figure 1.6: Mitochondrial fission and fusion.

Mitochondria continuously undergo fission (a) and fusion (b) to maintain their health. Fission is regulated by dynamin-related protein 1 (Drp1) which oligomerizes around the outer mitochondrial membrane and is recruited by fission protein 1 (Fis1). Full oligomerization of Drp1 creates spiral chains that wrap around mitochondria and complete fission. Fusion is accomplished by dimerization of mitofusin-1 and -2 (Mfn-1/Mfn-2) and Optic Atrophy-1 (OPA-1) which completes outer and inner membrane fusion respectively. Adapted from [201].

neurodegenerative diseases are characterized by defective autophagy and failure to remove harmful protein aggregates [384, 48]. Autophagy is dynamically regulated by starvation and other stress factors and is initiated through sequestering organelles and proteins in spherical membrane structures called autophagosomes. Eventually, autophagosomes fuse with lysosomes containing hydrolases to form autolysosomes that degrade the sequestered material (figure 1.7) [384]. The formation of the autophagosome membrane is regulated by an array of autophagy-related proteins (Atg) and the microtubule-associated protein 1 light chain 3 (LC3) [230, 322, 388]. Two forms of LC3 exist: cytosolic LC3-I and phosphatidylethanolamine-conjugated LC3-II which inserts in the autophagosome membrane. Conversion of LC3-I to LC3-II is indicative for the formation of autophagosomes [322, 35]. Importantly, because LC3-II is both present in the outer and inner part of the autophagosome membrane, LC3-II itself gets partially degraded in autolysosomes (figure 1.7). Therefore, assessment of LC3-I and LC3-II levels is often combined with the use of lysosomal inhibitors to determine the rate of autophagy, also called the autophagic flux [229, 322].

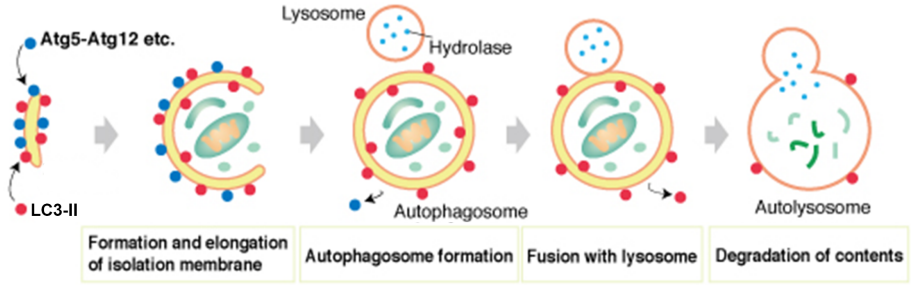

Figure 1.7: The process of autophagy.
Autophagy is initiated by the formation and elongation of an autophagosome membrane to form autophagosomes that capture proteins and organelles. This process is regulated by autophagy-related proteins (Atg) and phosphatidylethanolamine-conjugated LC3-II which insert in the membrane. Next, autophagosomes fuse with lysosomes containing hydrolases to form autolysosomes which degrade the sequestered material, thus completing the autophagic process. Adapted from http://ruo.mbl.co.jp/e/product/protein/lc3.html

1.5 Matrix metalloproteinases

More than fifty years ago, a new field in biomedical research arose when in 1962 Jerome Gross and colleagues described an interesting collagenolytic activity during metamorphosis in tadpoles [126]. This activity turned out to be interstitial collagenase, the first member of the enzyme family called matrix metalloproteinases (MMPs) and in the following decades, much more members were discovered. MMPs are in fact Zn^{2+}-dependent endopeptidases that touch almost every aspect of normal and pathological mammalian biology from egg cell fertilization, embryonic development, tissue repair, immune and nervous system function to cancer, inflammation, autoimmune diseases, vascular diseases and neurodegenerative disorders [377, 33, 97, 5]. They tightly regulate cell behavior in these processes by modulating the extracellular matrix, hormones, cytokines, chemokines, adhesion molecules, growth factors, receptors and an array of intracellular substrates [295, 40].

1.5.1 Number, structure and classification

The number of distinct MMPs differs between species. For example, *C. elegans* only has three MMPs [106], *Arabidopsis thaliana* has five [206] and both humans and mice have 23 different MMPs [209, 156]. For the number of MMPs in human and mice, slightly contradictory literature is present. Yong et al. (2005) state that humans possess 24 MMPs and mice 23 because they claim that humans have two different forms of MMP-23 (A and B) [377]. In fact, human MMP-23A is encoded by a pseudogene and thus cannot be regarded as a functional MMP protein. Therefore, both humans and mice possess 23 MMPs with the only difference that mice have two subtypes of MMP-1(ColA and ColB) and lack the orthologue of human MMP-26 [377, 156].

MMPs are multidomain enzymes characterized by a highly conserved catalytic domain with three histidine-residues binding a central Zn^{2+} ion [377, 40]. In general, the structure of a typical MMP consists of an N-terminal signal peptide, a prodomain, a catalytical domain, a linker or hinge region, and a C-terminal hemopexin-like domain (figure 1.8). MMPs are synthesized as pre-proenzymes

and the signal peptide that targets the enzyme to the endoplasmatic reticulum is removed during translation. The prodomain contains a conserved cysteine residue with a thiolgroup that interacts with the Zn^{2+} ion of the catalytic site to maintain the latency of the enzyme [246]. The catalytic domain dictates cleavage-site specificity through its active site cleft, subsite pockets that interact with amino acids adjacent to the peptide scissile bond and through substrate-binding exosites located outside the active site [265, 314]. The hinge region makes the MMP extremely flexible for the proper positioning of the catalytic domain relative to the hemopexin-like domain to efficiently interact with substrates [264]. The C-terminal hemopexin-like domain is necessary for protein-protein interaction and contributes to substrate specificity and regulation of enzyme activity by interacting with specific substrates and endogenous inhibitors [349, 276]. Moreover, MMPs can act as ligands through their hemopexin-like domain, thereby initiating downstream signal cascades by binding to receptors [152, 276]. Exceptions to this general domain structure are MMP-7 (matrilysin), MMP-26 (endometase/matrilysin-2) and MMP-23, which lack the hinge region and hemopexin-like domain. Instead, the C-terminal of MMP-23 consists of unique cysteine-rich, proline-rich, immunoglobulin-like, and IL-1 type II receptor-like domains. MMP-2 (Gelatinase A) and MMP-9 (Gelatinase B) have gelatin-binding fibronectin-like domains to efficiently interact with gelatin and gelatin-like substrates. Finally, there are four membrane-type MMPs (MMP-14, -15, -16 and -24) characterized by a transmembrane domain and other MMPs have a glycophosphatidyl inositol (GPI) membrane-anchoring signal (MMP-17 and MMP-25).

Different classifications of MMPs exist in literature [293, 269, 349, 97, 152] and one popular way to classify them is based on their domain composition. Nevertheless, little consensus about this classification is present in the field since domain structure does not predict function. Other types of MMP organization entail the subdivision based on activation mechanism, substrate preference or cellular localization. A combination of these classifications is presented in figure 1.8.

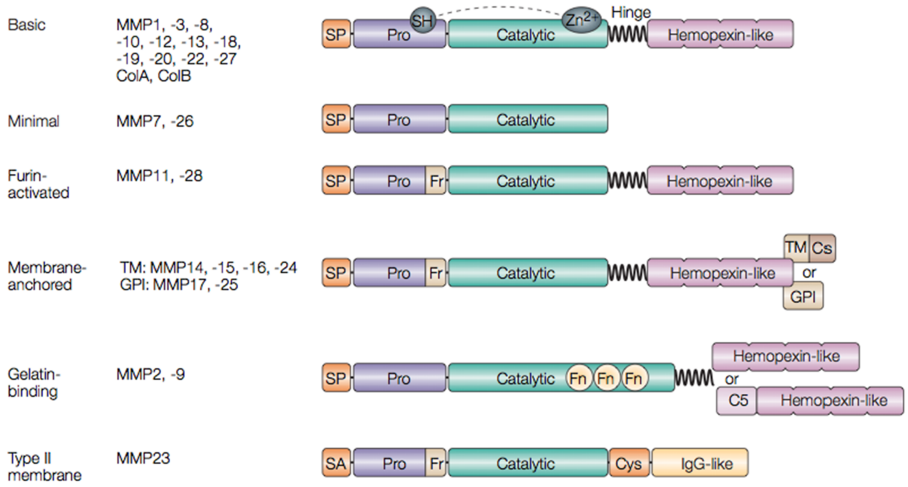

Figure 1.8: Classification of matrix metalloproteinases.
This overview shows the general domain structure of MMPs. MMP-7 and -26 are minimal domain MMPs because they lack the hinge region and hemopexin-like domain. Certain MMPs contain a furin-cleavage site (Fr) for intracellular activation and a subset of these MMPs are membrane-anchored and characterized by a transmembrane (TM) domain, glycophosphatidyl inositol (GPI) anchor (MMP-17 and -26) or an amino (N)-terminal signal anchor (SA) (MMP-23). MMP-2 and -9 are distinctive for their fibronectin-like (Fn) domains to bind gelatin efficiently. Abbreviations: C5, type-V-collagen-like domain; Col; collagenase-like protein; Cs, cytosolic; Cys, cysteine array; Fn, fibronectin repeat; Fr, furin-cleavage site; IgG, immunoglobulin; Pro, pro-domain; SH, thiol group; SP, signal peptide; Zn^{2+}, zinc ion. Adapted from [269].

1.5.2 Regulation of MMP activity

To perform their function optimally in both normal and pathological conditions, MMPs must be present in the right cell type, the correct (peri)cellular location, at the right time, in the right amount, and they must be activated or inhibited appropriately. Therefore they are tightly regulated at different levels: transcription, compartmentalization on or near the cell surface, zymogen activation, and enzyme inactivation/degradation [269, 97]. The final catalytic activity is further determined by substrate affinity and availability.

1.5.2.1 Transcription

MMP promotors harbor several cis-elements allowing for a precise regulation of gene expression by a variety of transcription factors [314, 374]. Several MMPs share cis-elements suggesting that these MMPs are transcriptionally regulated together [374]. One major regulator of MMP gene expression is the transcription factor activator protein-1 (AP-1) which consists of Fos family and Jun family protein heterodimers [359, 314]. Most MMP-genes contain an AP-1 site and a classic TATA box at the promotor site, exceptions being MMP-8, -11 and -21 which lack the AP-1 site. MMP-2, -14 and -28 lack both the AP-1 site and TATA box. The presence of an AP-1 site renders the MMP-genes responsive to inducible factors such as cytokines and growth factors, including interleukins, interferons, TNF-α, and the extracellular matrix metalloproteinase inducer EMMPRIN [314, 374]. Moreover, several factors including growth factors, cortisol and integrins can also modulate post-transcriptional mRNA levels by directly stabilizing or destabilizing the mRNA thereby influencing its half-life [374]. In addition, alternative splicing and promotor usage can further determine the net MMP activity. For instance, MMP-11 can be translated directly as an active enzyme through an alternative transcript lacking the signal peptide and prodomain [200]. Another example of the complex regulation of MMP activity at the level of transcription is presented by the observation that nuclear MMP-3 is able to act as a transcription factor for the connective tissue growth factor (CTGF) gene in chondrocytes [92]. CTGF in turn increases transcription of MMP-1, -2, -3, -7 and -14 [45, 40]. Additionally, CTGF itself serves as a substrate for these MMPs which can terminate the positive feedback loop [68]. In this way, MMPs are able to influence the level of their own transcription.

In the adult human and rodent brain, a wide range of MMPs have low mRNA levels and transcription is mainly upregulated during early postnatal development [152]. However, MMPs are transcriptionally upregulated in reponse to neuronal activity, injury and neurological disorders [180, 225, 152, 114]. For example, MMP-9 mRNA levels increase in the rat hippocampus in reponse to systemic administration of the glutamate receptor agonist kainate [318].

1.5.2.2 Compartmentalization

Confinement of MMP proteolysis to certain cellular compartments is essential to maintain catalytically favorable levels of both enzyme and substrate [327]. Moreover, undirected release of an active MMP could lead to an unwanted degradation cascade [285, 327]. It remains a key question in MMP biology of how specific proteinase-substrate interactions are regulated to limit MMP action to specific, targeted substrates since this determines a large part of MMP specificity [285]. One possible mechanism to ensure a sufficiently high enzyme concentration within the proximity of the desired substrate is by confining MMPs to pericellular niches by anchoring to the cell membrane or by interaction with extracellular macromolecules [314, 97, 285].

The membrane bound MMPs (MT-MMPs) can be concentrated to specific cell surface locations by partition into lipid rafts and for example MT1-MMP (MMP-14) can form a tripartite complex with proMMP-2 and an endogenous inhibitor to locally activate the latent MMP-2 molecule [71, 314]. In addition to the compartmentalized nature of MT-MMPs, several observations of MMP-cell interaction have been reported such as MMP-7 that is able to anchor to cholesterol and surface proteoglycans [381], and MMP-9 to surface proteoglycans [381] and the hyaluronic acid receptor CD44 [380]. Anchoring to integrin receptors has been shown for MMP-1 [87] and MMP-2 [71]. Direct MMP activation by allosteric interaction with these receptors and extracellular macromolecules can influence the level of local catalytic efficiency, thereby adding another level to compartmentalize MMP activity [327]. MMPs can also undergo different cell sorting by an inefficiently translated signal peptide or loss of this peptide by alternative splicing [92, 40]. In addition, endocytosis provides a mechanism to recycle and relocate MT-MMPs (e.g. MMP-14) [290] and to transfer exogenous MMPs to the cytosol (e.g. MMP-3 and MMP-7) [328, 319], which can then further travel to the nucleus (e.g. MMP-3) [307, 92]. Finally, recent evidence shows that MMP-9 mRNA is transported to dendrites in hippocampal neurons and is locally translated in response to glutamate stimulation [152, 89].

1.5.2.3 Zymogen activation

MMPs are mostly synthesized as inactive zymogens and their latency is maintained by a cysteine in the prodomain that interacts with the catalytic Zn^{2+} ion and forms a complex that blocks the active site. MMPs can undergo a direct or stepwise activation (figure 1.9), which results in the dissociation of the cysteine residue from the complex, a process called the "cysteine switch" [340]. An important aspect of the cysteine switch mechanism is that the prodomain does not necessarily need to be removed to acquire an active enzyme [285]. Generally, there are three main activation mechanisms that can be distinguished: 1) a direct proteolytic cleavage of the prodomain, 2) a non-proteolytic modification of the cysteine residue and 3) an allosteric perturbation of the zymogen by binding to a receptor or substrate [285, 304, 40]. In addition, translation of alternative spliced mRNA lacking the prodomain can directly yield active MMPs (see previously) [200, 40].

Non-proteolytic activation results in the destabilization of the cysteine-Zn^{2+} coordination and gives rise to a partially activated MMP intermediate [243]. The final step involves the action of an MMP or its intermediate, meaning that MMPs can activate each other [243, 349]. Proteinases such as furin and MMPs, low pH, high temperatures and chemical agents such as 4-aminophenylmercuric acetate (APMA), detergents (e.g. SDS), heavy metals, alkylating agents, oxidants (e.g. ROS) and reactive nitrogen species (NOS) can activate MMPs [349, 285]. Non-proteolytic activation may lead to subsequent autoproteolytic degradation of the propeptide resulting in autocatalytic activation of the MMP [343]. Interestingly, Tocchi et al. (2013) reported an interaction between MMP-7 and its CSPG substrate that augments the autocatalytic activity of the enzyme, demonstrating that substrate binding can impact MMP activity by allosteric perturbation of the zymogen. Importantly, allosteric activation mechanisms have been characterized for several MMPs [365, 285, 327].

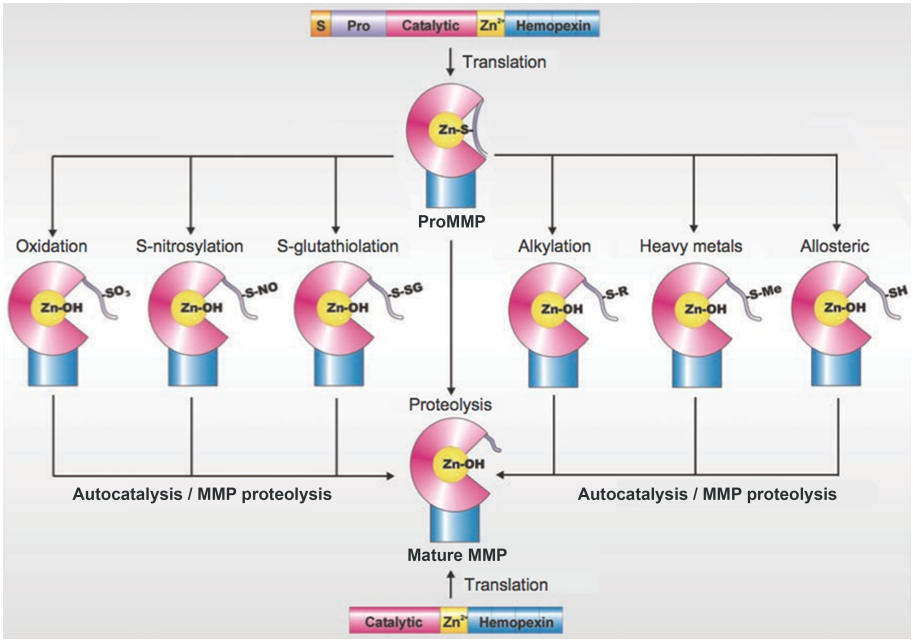

Figure 1.9: Activation mechanisms of proMMPs.
MMPs are synthesized as inactive zymogens (proMMPs) and are most commonly activated by direct proteolytic cleavage of the prodomain which yields mature MMPs. Non-proteolytic agents can disrupt the catalytic cysteine-Zn^{2+} coordination which results in partially active MMPs that can undergo autocatalysis or proteolysis by other MMPs to form mature MMPs. Binding to a receptor or substrate can distort the catalytic domain which leads to allosteric activation. In addition, alternative splicing may yield MMP transcripts lacking the signal peptide and prodomain which translate into constitutively active enzymes. Adapted from [40].

1.5.2.4 Endogenous MMP inhibition

In the blood and lymphatic system MMPs are inhibited by α_2-macroglobulin whereas in mammalian brain tissue the endogenous inhibitors constitute four members of the tissue inhibitors of metalloproteinase (TIMP) family [97]. TIMP expression corresponds to the expression of MMPs and they bind MMPs in a 1:1 stochiometry so an imbalance in expression can significantly effect overall MMP activity [5]. The N-terminal domain of the TIMP interacts with the catalytic domain, whereas the C-terminal domain interacts with the MMP hemopexin

domain and both interactions determine the inhibitory specificity. For example, TIMP-1 inhibits MMP-3 and MMP-9 more readily than MMP-2, which is mostly inhibited by TIMP-2 [314, 97]. Paradoxically, TIMP-2 is necessary for proper activation of proMMP-2 *in vivo* by binding to MMP-14 and proMMP-2 [314].

In normal, unstimulated adult CNS the expression of TIMP-1 is low whereas TIMP-2 and -3 are expressed more abundantly by neurons and astrocytes [97, 227]. TIMP-4 is exclusively expressed in the cerebellum and dorsal root ganglia with increased expression into adulthood [227]. Besides inhibition of MMPs, TIMPs have MMP-independent functions such as regulating cell growth, cell survival, apoptosis and neurite outgrowth by binding to various cell surface receptors [305, 315, 323]. In addition, other molecules with MMP inhibiting properties have been described such as the β-amyloid precursor protein which can inhibit MMP-2 [141, 245].

1.5.3 Functions in the CNS

Subsets of MMPs and TIMPs are expressed in the CNS by many cell types including neurons, astrocytes, microglia, vascular endothelial cells and choroid plexus epithelial cells [227]. In accordance to their widespread expression profiles, MMPs are implicated in a myriad of CNS pathologies and are necessary for normal brain development and function [378, 5]. For the purpose of this dissertation, I will mainly focus on the functions of MMPs in neurite outgrowth and guidance, and plasticity.

1.5.3.1 Neurite outgrowth and guidance

MMPs regulate neurite extension and guidance in various ways. For example, MMPs regulate the signaling of the axonal chemoattractant netrin-1, by ectodomain shedding of netrin-1 receptors. Netrin-1 and its receptor are required for proper axon outgrowth, branching and guidance [220, 69]. Other classes of guidance molecules are also susceptible to MMP processing. Ectodomain cleavage of the Ephrin-B2 receptor by the gelatinases MMP-2 and MMP-9 induces growth-cone collapse both in vitro and in vivo [193]. In addition,

semaphorin-3A (Sema3A)-induced dendritic outgrowth of cortical neurons is regulated by MMP-2 [122] and Sema3A negatively regulates the expression of MMP-3 [123]. Moreover, the growth-promoting effect of Sema3C on cortical axons requires MMP activity [123].

Neurite outgrowth can also be regulated by MMPs through the activation of growth factors such as nerve growth factor (NGF), insulin-like growth factor (IGF) and BDNF. BDNF and NGF are involved in axonal outgrowth in vitro and in dendritic growth in the visual cortex [213, 199] and both growth factors are known substrates of MMPs [188, 227]. IGF-1 stimulates the growth of dendrites in the somatosensory cortex [251] and proteolytic activity of MMPs is required to regulate the bio-availability of IGF-1 through cleavage of IGF-binding proteins (IGFBPs) [109, 53]. Another mechanism by which MMPs can influence neurite outgrowth is through the processing of growth inhibiting CSPGs. MMPs can degrade these proteoglycans to make the ECM permissive for neurite outgrowth [391]. Conclusively, MMPs can be considered as important mediators of neurite outgrowth and guidance.

1.5.3.2 MMPs and neuroplasticity

MMPs are capable of remodeling synaptic circuits and are vital for behavioral and experience-dependent plasticity [152]. For example, an important modulator of hippocampal synaptic plasticity is MMP-9, which is essential for late-phase LTP [247, 260, 356, 360] and regulates dendritic spine dynamics through β1-integrin signaling [356, 80, 224, 312]. In accordance, MMP-9 null mice have defects in late phase LTP and this hippocampal phenotype is rescued by application of MMP-9 [247, 227]. MMPs can also modulate the induction of LTP [182] by processing growth factors such as BDNF [188, 227]. Moreover, several actin-binding proteins including Arp2/3, cortactin and cofilin are putative MMP substrates and have been implicated in MMP-mediated structural plasticity [216, 80, 40].

At the level of behavior, Meighan et al. (2006) found that expression of hippocampal MMP-3 and MMP-9 was transiently increased in rats during Morris water maze acquisition and this process was NMDA receptor-dependent. Infusion

of an MMP inhibitor impairs their learning ability and affects the expression of the dendritic cytoskeletal protein cortactin [216]. Another important study was done by Wright et al. (2009) in which MMPs were inhibited during habituation learning, resulting in the inability of rats to habituate to a stimulus-induced head-shake response and this effect was found to be largely specific to MMP-3 [369]. In addition, MMP-3 is also necessary for memory consolidation in fear-conditioning [262] and several other studies also indicate that MMPs are implicated in learning and memory [178, 114]. In summary, a large body of evidence implicates several MMPs in structural and functional plasticity in the hippocampus and striatum. However, much less is known about their function in cortical plasticity. General MMP inhibition was recently reported to selectively prevent the potentiation of the open-eye after 7 days of MD in the visual cortex of juvenile rats [309]. In this model, MMP inhibition mainly affected the spine dynamics of layer II/III pyramidal cells in the binocular zone, indicating that MMPs are necessary for experience-dependent structural plasticity [309]. Also, MMP-9 knockout mice are characterized by a decrease in experience-dependent plasticity of the barrel cortex upon sensory deprivation [163]. Tiraboschi and colleagues recently discovered that reinstatement of OD plasticity in adult rats invokes an upregulation of MMP-2 and MMP-9 genes, possibly contributing to the required structural plasticity [326]. It is assumed that MMPs are also able to influence cortical plasticity in various ways, for example by modulating PNN, which are composed of CSPGs. CSPGs are known substrates of several MMPs, especially MMP-3 [239, 237] and enhanced expression of MMP-2 and MMP-9 coincides with a reduction of PNN in the cerebellum during environmental enrichment [108]. Moreover, Mataga and colleagues showed that the serine protease tPA is upregulated in V1 after two days of MD and is necessary for structural OD plasticity, which provides direct evidence that visual cortex plasticity is dependent on extracellular proteolytic activity [210]. Interestingly, tPA is able to activate several MMPs [243, 349], providing a potential mechanism by which MMPs could exert an effect on OD plasticity [309]. MMPs could also be involved in cortical plasticity through regulating the bio-availability of IGF-1 or TNF-α signaling. IGF-1 has been reported to modulate GABAergic inhibition in environmental enrichment and OD plasticity paradigms [51, 212], whereas TNF-α, just as BDNF, is essential for homeostatic plasticity [164, 96] and can

be activated by several MMPs [116, 314]. To conclude, it is well-established that MMPs are important mediators of various forms of neuroplasticity although their exact mechanisms of operation still remain elusive.

1.5.4 MMPs as therapeutic targets

Over 25 years ago, MMPs were thought to be primarily implicated in the degradation of the ECM between tumor cells and blood vessel linings to promote cancer progression [341, 120]. Therefore, the first clinical trials were set up to try to inhibit MMP activities in metastatis and angiogenesis [266]. At that time, only three MMPs were characterized and their function was thought to be merely detrimental. As highlighted previously, the MMP biology has become far more complex since then and over the years it has been established that MMPs, despite their detrimental role in a myriad of diseases, are vital for the normal development and functioning of the brain, other organs and even an entire organism [5]. The dual role of MMPs is apparent in for example cerebral ischemia or stroke where MMPs first cause blood-brain-barrier disruption and inflammation whereas in later stages they promote angiogenesis and are necessary for functional recovery by promoting brain plasticity [61, 5]. Also in cancer several MMPs are able to prevent metastasis by cleavage and inactivation of chemokines [266]. Therefore in retrospect, it is not surprising that almost all broad spectrum MMP inhibitors (MMPI) and even the more specific ones, failed in extensive phase III clinical trials [33, 58, 265]. Failure of these clinical trials can be explained by several reasons, including: poor oral bioavailability, metabolic instability, insufficient specificity, dose-limiting toxicity and inadequate spatial and temporal administration of MMPIs [58, 105, 341]. In addition, because crucial differences exist between the protease and substrate degradomes of mice and humans, discrepancies between the effects of MMPIs in preclinical mice experiments and human clinical trials undermined the therapeutic potential of these MMPIs [266, 341]. Early clinical trials with prolonged application of broad-spectrum MMPIs revealed unwanted side-effects such as musculoskeletal pain and inflammation, indicating the need for more specific MMPIs [85]. To date, only one MMPI (Periostat, doxycyline)

past clinical phase III and was approved by the FDA to be used in periodontitis [267].

A major obstacle in MMPI research is to synthesize specific, potent MMPIs for any of the known MMPs because of similarities in their catalytic cleft, although promising advancements are being made [265, 88, 75, 65]. One of the most important aspects for the future success of MMPIs is a complete characterization and validation of the MMP targets and antitargets in a specific physiological process. Only then will we be able to inhibit MMPs with the greatest efficacy in a spatially and temporally controlled manner.

Chapter 2

Altered neuronal architecture and plasticity in the visual cortex of adult MMP-3-deficient mice

[1]Jeroen Aerts, [1]Julie Nys, [2]Lieve Moons, [1]Tjing-Tjing Hu and [1]Lutgarde Arckens

[1]Laboratory of Neuroplasticity and Neuroproteomics, KU Leuven, Leuven, Belgium
[2]Laboratory of Neural Circuit Development and Regeneration, KU Leuven, Leuven, Belgium

Published in Brain Structure and Function, 2014, DOI 10.1007/s00429-014-0819-4

2.1 Introduction

The capacity of the mammalian brain to change its functional and anatomical organization based on sensory experience is defined as neuroplasticity. To ensure a correct development of sensory systems, genetically determined molecular programs control the formation of connections that are further sculpted by neural activity and are able to adapt after injury or sensory manipulation through experience-dependent plasticity [271, 310]. The visual system is the prime model for studying brain plasticity, including changes in deprived as well as non-deprived areas in response to sensory impairment, referred to as cross-modal plasticity. In the visual cortex of adult mice we recently revealed a potential for cross-modal plasticity following monocular enucleation (ME) [334, 256]. We provided evidence for an extensive reactivation of the visual cortex within 7 weeks post-ME. This reactivation was driven by an initial open-eye potentiation followed by cross-modally driven plasticity in the medial an lateral monocular zones starting from adjacent non-visual cortices around 3 weeks post-ME [334]. However, the molecular determinants regulating these two distinct plasticity processes still remain unclear. In that regard, matrix metalloproteinases (MMPs), Zn^{2+}-dependent endopeptidases that modulate extracellular matrix proteins, chemokines, cytokines, growth factors, receptors and a range of intracellular substrates, have over the years been identified as major regulators of normal brain development and neuroplasticity [377, 97, 40, 205]. Indeed, it is well established that MMPs are necessary for proper axon guidance and elongation [123, 261], neurite remodeling [143, 339, 225, 376], dendritic spine dynamics and elongation [318, 143, 224], synaptic plasticity [90, 225] and learning and memory [247, 216, 369]. Several MMPs, including MMP-3, are expressed in the cortex both under normal and pathological conditions such as stroke [308, 123, 227, 122]. Moreover, it has been shown that MMP-3 is necessary for proper cortical axon extension and guidance through interaction with semaphorin-3A and -3C [123]. MMP-3 is able to cleave and activate several other MMPs [258, 240] including MMP-9, which is a major regulator of dendritic spine dynamics, and late-phase LTP [318, 223, 224]. Recently, Spolidoro et al. (2012) uncovered a role for MMPs in critical period plasticity of the visual cortex in monocular deprived (MD) rats. Infusion of a broad-spectrum MMP inhibitor

prevented both the potentiation of the open-eye response and the increase in spine density on layer II/III pyramidal neurons after MD [309]. However, studies focusing on MMP-3 in visual cortex plasticity are lacking. Here we investigated the role of this specific endopeptidase in ME-induced plasticity of the visual cortex using adult MMP-3 deficient (MMP-$3^{-/-}$) mice. An assessment of MMP-3 deficiency on the structure and functionality of the adult visual cortex is crucial to understand plasticity-related manipulations in these mice. Here, we describe a phenotypical characterization of the visual cortex of MMP-$3^{-/-}$ mice using Golgi-cox staining, revealing an aberrant neuronal morphology. Western analysis of cytoskeletal proteins disclosed a differential composition of neurofilament proteins complementing these findings. Finally, to assess these impairments at a functional level we performed ME to probe for an involvement of MMP-3 in experience-dependent cortical plasticity.

2.2 Material and methods

2.2.1 Animals

All experiments were performed in adult (120 days old) wildtype (WT) and MMP-3 deficient (MMP-3$^{-/-}$) mice with a similar genetic background (50% Bl6 x 25% B10 x 25% RIII) (Mudgett, Merck Labs) which were housed under standard laboratory conditions under an 11/13h dark/light cycle with food and water available ad libitum. All experiments have been approved by the Ethical Committee of the university and were in strict accordance with the European Communities Council Directive of 22 September 2010 (2010/63/EU) and with the Belgian legislation (KB of 29 May 2013). Every possible effort was made to minimize animal suffering and to reduce the number of animals.

2.2.2 Golgi-cox staining

WT (n = 3) and MMP-3$^{-/-}$ (n = 3) mice received an intraperitoneal injection of sodium pentobarbital (Nembutal, 600 mg/kg, Ceva Sante Animale) before being perfused transcardially with 1% paraformaldehyde (PFA, Sigma-Aldrich, St. Louis, MO) in 0.15M phosphate-buffered saline (PBS, pH 7.42) at 37 °C. Brains were dissected and post-fixated in 4% PFA in PBS for 1 hour after which they were impregnated with the Golgi staining solution (FD Rapid GolgiStain kit, FD Neurotechnologies Inc., USA) for 12 to 14 days in complete darkness. The impregnated brains were further processed using a vibratome (Leica VT1000S, Leica Microsystems GmbH, Wetzlar, Germany) into 80 μm-thick coronal sections. These sections were stained in developing solution (FD Rapid GolgiStain Kit), placed on glass slides and air dried for three days before being dehydrated and coverslipped for imaging with bright field microscopy (Zeiss Axio Imager Z.1, software program Axiovision Rel. 4.6, Carl Zeiss Benelux).

2.2.3 Morphometric quantification

The dendritic composition of layer V pyramidal cells (n = 12-15 / animal) exhibiting complete Golgi impregnation, was manually traced on flattened Z-stack images using the brush tool in Adobe Photoshop CS5 and a pen tablet (Wacom Co., Ltd.). To exclude possible misinterpretations of branching patterns, the tracings done on the flattened images were checked against the original Z-stack data. For each extracted neuron the apical shaft length, mean oblique length, number of obliques, number of branching points and spine density on the apical shaft were measured using Axiovision Rel. 4.6 (Carl Zeiss, Benelux). The spine density was determined at a final magnification of x1000 by manually counting the spines on two consecutive 25 μm segments on the apical shaft of each neuron starting at a distance of 50 μm away from the cell body. The dendritic diameter was noted every 25 μm. For each segment the length of up to ten spines was measured and only spines with a clear connection to the apical shaft were included. For each condition, the data was presented as the mean $\pm$ standard error of the mean (SEM).

2.2.4 Western Blotting

For each mouse (WT: n = 6, MMP-3$^{-/-}$: n = 6) the visual cortex was collected from 100 μm-thick coronal cryosections spanning Bregma levels -2.00 to -4.60. Proteins were extracted with a lysis buffer (50 mM Tris, 5 mM EDTA, 1% Triton X-100, 1 mM DTT, pH 7.4 and complete protease inhibitor cocktail (Roche Diagnostics Ltd, Mannheim, Germany)) and the samples were centrifuged (8000 x g) for 5 minutes at 4 °C. The supernatant was isolated and the total protein concentration was determined by means of a QubitTM fluorometer (Invitrogen, Merelbeke, Belgium). Samples were stored at -80 °C. For immunodetection of non-phosphorylated neurofilament-high (NF-H), phosphorylated neurofilament-high/-medium (pNF-H/-M), neurofilament-low (NF-L) and α-internexin (NF-66), equal amounts of protein (10 μg) were loaded onto 4-12% Bis-Tris Midi gels (NuPAGE Novex, Invitrogen) and transferred to a polyvinylidene fluoride (PVDF) (NF-L) or nitrocellulose (NF-H, pNF-H/M and NF-66) membrane. The choice of membrane was empirically determined based on signal-to-noise

ratio. Overnight incubation with the monoclonal antibody SMI-32R (anti-NF-H, 1:500, Covance Research Products, USA; Sternberger and Sternberger 1983), SMI-31R (anti-pNF-H/pNF-M, 1:1000, Covance Research Products, USA; Sternberger and Sternberger 1983), anti-NF-L (1:5000, Mab1615, Merck Millipore, Germany) and anti-NF-66 (1:5000, NBP1-49175, Novus Biologicals, USA) was followed by 30 minutes incubation with HRP-labeled secondary antibodies (1:50000, Dako, Denmark). The immunoreactive bands were visualized using a luminol-based enhanced chemiluminescent kit (SuperSignal West Dura, Thermo Scientific, USA). In order to correct for inter-gel variability and to normalize the concentration of the specific detected proteins to the total amount of protein present, we performed a total protein stain (TPS) prior to immunodetection with LavaPurple (Gelcompany, USA) according to manufacturer's instructions. After the staining, dry blots were scanned with a ChemiDocTM MP Imaging System (Bio-Rad Laboratories, USA). The protein bands were semi-quantitatively evaluated by densitometry (Image Lab 4.1, Bio-Rad Laboratories, USA). First, to account for inter-gel variability including loading differences, incomplete transfer or position on the blot, a TPS was employed rather than the use of a single reference protein [6, 146]. For each protein of interest, the optical density value per mouse was normalized to its corresponding TPS. Also, to compare samples between different gels, normalized data were expressed relative to the reference sample, i.e. a pool of all samples.

2.2.5 Monocular enucleation and in situ hybridization

Monocular enucleation of the mice (n = 4 / condition) was performed as previously described [2, 256, 333]. Briefly, under anesthesia by intraperitoneal injection of a mixture of ketamine hydrochloride (75 mg/kg, Dechra Veterinary Products, Eurovet) and medetomidine hydrochloride (1 mg/kg, Orion Corporation, Janssen Animal Health), the right eye was carefully removed and if needed, the orbit was filled with hemostatic cotton wool (Qualiphar, Bornem, Belgium). After injection with atipamezol hydrochloride (1 mg/kg, Orion Corporation, Elanco Animal Health) to reverse anesthesia, the animals were allowed to recover on a heating pad. They were all administered 0.05 ml of antibiotics (Kefzol, 1 g Natrii cefazolin and 15 mg Lidocaini hydrochloridum

anhydricum in 4 ml 0.9% NaCl, Eurocept Pharmaceuticals) intramuscularly to prevent post-surgical infections. After the enucleation procedure, mice were again housed under the same normal light conditions in standard cages for a survival period of seven weeks. Prior to sacrifice, the animals underwent an overnight dark-exposure followed by 45 min of bright light to obtain an optimal visually evoked *zif268* expression [367, 161, 9, 387, 336]. For in situ hybridization experiments, all mice received an overdose of sodium pentobarbital (Nembutal, 600 mg/kg, Ceva Sante Animale) by intraperitoneal injection prior to sacrifice by cervical dislocation. The brains were rapidly removed and immediately frozen in 2-methylbutane (Merck, Overijse, Belgium) at a temperature of -40 °C and stored at -80 °C until sectioning. Twenty-five μm-thick sections were prepared on a cryostat (Microm HM 500 OM, Walldorf, Germany), mounted on 0.1% poly-L-lysine (Sigma–Aldrich, St. Louis, MO)-coated slides and stored at -20 °C until further processing.

In situ hybridization was performed with a mouse-specific synthetic oligonucleotide probe (Eurogentec, Seraing, Belgium) with sequence 5'-ccgttgctcagcagcatcatctcctccagtttggggtagttgtcc-3' for *zif268*. This oligonucleotide probe has been used successfully for the analysis of *zif268* mRNA expression in the mouse brain in previous publications [334, 366, 256]. As described earlier [10, 55], each probe was 3'-end labeled with ^{33}P-dATP using terminal deoxynucleotidyl transferase (Invitrogen, Paisley, UK). Unincorporated nucleotides were separated from the labeled probe with miniQuick SpinTM Oligo Columns (Roche Diagnostics, Brussels, Belgium). Series of cryostat sections (every 50 μm) were fixed, dehydrated and delipidated. The radioactively labeled probe was added to a hybridization cocktail (50% (vol/vol) formamide, 4x standard saline sodium citrate buffer, 1 x Denhardt's solution, 10% (wt/vol) dextran sulphate, 100 μg/ml herring sperm DNA, 250 μg/ml tRNA, 60 mM dithiothreitol, 1% (wt/vol) N-lauroyl sarcosine, 20 mM $NaHPO_4$, pH 7.4) and applied to the cryostat sections (10^6 cpm per section) for an overnight incubation at 37 °C in a humid chamber. The following day, sections were rinsed in 1x standard saline sodium citrate buffer at a temperature of 42 °C, dehydrated, air-dried and exposed to an autoradiographic film (Biomax MR, Kodak, Zaventem, Belgium). Films were developed in Kodak D19 developing solution after 7 days and fixation was performed in Rapid fixer (Ilford Hypam, Kodak). For each mouse,

autoradiographic images from three adjacent sections were scanned at 1200 dpi (CanoScan LIDE 600F, Canon, USA). Pseudo-color maps were generated with a custom-made MATLAB script (MATLAB R2008b, The MathWorks Inc., Natick, MA) and represent a false coloring of the gray values: a low gray value is represented in black/green, a high gray value in white/yellow, indicating a low signal response or a high signal response respectively. This is done in accordance with a gray scale ranging from black (0) to white (255).

2.2.6 Histology

Histology was performed on each section to aid interpretation of the activity patterns obtained by in situ hybridization. The cryostat sections for *zif268* were therefore Nissl-counterstained (Cresyl violet 1%, Fluka Chemika, Sigma-Aldrich) according to standard procedures. Comparisons were made to a stereotaxic mouse brain atlas [110]. Images of the stained coronal sections were obtained with a light microscope (Zeiss Axio Imager Z.1) equipped with an AxioCam MRm camera (1388x1040 pixels) using the software program Axiovision Rel. 4.6 (Carl Zeiss Benelux).

2.2.7 Localization of visual areal boundaries with Nissl patterns

To anatomically delineate the areal borders of the different visual subdivisions a comparison was made with Nissl counterstained sections as described previously by Van Brussel et al. (2009; 2011) and Nys et al. (2014) [333, 334, 256]. All topographic denominations were adopted from these papers. Concurrently, we applied the mapping of functional subdivisions of the visual cortex as located by Van Brussel et al. (2009) where the eye-specific inputs were identified using enucleation of one eye combined with stimulation of the remaining eye. Combined, these methods allowed for the generation of animal specific coronal atlases of the visual cortex and thus provided a reliable guide for the interpretation of *zif268* in situ hybridization results. In all figures, large arrowheads indicate the total extent of the visual cortex while small arrowheads indicate areal borders. We always distinguished five regions from medial to

lateral: medial extrastriate cortex (V2M), primary visual cortex (V1), which was further subdivided in the monocular (V1m) and the binocular (V1b) part and lateral extrastriate cortex (V2L), which was also subdivided in a monocular (V2Lm) and a binocular (V2Lb) region. In relation to functional inputs, we defined the V1–V2L border as the central binocular zone (Bz), a large part of V2M and V1m as the medial monocular zone (Mmz), and V2Lm as the lateral monocular zone (Lmz). In figures 4 and 5, the location of the binocular zone has been indicated with the gray letter b. Adjoining monocularly driven parts of V1 and V2L are marked with a gray letter m.

2.2.8 Quantitative analysis of ISH results

As described before [256], optical density values (mean gray value per pixel) from the autoradiograms of different experimental and control groups were quantified using a custom-made MATLAB script (MATLAB R2008b, The MathWorks Inc., Natick, MA). For each condition at least 3 mice were included and for each mouse three 25 µm-thick sections were selected between -3.00 mm and -4.00 mm relative to Bregma [110]. In order to demarcate the region of interest in the left hemisphere, we determined the top edge of the cortex, the border between the granular layer IV and infragranular layer V and the boundary where layer VI meets the white matter. These layer-related borders were computed by a contour smoothing algorithm based on the Gaussian weighted least squares fit [27] from manually drawn lines on the autoradiogram. The different areal and functional boundaries as derived from Nissl patterns were subsequently registered to the curvature of the top and bottom boundaries. Next, the delineated region of interest was equally divided into 24 segments [62] creating two lattices of 24 quadrangles, corresponding to the upper (LII-IV) and lower (LV-VI) layers. To compensate for possible variation in brain size and morphology, we translated the lattice on each autoradiogram over the cortical curvature, fixing the border of a specific segment to an areal border (border segment 19/20 is area border V1m/V2M). For each segment created this way, the relative optical density was calculated as the mean gray value of all pixels within this quadrangle normalized to the mean gray value of a square measured in the thalamus (a defined region with no *zif268* expression above background). This procedure was required

to compare autoradiograms across experiments [270, 334]. Relative molecular activity was expressed in percentages based on the following formula: (1 - (cortical *zif268*/thalamic background)) x 100. We compared *zif268* expression between different experimental and control groups for upper and lower layers of the visual cortex separately. Furthermore, relative expression patterns were assessed along the anatomically defined visual subdivisions as well as in the functionally distinct areas consisting of the central binocular zone and two flanking monocular zones.

2.2.9 Statistics

All Western blot data and data of the Golgi-cox staining except for the spine length distribution, were presented as mean ± SEM. A normal distribution was verified using the Kolmogorov–Smirnov test and parallel equal variance between groups was tested. If the test requirements were fulfilled, an unpaired Student's t-test for pairwise comparison was used (*P $<$ 0.05, **P $<$ 0.01, ***P $<$ 0.001). When criteria for this parametrical test were not fulfilled, a Mann-Whitney U rank sum test for pairwise comparison of independent samples was applied (*P $<$ 0.05, **P $<$ 0.01, ***P $<$ 0.001). For comparing the distribution of spine length across groups, a chi-square analysis was performed and data was presented as the percentage of total spine number per spine length interval.

To compare the ISH results for each condition, the data of relative optical densities was presented as mean ± SEM. A normal distribution was verified using the Kolmogorov–Smirnov test and parallel equal variance between groups was tested. If the test requirements were fulfilled, for the ISH data a two-way ANOVA was used with factors zone (functional: binocular, medial monocular or lateral monocular zone) and genotype (WT or MMP-3$^{-/-}$) or deprivation (control of 7wME) to test for ME-specific changes in *zif268* expression. Fisher's LSD post hoc tests were used for pairwise comparisons and a probability level of $<$ 0.05 (α-level was set to 0.05) was accepted as statistically significant (*P $<$ 0.05, **P $<$ 0.01, ***P $<$ 0.001). When criteria for this parametrical test were not fulfilled, a non-parametrical Kruskal-Wallis analysis with a Mann-Whitney U rank sum test for pairwise comparison of independent samples was applied.

When no interaction between the two factors studied was observed a one-way ANOVA with an unpaired Student t-test for pairwise comparison was used (*P < 0.05, **P < 0.01, ***P < 0.001). Statistical analyses were performed using SigmaStat 3.1 (SYSTAT software).

2.3 Results

2.3.1 Truncated neuronal morphology and impaired translaminar projections in the visual cortex of MMP-3 deficient mice

Golgi-Cox staining revealed normal vertical projections across all cortical layers in V1 of WT mice. In contrast, MMP-3$^{-/-}$ mice displayed an apparent, truncated translaminar organization (figure 2.1a-b). To address this anatomical feature in more detail, we analyzed layer-specific pyramidal neurons, since they are typically characterized by long apical dendrites supporting the vertical oriented appearance of the stained cortex. Layer V pyramidal cells of MMP-3$^{-/-}$ mice displayed a significant reduction ($P < 0.001$) in the length of the apical shaft (figure 2.2a-c) and a comparable number of apical branches called obliques ($P = 0.666$), together resulting in a higher density of apical obliques (# apical obliques/ apical shaft length, $P < 0.001$) compared with WT mice (figure 2.2d-e). No differences between the two genotypes concerning mean oblique length ($P = 0.490$) or branching complexity (mean # branch points per neuron, $P = 0.298$) were observed (figure 2.2f-g). These measurements indicate that MMP-3$^{-/-}$ mice have a shorter apical shaft with more apical obliques per unit of length. Spine density on the apical shaft was the same in both genotypes ($P = 0.893$) whereas the distribution of spine length showed significantly shorter spines (chi-square = 10.701, df = 3, $P = 0.013$) in MMP-3$^{-/-}$ mice compared with WT (figure 2.2h-j). These results indicate a higher prevalence of shorter, more mature spines in the cortex of MMP-3$^{-/-}$ mice. No differences in soma size were observed. Dendritic diameter did not differ in each measured segment so no correction factor for spine density was employed [153].

2.3.2 Cytoskeletal protein anomalies in the visual cortex as a result of MMP-3 deficiency

To corroborate the truncated neuronal morphology in the MMP-3$^{-/-}$ mice on a molecular level, we compared the expression levels of different neurofilament

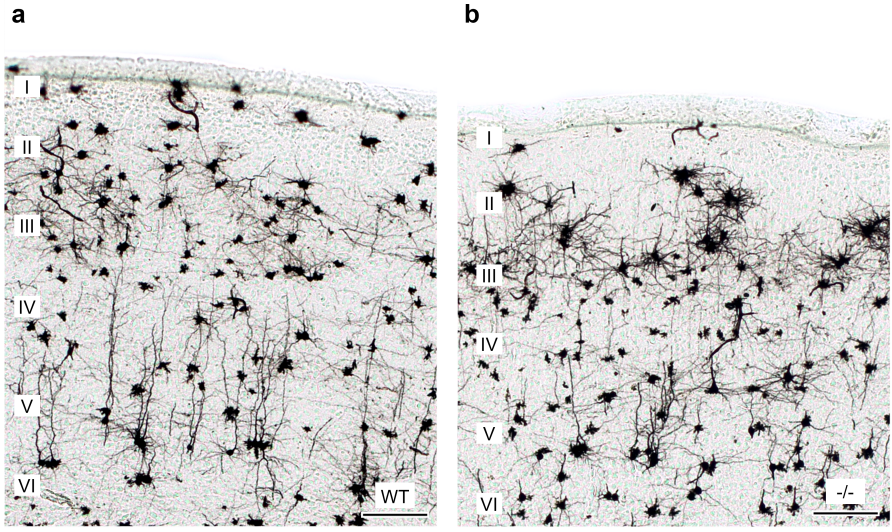

Figure 2.1: Representative bright field images of Golgi-Cox stained primary visual cortex of WT (a) and MMP-3$^{-/-}$ (b) mice.
A perturbed translaminar organization characterizes the visual cortex of MMP-3$^{-/-}$ mice. Scale bars: 150 μm.

protein subunits in cortices of both genotypes using Western analysis since they constitute the major components of the neuronal cytoskeleton. All analyzed neurofilament protein subunits were found to be significantly upregulated in the visual cortex of MMP-3$^{-/-}$ mice (figure 2.3a-e: non-phosphorylated neurofilament-high (NF-H), $P = 0.026$, ratio = 1.9; phosphorylated neurofilament-high (pNF-H), $P = 0.011$, ratio = 2.2; phosphorylated neurofilament-medium (pNF-M), $P = 0.002$, ratio = 3.0; neurofilament-low (NF-L), $P < 0.001$, ratio = 5.9 and α-internexin (NF-66), $P < 0.001$, ratio = 2.3). These results are indicative for an altered neurofilament protein subunit composition and phosphorylation state.

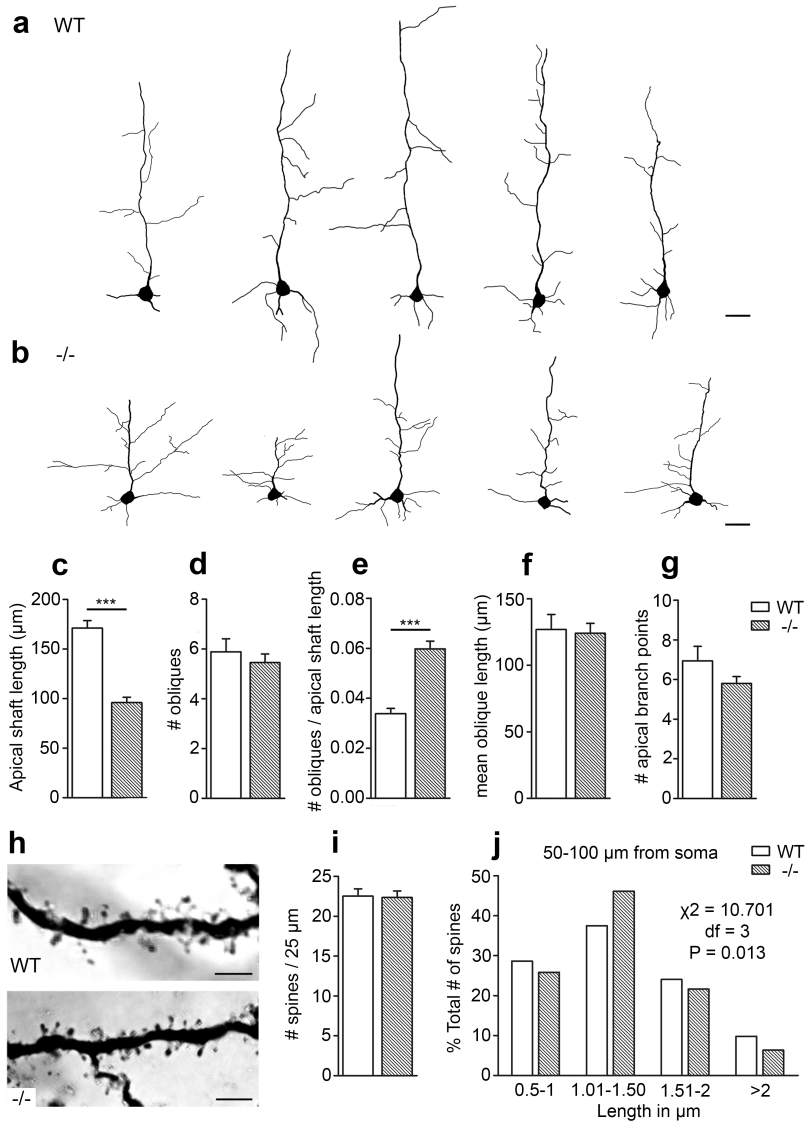

Figure 2.2: Morphological analysis of layer V pyramidal neurons in the visual cortex of WT and MMP-3$^{-/-}$ mice.

a-b) Representative traced pyramidal neurons of WT and MMP-3$^{-/-}$ mice. Scale bars: 20 μm. Morphometric evaluation of the apical shaft length (c), absolute number of obliques (d), relative number of obliques (e), mean oblique length (f) and number of apical branch points (g) evidence a significant shorter apical dendrite and higher density of apical obliques in MMP-3$^{-/-}$ mice. Values in c-g represent mean $\pm$ SEM. Student's t-test: *** $P < 0.001$ (c) and Mann-Whitney-U test *** $P < 0.001$ (e). h) Representative Golgi-cox stained dendritic spines on the apical shaft. Final magnification: 1000x. Scale bars: 5 μm. i) Dendritic spine density is not altered by MMP-3 deficiency. j) Frequency distribution of dendritic spine length measured from 50-100 µm from the soma indicate a higher abundance of shorter spines in MMP-3$^{-/-}$ mice (Chi-square = 10.701, df = 3, P = 0.013).

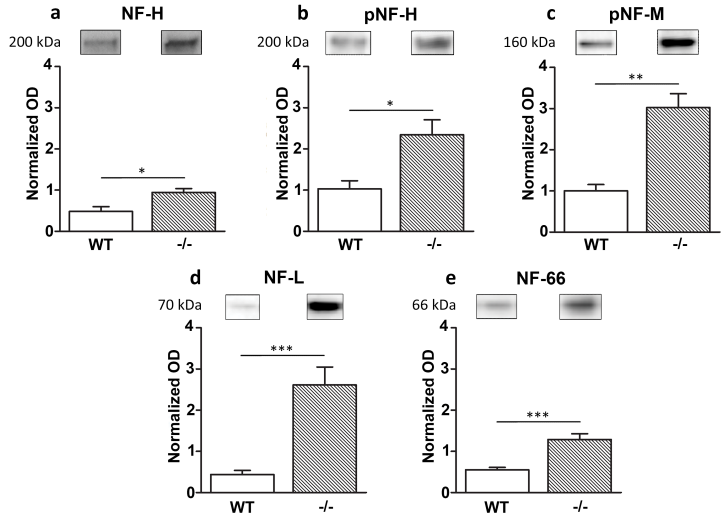

Figure 2.3: Analysis of different neurofilament protein subunit levels in the visual cortex of WT and MMP-3$^{-/-}$ mice.

All analyzed neurofilament protein subunits are significantly upregulated in MMP-3$^{-/-}$ mice: (a) non-phosphorylated neurofilament-high (NF-H), P = 0.026; (b) phosphorylated neurofilament-high (pNF-H), P = 0.011; (c) phosphorylated neurofilament-medium (pNF-M), P = 0.002; (d) neurofilament-low (NF-L), P < 0.001 (e) and α-internexin (NF-66), P < 0.001 with *P < 0.05, **P < 0.01, ***P < 0.001. Above each graph representative bands and their corresponding molecular weight are shown. Values in a-e represent mean ± SEM.

2.3.3 An aberrant visual and cross-modal response to monocular enucleation in MMP-3 deficient mice

In order to assess the response of the visual cortex to ME as a plasticity readout, we performed radioactive in situ hybridization (ISH) for the activity marker gene *zif286*, as a reliable reporter for light-induced neural activity [333, 334, 256]. ME is a useful model to investigate not only open-eye potentiation (unimodal) but also the cross-modal component of visual cortical plasticity in the mouse [334, 256]. Here we applied the same deprivation protocol to WT and MMP-3$^{-/-}$ mice to assess the functional outcome of ME in the context of the drastically altered neuronal architecture in MMP-3$^{-/-}$ mice. To exclude possible intrinsic

effects of MMP-3 deficiency on visually evoked *zif268* expression, we compared the activity profiles of WT control and MMP-3$^{-/-}$ control mice. No significant differences were found between these two conditions (figure 2.4), suggesting MMP-3 deficiency itself has no apparent effect on *zif268* expression in the visual cortex. Furthermore, it is known that variation in the genetic background affects the capacity for ocular dominance (OD) plasticity in mice [135] and normal adult C57Bl/6J mice display an extensive reactivation along the full extent of the visual cortex within seven weeks of ME. Hence, we tested whether the genetic background of the WT mice influenced the reactivation pattern seven weeks post-ME by comparing age-matched WT mice versus seven weeks enucleated littermates (figure 2.5a-b). Only the infragranular layers of the medial monocular zone (Mmz: V1m and V2M) of the enucleated mice (WT 7wME) showed a significant reduction (figure 2.5d Mmz: $P = 0.009$; figure 2.5c Mmz: $P = 0.057$) in *zif268* expression compared to the age-matched controls (WT control). Yet the binocular zone (Bz: V1b and V2Lb) and lateral monocular visual cortex (Lmz: V2Lm) exhibited no difference in *zif268* expression between conditions (figure 2.5c, Bz: $P = 0.715$, Lmz: $P = 0.523$; figure 2.5d, Bz: $P = 0.495$, Lmz: $P = 0.886$). These results are very comparable to previous observations in C57Bl/6J mice [334, 256], ruling out a clear effect of the WT genetic background on ME-induced cortical plasticity.

Next, the *zif268* expression in the visual cortex of WT 7wME was compared to that of MMP-3$^{-/-}$ 7wME to primarily determine the effect of MMP-3 deficiency on cross-modal plasticity (figure 2.6a-b). A massive decrease in *zif268* expression in the two monocular zones across all layers (figure 2.6c, Lmz: $P = 0.012$; Mmz: $P < 0.001$; figure 2.6d, Lmz: $P = 0.003$; Mmz: $P < 0.001$) was observed in MMP-3$^{-/-}$ 7wME mice compared to WT 7wME. The hypoactivity in response to ME was mostly located in monocular driven areas since the relative neural activity remained confined to the Bz (figure 2.6b). The *zif268* expression in the Bz was only significantly different in the infragranular layers (figure 2.6d, Bz: $P = 0.007$) and not in the supragranular layers (figure 2.6c, Bz: $P = 0.072$). Taken together, these results indicate perturbed cross-modal plasticity and open-eye potentiation in the visual cortex of adult MMP-3$^{-/-}$ mice.

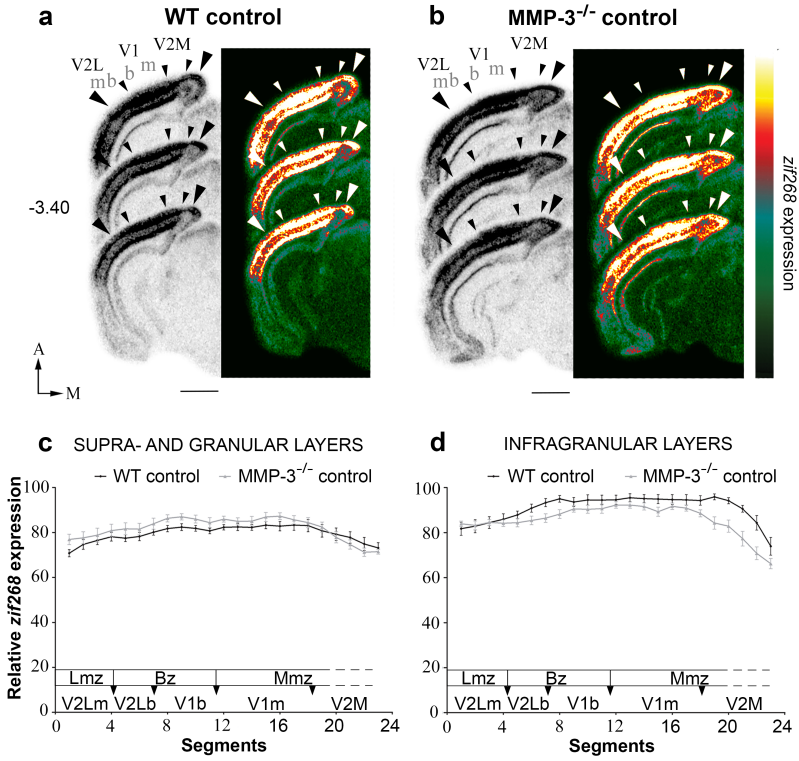

Figure 2.4: *Zif268* expression in the visual cortex of WT and MMP-3$^{-/-}$ mice reveals no significant differences.

For both conditions images of the left visual cortex from three adjacent sections around Bregma level -3.40 mm are shown. The corresponding pseudo-color representations of signal intensity differences are displayed next to each triplet of ISH sections. The medio-lateral extent of the visual cortex is marked by the two large arrowheads and interareal boundaries with smaller arrowheads, as identified in the histologically processed slices (Nissl, see methods). Line graphs (c,d) illustrate the relative *zif268* expression for the upper (LII-LIV) (c) and lower (LV-VI) (d) layers along the five predefined visual subdivisions (black arrowheads, corresponding with the small arrowheads in the images of a and b as measured by the average optical density in each segment, using a custom-made MATLAB script, for WT controls (black lines) and MMP-3$^{-/-}$ controls (gray lines) animals. No significant differences between the subregion-specific activity profiles of WT and MMP-3$^{-/-}$ control levels were found which indicates that MMP-3 deficiency has no overt effects on normal *zif268* expression levels. Error bars represent the SEM of the mean optical density in each segment. Abbreviations: A, anterior; P, posterior; M, medial; L, lateral; V2M, medial extrastriate cortex; V1m, monocular primary visual cortex; V1b, binocular primary visual cortex; V2Lb, binocular lateral extrastriate cortex; V2Lm, monocular lateral extrastriate cortex; Lmz, lateral monocular zone; Bz, binocular zone; Mmz, medial monocular zone; m, monocular; b, binocular; ME, monocular enucleation; w, weeks. Scale bars: 2 mm.

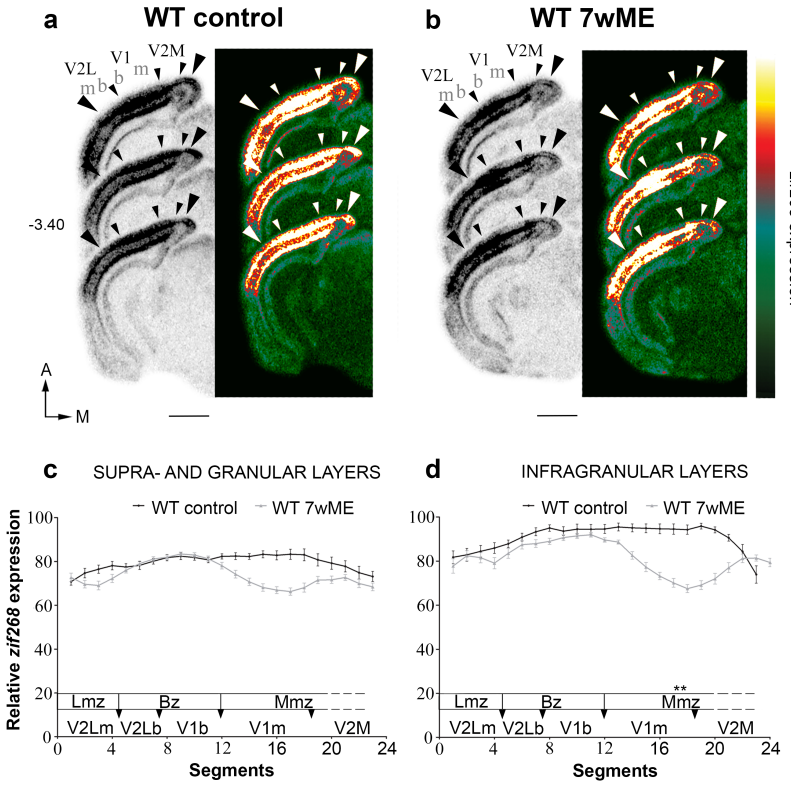

Figure 2.5: *Zif268* expression in the visual cortex of WT control (a) and WT mice enucleated for seven weeks (b) reveals different reactivation patterns.

For both conditions images of the left visual cortex from three adjacent sections around Bregma level -3.40 mm are shown. The corresponding pseudo-color representations of signal intensity differences are displayed next to each triplet of ISH sections. The medio-lateral extent of the visual cortex is marked by the two large arrowheads and interareal boundaries with smaller arrowheads, as identified in the histologically processed slices (Nissl, see methods). Line graphs (c,d) illustrate the relative *zif268* expression for the upper (LII-LIV) (c) and lower (LV-VI) (d) layers along the five predefined visual subdivisions (black arrowheads, corresponding with the small arrowheads in the images of a and b as measured by the average optical density in each segment, using a custom-made MATLAB script, for controls (black lines) and 7wME (gray lines) animals. In WT 7wME the subregion-specific activity profiles do not differ from WT control levels except for the medial monocular zone in the infragranular layer, interpreted as evidence for visual and cross-modal reactivation. Error bars represent the SEM of the mean optical density in each segment. Statistics with *P $<$ 0.05, **P $<$ 0.01, ***P $<$ 0.001. Abbreviations: A, anterior; P, posterior; M, medial; L, lateral; V2M, medial extrastriate cortex; V1m, monocular primary visual cortex; V1b, binocular primary visual cortex; V2Lb, binocular lateral extrastriate cortex; V2Lm, monocular lateral extrastriate cortex; Lmz, lateral monocular zone; Bz, binocular zone; Mmz, medial monocular zone; m, monocular; b, binocular; ME, monocular enucleation; w, weeks. Scale bars: 2 mm.

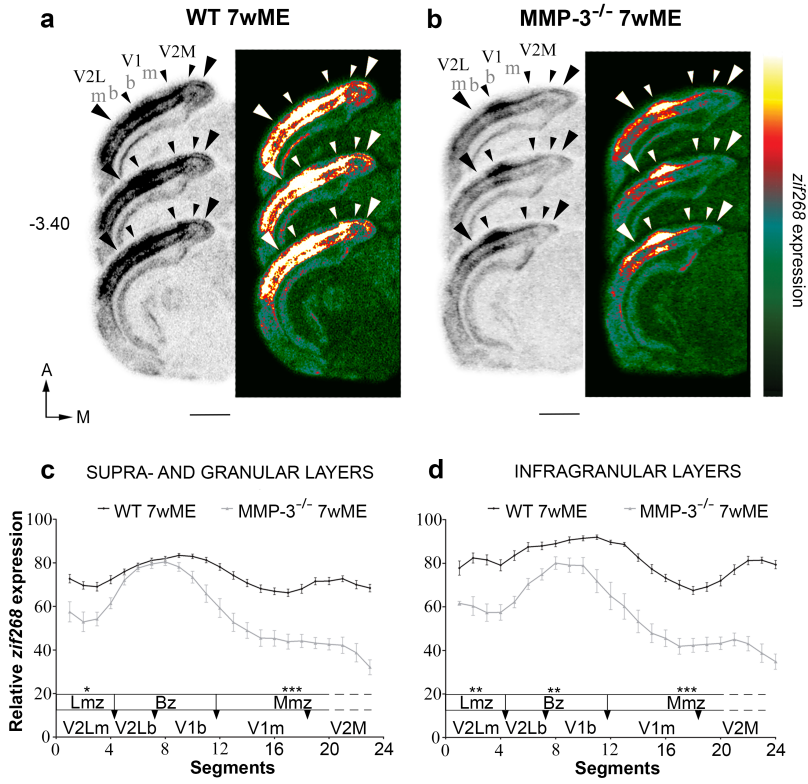

Figure 2.6: *Zif268* expression in the visual cortex of WT (a) and MMP-3$^{-/-}$ (b) mice seven weeks post-enucleation reveals different reactivation patterns.

For both conditions images of the left visual cortex from three adjacent sections around Bregma level -3.40 mm are shown. The corresponding pseudo-color representations of signal intensity differences are displayed next to each triplet of ISH sections. The medio-lateral extent of the visual cortex is marked by the two large arrowheads and interareal boundaries with smaller arrowheads, as identified in the histologically processed slices (Nissl, see methods). Line graphs (c,d) illustrate the relative *zif268* expression for the upper (LII-LIV, c) and lower (LV-VI, d) layers along the predefined visual subdivisions (black arrowheads, corresponding with the small arrowheads in the images of a and b) as measured by the average optical density in each segment, using a custom-made MATLAB script, for WT (black lines) and MMP-3$^{-/-}$ (gray lines) animals. A lack of cross-modal plasticity in MMP-3$^{-/-}$ mice seven weeks post-enucleation is clearly visible as evidenced by the remarkable decrease in *zif268* expression in all monocular driven areas. Open-eye potentiation in these animals seems perturbed since the *zif268* pattern does not expand into V1m and V2Lm. Error bars represent the SEM of the mean optical density in each segment. Statistics with *P $<$ 0.05, **P $<$ 0.01, ***P $<$ 0.001. Abbreviations: A, anterior; P, posterior; M, medial; L, lateral; V2M, medial extrastriate cortex; V1m, monocular primary visual cortex; V1b, binocular primary visual cortex; V2Lb, binocular lateral extrastriate cortex; V2Lm, monocular lateral extrastriate cortex; Lmz, lateral monocular zone; Bz, binocular zone; Mmz, medial monocular zone; m, monocular; b, binocular; ME, monocular enucleation; w, weeks. Scale bars: 2 mm.

2.4 Discussion

2.4.1 Linking MMPs to dendrite arborization

Within this study we demonstrate that genetic inactivation of MMP-3 has profound effects on the structural and functional integrity of the visual cortex in adult mice. In fact, images of Golgi-Cox-stained cortices could be assigned to either originating from WT or MMP-3$^{-/-}$ mice, based on structural appearance. In more detail, layer V pyramidal cells of MMP-3$^{-/-}$ mice displayed significantly shorter apical dendrites and more apical obliques per unit of length, providing one explanation for the truncated translaminar appearance of the Golgi-Cox-stained MMP-3$^{-/-}$ cortex. Consistent with our results, recent work by Van Hove et al. (2011) showed a reduced dendritic tree size of cerebellar Purkinje cells in MMP-3$^{-/-}$ mice compared with WT, both at P12 and P90 [339]. This study clearly revealed that genetic inactivation of MMP-3 has profound effects on brain development with a neuronal phenotype that persists into adulthood.

The exact mechanism by which MMP-3 mediates the abnormal dendritic arborization remains elusive but MMP-dependent activation of neurotrophins provides an attractive mechanism. Several neurotrophins and growth factors such as insulin-like growth factor-1 (IGF-1) are known to not only influence dendritic outgrowth but also to play a role in visual cortex plasticity [213, 251, 197, 212]. They might therefore be suggested as putative MMP-3 targets mediating the observed phenotype. All known mammalian neurotrophins act as major regulatory signals in the lamina-specific development of apical and basal dendrites in the visual cortex of the mouse [213]. Specifically, brain-derived neurotrophic factor (BDNF), a known substrate of MMP-3 [188, 227] regulates the growth and branching of layer V pyramidal cells in the visual cortex [213]. Nerve growth factor has similar effects as BDNF on dendritic arborization and regulates MMP-3 expression [255] and can be activated by MMP-7 [188], itself an *in vitro* substrate of MMP-3 [214].

Other alternative mechanisms might involve MMP mediated integrin [303] and semaphorin signaling [123]. Several MMPs can be linked to integrin-mediated signaling pathways by interaction with ECM molecules [303, 356, 223] and

genetic ablation of integrin-mediated signaling results in post-developmental, progressive retraction of dendritic arbors of layer V pyramidal neurons in the somatosensory and visual cortex of the mouse [233, 225]. On the other hand, a functional link between MMPs and guidance molecules, including semaphorins has previously been established [215]. Specifically, MMP-3 is required for semaphorin-3C-dependent cortical axon outgrowth and is negatively regulated by the axonal growth inhibitory semaphorin-3A [123]. Besides having effect on axons, class 3 semaphorins regulate dendritic growth and branching [249, 104, 157]. Alternatively, MMP-3 may be implicated in sculpting dendritic architecture by regulating the bio-availability of IGF-1 through selective cleavage of IGF-binding protein-3 [109, 227] and IGF-1 is crucial for apical dendritic growth in layer II pyramidal neurons [251].

2.4.2 MMPs regulate dendritic spine development and dynamics

It has been previously established that MMPs are expressed in dendritic spines [180] and are necessary for dendritic spine maturation and actin dynamics by phosphorylation of cofilin through β1-integrin-dependent signaling [80, 356, 56] or by directly cleaving the actin filament-severing protein gelsolin and other cytoskeletal proteins [40, 347]. Indeed, we observed a significant shift in dendritic spine length distribution towards shorter spines in MMP-3$^{-/-}$ mice, indicating a role for this metalloproteinase in spinogenesis and spine maturation. Earlier studies on dendritic spines and MMPs revealed that inhibition of MMPs by minocycline induces spine maturation in cultured hippocampal neurons [25] while in contrast, elevated activity of MMP-7 and MMP-9 increases spine length both in vitro and in vivo respectively [224, 26, 97]. Since MMP-9 can be activated by MMP-3 [258, 214] and MMP-3$^{-/-}$ mice are characterized by a reduced proMMP-9 activation in vivo [160], it is conceivable that a reduced MMP-9 activity is responsible for the observed shift in spine length distribution towards shorter, more mature spines. Whether MMP-3 is an efficient activator of MMP-7 *in vivo* is still a matter of debate [285], making it more difficult to attribute the observed dendritic spine phenotype to a reduced activity

of MMP-7. Also, a recent study by Spolidoro et al. (2012) demonstrated that MMP inhibition prevented the increase in immature spines in the visual cortex of juvenile rats after seven days of monocular deprivation (MD) [309], substantiating MMP-mediated structural plasticity in the visual system.

2.4.3 Neurofilament protein upregulation

The observed aberrant dendritic morphology of MMP-3$^{-/-}$ pyramidal neurons is indicative for abnormal cytoskeletal dynamics. Hence, we wanted to discern the contribution of neurofilament proteins (NF) to this phenotype since they constitute the major components of the neuronal cytoskeleton. Surprisingly, when comparing the NF content in the visual cortex of WT and MMP-3$^{-/-}$ mice, we found a significant upregulation in MMP-3$^{-/-}$ mice for α-internexin (NF-66) and the light (NF-L), medium (NF-M) and heavy (NF-H) subunits, both phosphorylated (p) and non-phosphorylated. All analyzed subunits displayed a different degree of upregulation, ranging from 1.9-fold (NF-H) to 5.9-fold (NF-L), suggesting an overall change in NF subunit stoichiometry in MMP-3$^{-/-}$ mice. A normal NF subunit stoichiometry is essential for proper NF assembly and transport and alterations in stoichiometry have been implicated in several neurodegenerative diseases [159, 174, 316, 184, 15]. Kong et al. (1998) revealed that by transgenic overexpression of different neurofilament subunits, an increased ratio of NF-H and/or NF-M to NF-L inhibited dendritic arborization in spinal motor neurons. An imbalance in the ratio of different NF subunits can alter NF assembly properties and slow down NF transport into neuronal processes which is likely to cause structural changes in dendrites [179, 67, 15]. Additionally, increased phosophorylation of NF-H and NF-M subunits can cause slower NF transport potentially by preventing attachment to molecular motors [67, 63, 15].

2.4.4 Genetic removal of MMP-3 abolishes cross-modal plasticity and perturbs open-eye potentiation

Since the MMP family has recently been implicated in visual cortex plasticity [309], we here probed for cross-modal plasticity in MMP-3$^{-/-}$ mice by means of the long-term monocular enucleation (ME) paradigm [256, 334]. The *zif268* activity profile of WT enucleated mice (WT 7wME, figure 4) revealed a nearly full reactivation along the entire medio-lateral visual cortex thereby resembling *zif268* expression levels in WT control animals with only a slight decrease in activity in the infragranular layer of the medial monocular zone (figure 2.5d). These results are consistent with previous data obtained in adult C57Bl/6J mice [256, 334] and indicate that the different genetic background of our WT mice compared to C57Bl/6J has a negligible effect on the cortical plasticity phenomena studied here [135]. In contrast, the lack of cross-modal reactivation in adult MMP-3$^{-/-}$ mice 7wME (figure 2.6) is most likely a result of the truncated translaminar organization described above. Since pyramidal neurons in the visual cortex are essential for intra-areal and inter-areal information processing [311, 83, 155], the dendritic phenotype observed in MMP-3$^{-/-}$ likely disrupts the intra-areal and inherently the cortico-cortical framework necessary for cross-modal plasticity [256, 334, 268]. Besides the apparent absence of cross-modal plasticity, open-eye potentiation seemed perturbed as well. Indeed, the *zif268* pattern remained confined to the binocular zone and did not expand into the monocular regions as expected based on previous publications [64, 165, 101, 256]. Furthermore, the permanently decreased *zif268* expression in the infragranular layer of the binocular zone also supports this interpretation of an altered open-eye potentiation. General MMP inhibition was recently reported to selectively prevent the potentiation of the open-eye after 7 days of MD in the visual cortex of juvenile rats [309]. This experience-dependent potentiation is necessary for a complete OD shift [111, 300] and ME induces robust OD plasticity driven by the remaining eye [64, 165]. Considerable molecular data has been obtained from classic MD experiments. In that regard, it is established that several neurotrophins, which are substrates of MMPs, modulate the outcome of MD [197, 202, 29] where administration of NGF or BDNF disrupts OD plasticity [197]. Moreover, BDNF is critically involved in the induction of long-term potentiation

(LTP) in dendrites and spines [182]. Although MMP-3 is necessary for activation of these neurotrophins, genetic inactivation of MMP-3 likely induces complex degradomic cascades [266, 38] including compensatory upregulation of other redundant MMPs that can activate these neurotrophins [97, 95]. Furthermore, it is known that MMP-9, a putative downstream target of MMP-3 is necessary to maintain LTP and is upregulated by synaptic activity [360, 152, 247]. Classic OD plasticity cannot be explained solely by homosynaptic mechanisms [139, 16]. Homeostatic plasticity has been suggested to also play a role [164, 72, 236]. Accordingly, tumor necrosis factor-α (TNF-α) deficient mice lack the open-eye response typical for MD which has been attributed to perturbed homeostatic synaptic scaling [164]. Pro-TNF-α is activated by several MMPs, including MMP-3 [116, 314] so the lack of MMP-3 can therefore perturb the response of the remaining eye possibly via TNF-α. However, general MMP-inhibition did not alter homeostatic plasticity in the primary visual cortex of juvenile rats following seven days of MD [309]. Taken together, it is conceivable that lack of MMP-3 and the resulting degradome disrupts this experience-dependent potentiation process, contributing to the observed phenotype.

2.4.5 Conclusions

Genetic inactivation of MMP-3 clearly has profound effects on the structural and functional integrity of the visual cortex of adult mice. MMP-3 is necessary to constitute a normal phenotype of layer V pyramidal neurons since genetic ablation of this enzyme severely impacts apical dendritic length, branching and spine length. Additionally, we revealed an aberrant cortical plasticity phenotype characterized by a perturbed open-eye potentiation and lack of cross-modally driven reactivation. Most likely this is the result from the apparent truncated translaminar cortical organization that disrupts the intra-areal and cortico-cortical communication needed for experience-dependent plasticity in combination with the perturbed set of MMP-3 substrates. To our knowledge, this is the first study that reports NF protein upregulation in an MMP deficiency model. Further experiments are needed to elucidate whether or not MMPs can directly interact with NF proteins to modulate cytoskeletal dynamics and which molecular mediators constitute the observed phenotype.

Chapter 3

Altered expression of collapsin response mediator protein-5 and autophagosomes in the visual cortex of MMP-3 deficient mice

3.1 Introduction

As highlighted in the previous chapter, MMP-3 deficient (MMP-3$^{-/-}$) mice displayed a truncated neuronal architecture characterized by a reduction in apical dendritic length and dendritic spine length of layer V pyramidal neurons in the visual cortex (chapter 2) [3]. However, the molecular and cellular mechanisms mediating this cortical phenotype are still unclear. A functional proteomics approach of the visual cortex of wildtype (WT) and MMP-3$^{-/-}$ mice revealed a differential set of proteins that hinted to an altered expression of collapsin response mediator proteins (CRMPs) and proteins related to mitochondrial dynamics (appendix figure A.1 and table A.1). To investigate this, we focused on the analysis of all known CRMPs with a special attention to CRMP-5 which recently has been implicated in regulating mitochondrial function through mitophagy [35]. In addition, we examined mitochondrial fusion and fission proteins conveyed by the proteomics study.

Besides the generation of ATP, mitochondria are involved in reactive oxygen species (ROS) metabolism, calcium signaling and apoptosis [49]. They are mainly located in and transported to axons and the dendritic shaft and are associated with dendritic spines during development and plasticity [192, 43, 280, 49, 201]. Mitochondria maintain their health by continuously undergoing fission and fusion [74, 201]. Two key proteins, dynamin-related protein 1 (Drp1) and fission protein 1 (Fis1) mediate mitochondrial fission, whereas mitofusins (Mfn-1 and Mfn-2) and Optic Atrophy-1 (OPA-1) mediate mitochondrial fusion [74]. Many processes, including dendritic growth and branching, spinogenesis and neuroplasticity depend on proper mitochondrial dynamics and function [192, 49, 35].

CRMPs (for alternative names see appendix table A.2) are a family of five cytosolic phosphoproteins that were orginally identified as intracellular mediators of semaphorin signaling [44, 301]. However, recent evidence shows that CRMPs are involved in multiple cellular events, including microtubule polymerization, actin bundling and endocytosis leading to dendritic/axonal growth and neuronal differentiation [36, 11, 372, 364]. All CRMPs are highly expressed during development and their expression is downregulated in adulthood [44]. However,

in the cortex of adult mice CRMP-1, CRMP-2B and CRMP-5 are still detectable in the dendrite and soma of pyramidal neurons [32]. CRMP-5 has been specifically implicated in the regulation of dendritic outgrowth by modulating the growth promoting function of CRMP-2 [36]. CRMP-5 can be localized to dendritic mitochondria to induce mitophagy, linking CRMPs to mitochondrial dynamics [35]. Mitophagy or the degradation of mitochondria, is initiated through sequestering mitochondria in spherical membrane structures called autophagosomes. Autophagosomes in turn fuse with lysosomes to continue the degradation process. Formation of autophagosomes is regulated by microtubule-associated protein 1 light chain 3 (LC3) [322, 70, 388] and conversion of cytosolic LC3-I to phosphatidylethanolamine-conjugated LC3-II is indicative for the early formation of autophagosomes since LC3-II inserts into the autophagosome membrane [322, 35].

In this study we revealed a significant upregulation of CRMP-5 in the visual cortex of MMP-3$^{-/-}$ mice compared with WT using Western analysis, whereas the expression levels of other CRMPs (1-4) did not differ. CRMP-5 immunoreactivity was mainly localized in the soma and apical dendrites in in layer II/III and V of the visual cortex, both in MMP-3$^{-/-}$ and WT mice. In addition, a significant upregulation of LC3-II was observed in MMP-3$^{-/-}$ mice suggesting an accumulation of autophagosomes. Finally, no differences were detected in the expression levels of mitochondrial fusion and fission proteins Mfn-2 and Drp1 between both conditions, suggesting that a normal mitochondrial fusion and fission balance is present in MMP-3$^{-/-}$ mice.

3.2 Material and methods

3.2.1 Animals

All experiments were performed in adult (120 days old) MMP-3 wildtype (WT) and deficient (MMP-$3^{-/-}$) mice with a similar genetic background (50% Bl6 x 25% B10 x 25% RIII) (Mudgett, Merck Labs) which were housed under standard laboratory conditions under an 11/13h dark/light cycle with food and water available ad libitum. All experiments have been approved by the Ethical Committee of the university and were in strict accordance with the European Communities Council Directive of 22 September 2010 (2010/63/EU) and with the Belgian legislation (KB of 29 May 2013). Every possible effort was made to minimize animal suffering and to reduce the number of animals.

3.2.2 Western Blotting

For each mouse (WT: n = 6, MMP-$3^{-/-}$: n = 6) the visual cortex was collected from 100 μm-thick coronal cryosections spanning Bregma levels -2.00 to -4.60. Proteins were extracted with a lysis buffer (CRMPs: 7M urea, 2M thiourea, 4% CHAPS, 1% DTT, 40 mM Tris, and complete protease inhibitor cocktail (Roche Diagnostics Ltd, Mannheim, Germany); LC3-II, Mfn-2 and Drp1: RIPA buffer). and the samples were sonicated and heated for 5 minutes at 70 °C. Next, the samples were centrifuged (10000 x g) for 5 minutes at 4 °C. The supernatant was isolated and the total protein concentration was determined by means of a QubitTM fluorometer (Invitrogen, Merelbeke, Belgium). Samples were stored at -80 °C. For immunodetection of CRMP-1 to -5 equal amounts of protein (CRMP-1, -5: 10 μg, CRMP-2, -3: 15 μg, CRMP-4: 20 μg, LC3-II: 15 μg, Mfn-2, Drp1: 10 μg) were loaded onto 4-12% Bis-Tris Midi gels (Criterion XT, Bio-Rad Laboratories, USA) and transferred to a nitrocellulose (CRMPs) or PVDF (LC3B, Mfn-2 and Drp1) membrane. The choice of membrane was empirically determined based on signal-to-noise ratio. Overnight incubation with anti-CRMP-1 (1:4000, ab62709, Abcam), anti-CRMP-2 (1:10000, gift from Dr. Y. Ihara [127], C4G), anti-CRMP-3 (1:10000, ab128875, Abcam),

anti-CRMP-4 (1:10000, AB5454, Millipore), anti-CRMP-5 (1:5000, ab3620, Abcam), anti-LC3B (1:1000, 2775, Cell Signaling), anti-Mfn-2 (1:1000, M6319, Sigma) and anti-Drp1 (1:2000, ab123599, Abcam) was followed by 30 minutes incubation with HRP-labeled secondary antibodies (1:50000, Dako, Denmark). The immunoreactive bands were visualized using a luminol-based enhanced chemiluminescent kit (SuperSignal West Dura, Thermo Scientific, USA). In order to correct for inter-gel variability and to normalize the concentration of the specific detected proteins to the total amount of protein present, we performed a total protein stain (TPS) prior to immunodetection with LavaPurple (Gelcompany, USA) according to manufacturer's instructions. After the staining, dry blots were scanned with a ChemiDocTM MP Imaging System (Bio-Rad Laboratories, USA). The protein bands were semi-quantitatively evaluated by densitometry (Image Lab 4.1, Bio-Rad Laboratories, USA). First, to account for inter-gel variability including loading differences, incomplete transfer or position on the blot, a TPS was employed rather than the use of a single reference protein [6, 146]. For each protein of interest, the optical density value per mouse was normalized to its corresponding TPS. Also, to compare samples between different gels, normalized data were expressed relative to the reference sample, i.e. a pool of all samples.

3.2.3 Immunohistochemistry

WT (n = 3) and MMP-3$^{-/-}$ (n = 3) mice received an intraperitoneal injection of sodium pentobarbital (Nembutal, 600 mg/kg, Ceva Sante Animale) before being perfused transcardially with 1% paraformaldehyde (PFA, Sigma-Aldrich, St. Louis, MO) in 0.15M phosphate-buffered saline (PBS, pH 7.42) at 37 °C. Brains were dissected and post-fixated in 4% PFA in PBS overnight after which they were cut on a vibratome (Leica VT1000S, Leica Microsystems GmbH, Wetzlar, Germany) into 50 μm-thick coronal sections. An indirect labeling with signal amplification was used to visualize CRMP-5 in brain sections. Free-floating sections were incubated with a 0.3% H_2O_2 in Tris-buffered saline (TBS; 0.01M Tris, 0.9% NaCl, 0.3% Triton-X 100, pH 7.6). After pre-incubation with Pre Immune Goat serum (1:5 for 45 min), the sections were incubated overnight with the primary CRMP-5 antibody (1:500, ab3620, Abcam). The following day,

detection was performed using a biotinylated rabbit anti-goat immunoglobulin G (1:200, 30 min, Dako, Glostrup, Denmark) and an avidin-biotin-horseradish peroxidase solution (Vectastain Elite ABC, Vector Laboratories, Burlingame, CA). All incubations and rinses (3x10 min) were performed in TBS. The sections were immunostained using the glucose oxidase-diaminobenzidine-nickel method resulting in a black staining [306, 336]. Finally, the sections were mounted on gelatine-coated slides, air dried, dehydrated, cleared with xylene, coverslipped and viewed under a Zeiss Axio-Imager equipped with a Zeiss Axiocam (Carl Zeiss Benelux). Images were taken with the ZEN software (Carl Zeiss Benelux).

3.2.4 Statistics

All Western blot data are presented as mean ± SEM. A normal distribution was verified using the Kolmogorov–Smirnov test and parallel equal variance between groups was tested. If the test requirements were fulfilled, an unpaired Student's t-test for pairwise comparison was used (*P $<$ 0.05, **P $<$ 0.01, ***P $<$ 0.001). When criteria for this parametrical test were not fulfilled, a Mann-Whitney U rank sum test for pairwise comparison of independent samples was applied (*P $<$ 0.05, **P $<$ 0.01, ***P $<$ 0.001). Statistical analyses were performed using SigmaStat 3.1 (SYSTAT software).

3.3 Results

3.3.1 Upregulation of CRMP-5 in the visual cortex of MMP-3 deficient mice

In order to assess a possible link between the observed MMP-3$^{-/-}$ dendritic phenotype and CRMP expression levels, we conducted a Western analysis for all five CRMPs. Only CRMP-5 was significantly upregulated ($P = 0.006$) in the visual cortex of MMP-3$^{-/-}$ mice compared with WT, whereas the protein levels of CRMP-1,-2,-3 and -4 did not differ (figure 3.1a-e) (CRMP-1: $P = 0.445$; CRMP-2: $P = 0.102$; CRMP-3: $P = 0.508$; CRMP-4: $P = 0.839$). No apparent differences were observed in the cortical distribution of CRMP-5 when comparing the CRMP-5 stained visual cortex of MMP-3$^{-/-}$ mice with WT. CRMP-5 was predominantly located in the cell soma and dendrites in V1 with the highest expression in layers II/III and a distinct expression in layer V (figure 3.2).

3.3.2 Autophagosome accumulation and mitochondrial dynamics in MMP-3 deficient mice

A recent study by Brot et al. (2013) indicated that CRMP-5 induces mitophagy to regulate mitochondria levels at the dendrite [35]. Initial stages of mitophagy encompass the formation of autophagosomes around mitochondria that later fuse with lysosomes. To examine a possible contribution of autophagosomes to the MMP-3$^{-/-}$ phenotype, we measured the expression level of the lipidated form of LC3, LC3-II since it initiates autophagy by insertion into autophagosomes. Western analysis revealed a significant upregulation ($P = 0.004$) of a 15 kDa band corresponding to LC3-II (figure 3.3a). A vague band at 18 kDa corresponding to LC3-I was nearly undetectable in both conditions and was therefore not analyzed.

A recent 2-D DIGE study on the visual cortex of MMP-3$^{-/-}$ and WT mice revealed several differential proteins associated with mitochondrial function and dynamics. Therefore, we measured the expression levels of the mitochondrial

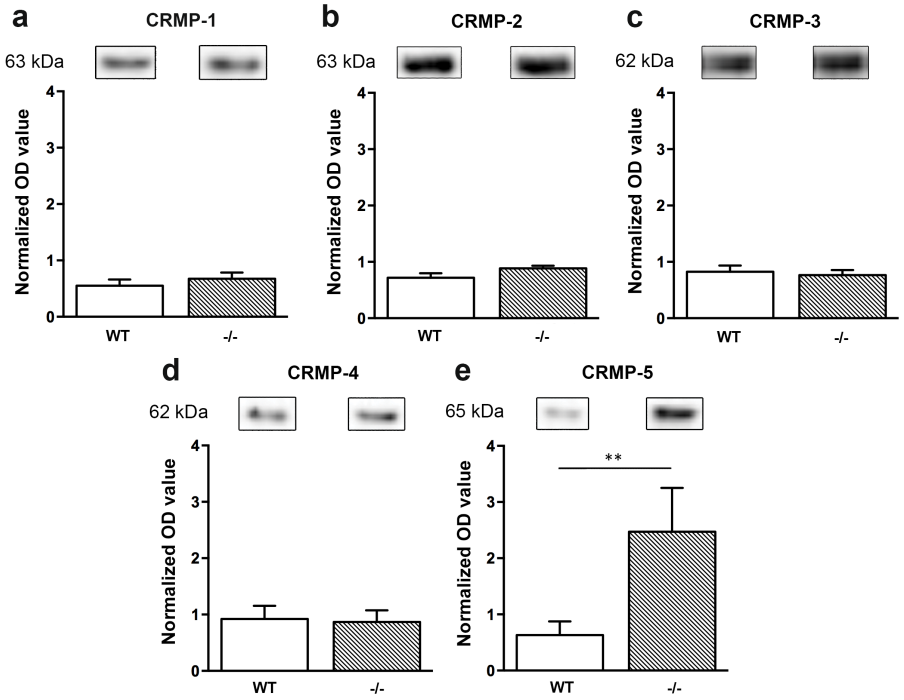

Figure 3.1: CRMP expression levels in the visual cortex of wildtype and MMP-3 deficient mice.

Expression levels of CRMP-1, -2, -3 and -4 did not differ in the adult visual cortex of wildtype (WT) compared with MMP-3 deficient (-/-) mice (a-d). However, CRMP-5 was upregulated in the visual cortex of MMP-$3^{-/-}$ mice compared with WT with **P < 0.01. Above each graph representative bands and their corresponding molecular weight are shown. Values in a-d represent mean $\pm$ SEM.

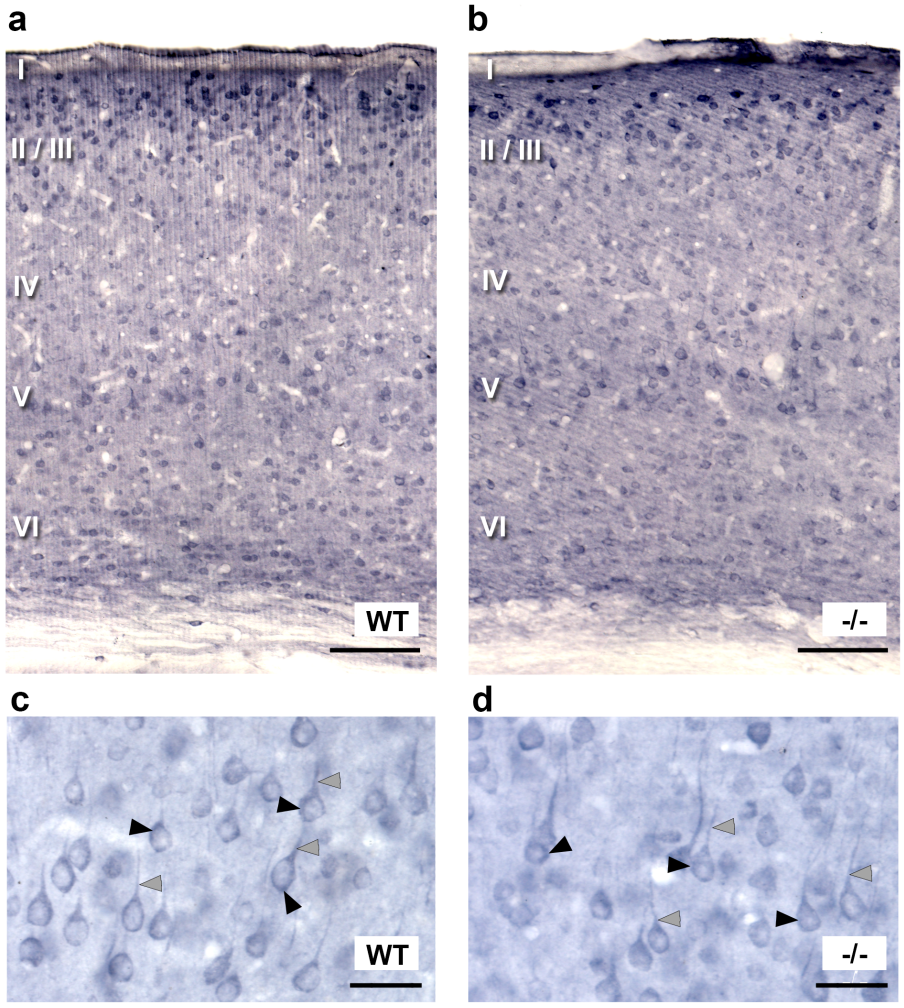

Figure 3.2: CRMP-5 immunoreactivity in the visual cortex of wildtype and MMP-3 deficient mice.

In both wildtype (WT) and MMP-3 deficient mice (-/-) CRMP-5 is predominantly located in layers II/III and V (a,b). No apparent difference in cellular localization was found when comparing layer V neurons in V1 of WT and MMP-$3^{-/-}$ mice (c,d) since in both conditions CRMP-5 could be detected in the soma (black arrowheads) and the apical dendrite (gray arrowheads). Scalebars in a,b: 50 μm. Scalebars in c,d: 20 μm.

fusion and fission proteins mitofusin-2 (Mfn-2) and dynamin-related protein 1 (Drp1) (figure 3.3b,c). The expression level of fusion protein Mfn-2 and fission protein Drp1 did not differ between MMP-3$^{-/-}$ and WT mice (Mfn-2: P = 0.238; Drp1: P = 0.326), suggesting that MMP-3 deficiency does not lead to defects in mitochondrial fusion and fission dynamics.

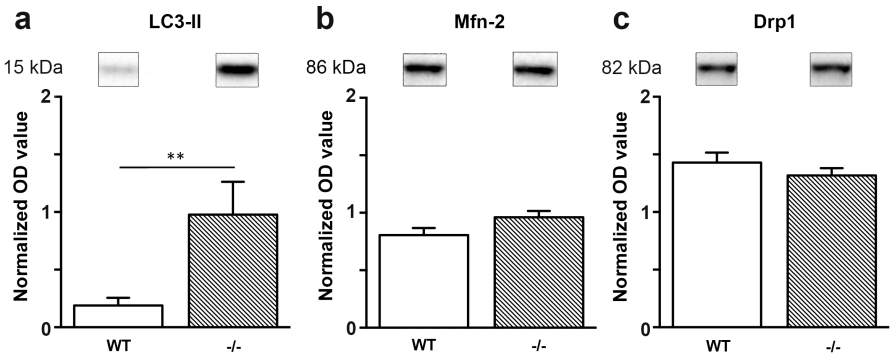

Figure 3.3: Expression levels of LC3-II, Mfn-2 and Drp1 in the visual cortex of wildtype and MMP-3 deficient mice.

The expression level of the autophagy marker LC3-II was significantly upregulated in MMP-3$^{-/-}$ mice compared with WT (**P $<$ 0.01) (a), indicating that MMP-3 deficiency leads to an increase in autophagosome generation. Expression levels of the mitochondrial fusion protein Mfn-2 and fission protein Drp1 did not differ between both conditions (b,c), suggesting a stable balance between fusion and fission dynamics in MMP-3$^{-/-}$ mice. Above each graph representative bands and their corresponding molecular weight are shown. Values in a-c represent mean ± SEM.

3.4 Discussion

The previous chapter highlighted the abnormal dendritic architecture of layer V pyramidal neurons in the visual cortex of MMP-3$^{-/-}$ mice, characterized by a reduction in apical dendritic length and spine length (chapter 2) [3]. To better understand this phenotype on a molecular level we focused on the family of collapsin response mediator proteins, autophagy and mitochondrial dynamics.

3.4.1 Upregulation of CRMP-5 as a potential cause of the MMP-3 deficient dendritic phenotype

Western analysis of all five CRMPs revealed an upregulation of CRMP-5 in the visual cortex of MMP-3$^{-/-}$ mice compared with WT, whereas the levels of other CRMPs did not differ (figure 3.1). Interestingly, CRMP-5 is necessary to specifically suppress dendritic outgrowth during development by inhibiting tubulin polymerization and counteracting the growth-promoting effects of CRMP-2, with CRMP-5 being the dominant signal [36, 37]. In agreement with our data, immunohistochemical localization of CRMP-5 has been previously reported in the soma and apical dendrites in the cortex of adult mice, whereas axons only express CRMP-5 at embryonic stages [32] (figure 3.2c,d). The same study indicated that CRMP-5 expression was mainly located in layer V pyramidal cells in the adult cortex, whereas we observed the highest expression in layers II/III (figure 3.2a,b). Although this could be in part the result of different specificities of the antibodies used in both studies. Taken together, both the involvement of CRMP-5 in dendritic outgrowth and the localization of CRMP-5 in pyramidal neurons provides a reasonable explanation for the truncated dendritic phenotype observed in MMP-3$^{-/-}$ mice [3].

It should be noted that the expression of several CRMPs, including CRMP-5 is downregulated during development [44] and the exact function of CRMPs in the adult brain remains elusive [291, 32]. Several studies indicate that CRMPs are also involved in spine maturation, synaptic plasticity and maintenance of neuronal circuits [34, 358, 373, 372] and CRMP-2 is a known substrate of MMP-9 [13]. Importantly, it is known that CRMP-5 is able to form heterooligomers with

other CRMPs , except CRMP-1 [113]. As a result, an upregulation of CRMP-5 could alter the function of these hetero-CRMP complexes. Interestingly, CRMP-5 and other CRMPs can modulate semaphorin 3A (Sema3A) signaling, both in development and the adult brain [291, 144]. Sema3A serves as a chemoattractant for the apical dendrites of cortical pyramidal neurons [278] and regulates the expression and activity of MMP-3 in the cortex [123], providing a possible link between CRMP-5 and MMP-3. Similarly, in the cerebellum of CRMP-5$^{-/-}$ mice the diameter of primary dendrites of Purkinje cells is decreased [373] and MMP-3$^{-/-}$ mice display a reduced Purkinje cell dendritic tree size [339], indicating that both CRMP-5 and MMP-3 are involved in the development and maintance of Purkinje cells. In summary, CRMP-5 can be put forward as a putative, underlying mediator of the altered dendritic architecture and cortical plasticity observed in MMP-3$^{-/-}$ mice [3].

3.4.2 MMP-3 deficiency elevates autophagosome generation but does not alter mitochondrial fusion and fission dynamics

A recent study by Sebastien Brot and colleagues indicated that CRMP-5 is located in mitochondria in vivo and regulates mitophagy by recruiting lysosomes at the mitochondrial level, thereby reducing the number of mitochondria in dendrites [35]. The initial stage of mitochondrial degeneration is the formation of autophagosomes [379] and is characterized by the conversion of LC3-I to the lipidated form LC3-II which inserts in the autophagosome membrane [322, 70, 35]. To examine whether CRMP-5 overexpression in MMP-3$^{-/-}$ mice can potentially mediate autophagosomal content, we performed Western analysis on LC3. MMP-3$^{-/-}$ mice displayed a signifcant upregulation of LC3-II in the visual cortex compared with WT (figure 3.3), indicative for autophagosome accumulation and mitophagy initiation. In accordance with these results, Brot et al. showed that overexpression of CRMP-5 in hippocampal neurons leads to an upregulation of LC3-II [35]. However, based on our data we can not conclude that this increase in LC3-II translates to increased autophagy because we did not measure the entire dynamic process of autophagy termed the

autophagic flux [229, 388]. LC3-II is located at the outer and inner membrane of the autophagosome and can be partially degraded when autophagosomes fuse with lysosomes. If LC3-II still increases after adding lysosomal inhibitors to the sample, this would indicate an enhancement of autophagic flux [229]. Measuring the relative abundance of LC3-II alone serves as an indicator for the amount of autophagosomes in the sample and provides a first indication to an increase in autophagy [229]. It is still possible however that the autophagosome accumulation is a result of autophagic inhibition by for example blockage of autophagosome-lysosome fusion [322, 176, 388]. It would be interesting to additionally examine the levels of lysosomal markers and evaluate the number of mitochondria by means of immunohistochemistry or electron microscopy to establish a definitive role for increased mitophagy in MMP-3$^{-/-}$ mice. We did not observe clear immunoreactivity for LC3-I in our Western analysis although the antibody used in this study has been extensively used for measuring both LC3-I and LC3-II in rodent brain samples [191, 91, 35, 320, 190]. This discrepancy might be explained by a differences in sample preparation methods combined with the antibody's preference to LC3-II [229].

We observed no differences in expression levels of mitochondrial fusion and fission proteins Mfn-2 and Drp1, indicating that a normal balance between fusion and fission is retained in MMP-3$^{-/-}$ mice. In accordance to this study, overexpressing CRMP-5 in hippocampal neurons did not have any effect on Drp1 levels [35], although the process of autophagy is linked to mitochondrial fusion and fission [379]. However, we did not evaluate the levels of other fusion and fission proteins such as Mfn-1, OPA1 and Fis1 which also regulate mitochondrial dynamics in concert with Mfn-2 and Drp1 [201].

3.4.3 Conclusions

This study evidences that genetic inactivation of MMP-3 has significant effects on the expression level of CRMP-5, whereas the cortical distribution of this phosphoprotein does not change apparently compared with WT mice. The observed overexpression of CRMP-5 provides a potential basis for the observed dendritic phenotype in MMP-3$^{-/-}$ mice. However, since we only studied CRMP

expression in the adult cortex, other processes may be at play related to the elusive role of CRMP-5 in the adult brain. Changes in LC3-II expression also hint towards a role for autophagy which could provide a framework for the cortical phenotype of MMP-3$^{-/-}$ mice by dysregulation of mitochondrial dynamics. In any case, further experiments are needed to establish a definitive role for autophagy and mitophagy in these knockout mice.

Chapter 4

Monocular enucleation affects the expression of specific MMPs in an age-dependent manner

4.1 Introduction

Matrix metalloproteinases (MMPs) constitute a family of Zn^{2+}-dependent endopeptidases that can be considered as key nodal components of a complex protease web [295]. In addition to the implication of MMPs in various CNS pathologies, MMPs have a beneficial role in shaping neural connections and modulating structural and functional plasticity [97, 227, 225]. For example, inhibition of MMP-3 and MMP-9 in the hippocampus of rats abolished spatial learning in a Morris water maze task by impairing long-term potentiation (LTP) [216, 368]. Recently, Spolidoro et al. (2012) uncovered a role for MMPs in ocular dominance plasticity in the visual cortex of monocular deprived juvenile rats. Infusion of a broad-spectrum MMP inhibitor prevented both the potentiation of the open-eye response and the concomitant increase in spine density on layer II-III pyramidal neurons after MD, indicating a role for MMPs in regulating structural and functional plasticity in the visual system [309]. As highlighted in the previous chapter, adult MMP-3 deficient (MMP-$3^{-/-}$) mice displayed an impaired monocular enucleation (ME)-induced open-eye potentiation and cross-modal plasticity in the visual cortex (chapter 2) [3]. Earlier work in adult P120 C57Bl/6J mice provided evidence for an extensive reactivation of the visual cortex within seven weeks post-ME [334, 256]. This reactivation was driven by an initial open-eye potentiation followed by cross-modally driven plasticity in the medial an lateral monocular zones starting from adjacent non-visual cortices around three weeks post-ME [334]. However, P45 C57Bl/6J mice subjected to the ME paradigm displayed a lack of cross-modal plasticity seven weeks post-ME, indicating that the potential for ME-induced cross-modal plasticity in the visual cortex is age-dependent in C57Bl/6J mice [256]. In relation to the data presented in chapter 2 and the fact that the cross-modal plasticity response of MMP-$3^{-/-}$ mice resembles that of P45 mice (figure 1.4) [256], MMP-3 can be put forward as a potential candidate for regulating the age-dependent component of cortical plasticity. Therefore, in this study we evaluated the expression level of MMP-3 using Western analysis in the medial monocular zone and binocular zone of both P45 and P120 ME mice to unravel a potential role of this enzyme in cross-modal plasticity and open-eye potentiation. In the same conditions we examined the levels of MMP-2 and MMP-9 using a combination

of Western analysis and gelatin zymography. Finally, we attempted to optimize a fluorescent assay to measure the activity of MMP-3 in homogenized brain samples.

4.2 Material and methods

4.2.1 Animals

All experiments were performed in C57Bl/6J mice obtained from Janvier Elevage (Le Genest-St-Isle, France), which were housed under standard laboratory conditions under an 11/13h dark/light cycle with food and water available ad libitum. All experiments have been approved by the Ethical Committee of the university and were in strict accordance with the European Communities Council Directive of 22 September 2010 (2010/63/EU) and with the Belgian legislation (KB of 29 May 2013). Every possible effort was made to minimize animal suffering and to reduce the number of animals.

4.2.2 Monocular enucleation

Monocular enucleation of the mice (n = 3 / condition) was performed as previously described [2, 256, 333]. Briefly, under anesthesia by intraperitoneal injection of a mixture of ketamine hydrochloride (75 mg/kg, Dechra Veterinary Products, Eurovet) and medetomidine hydrochloride (1 mg/kg, Orion Corporation, Janssen Animal Health), the right eye was carefully removed and if needed, the orbit was filled with hemostatic cotton wool (Qualiphar, Bornem, Belgium). After injection with atipamezol hydrochloride (1 mg/kg, Orion Corporation, Elanco Animal Health) to reverse anesthesia, the animals were allowed to recover on a heating pad. They were all administered 0.05 ml of antibiotics (Kefzol, 1 g Natrii cefazolin and 15 mg Lidocaini hydrochloridum anhydricum in 4 ml 0.9% NaCl, Eurocept Pharmaceuticals) intramuscularly to prevent post-surgical infections. After the enucleation procedure, mice were again housed under the same normal light conditions in standard cages for a survival period of one, three or seven weeks. Prior to sacrifice, the animals underwent an overnight dark-exposure followed by 45 min of bright light.

4.2.3 Western Blotting

The expression profiles of different MMPs was examined in the visual cortex of P45 and P120 mice one, three and seven weeks post-ME. To assess the MMP expression before manipulation we included samples of P45 and P120 mice without ME. For each mouse (n = 3 / condition) the monocular and binocular visual cortex was collected from 100 μm-thick coronal cryosections spanning Bregma levels -2.00 to -4.60. Proteins were extracted in a modified RIPA buffer (50 mM Tris HCl, 300 mM NaCl, 0,5 % Triton, 0,5 % sodium deoxycholate, 0,1 % SDS, pH 7.8) and the samples were sonicated and heated for 5 minutes at 70 °C. Next, the samples were centrifuged (10000 x g) for 5 minutes at 4 °C. The supernatant was isolated and the total protein concentration was determined by means of a BCA protein assay kit (Pierce, Thermo Scientific). Samples were stored at -80 °C. For immunodetection of MMP-2 and MMP-3 equal amounts of protein (10 μg) were loaded onto 4-12% Bis-Tris Midi gels (Criterion XT, Bio-Rad Laboratories, USA) and transferred to a polyvinylidene fluoride (PVDF) (MMP-3) or nitrocellulose (MMP-2) membrane. The choice of membrane was empirically determined based on signal-to-noise ratio. Overnight incubation with anti-MMP-2 (1:100, sc-8835-R, Santa Cruz) and anti-MMP-3 (1:100, ab52915, Abcam) was followed by 30 minutes incubation with HRP-labeled secondary antibodies (1:50000, Dako, Denmark). All antibodies were previously validated in other tissues and with recombinant MMPs as positive controls (for MMP-3 specifically see [338]). We also tested different anti-MMP-9 antibodies, without succes: 1:500-1:5000; ab137867, ab104686 and ab38898 (Abcam), AB19016 (Millipore) and two antibodies made in the lab of Prof. dr. G. Opdenakker (KU Leuven). The immunoreactive bands were visualized using a luminol-based enhanced chemiluminescent kit (SuperSignal West Dura, Thermo Scientific, USA). In order to correct for inter-gel variability and to normalize the concentration of the specific detected proteins to the total amount of protein present, we performed a total protein stain (TPS) prior to immunodetection with LavaPurple (Gelcompany, USA) according to manufacturer's instructions. After the staining, dry blots were scanned with a ChemiDocTM MP Imaging System (Bio-Rad Laboratories, USA). The protein bands were semi-quantitatively evaluated by densitometry (Image Lab 4.1,

Bio-Rad Laboratories, USA). First, to account for inter-gel variability including loading differences, incomplete transfer or position on the blot, a TPS was employed rather than the use of a single reference protein [6, 146]. For each protein of interest, the optical density value per mouse was normalized to its corresponding TPS. Also, to compare samples between different gels, normalized data were expressed relative to the reference sample, i.e. a pool of all samples.

4.2.4 MMP-3 activity assay

To asses the age-dependent effect of ME on MMP-3 activity in the visual cortex we measured the MMP-3 activity levels in adolescent (P45) and adult (P120) mice at three, five and seven weeks post-ME. For each group we included age-matched controls to allow a correct interpretation of the data. For each mouse (n = 3 / condition) the complete visual cortex was collected from 100 μm-thick coronal cryosections spanning Bregma levels -2.00 to -4.60. Proteins were extracted in a TCNB buffer (50 mM Tris, 10 mM $CaCl_2$, 150 mM NaCl, 0.05 % Brij-35, 1 % Triton X-100, pH 6.5 and EDTA-free protease inhibitor cocktail (Roche Diagnostics Ltd, Mannheim, Germany)) and the samples were centrifuged (10000 x g) for 15 minutes at 4 °C. The supernatant was isolated and the total protein concentration was determined by means of a BCA protein assay kit (Pierce, Thermo Scientific). Samples were stored at -80 °C.

The proteolytic activity of MMP-3 was assessed fluorometrically using a 5-FAM/QXL520 fluorescence resonance energy transfer (FRET) peptide (60580, Anaspec, San Jose, CA) according to a modified protocol adapted from Candelario-Jalil et al. 2011 [39]. We applied two different approaches to optimize the protocol for measuring MMP-3 activity in mouse brain tissue, focusing on the use of different protein A/G beads for immunocapturing MMP-3 (figure 4.1). To immunoprecipitate MMP-3 from the samples, 2 μg/ml of a monoclonal rabbit anti-MMP-3 antibody (ab52915, Abcam) was incubated with 20 μl protein A/G agarose beads (sc-2003, Santa Cruz Biotechnology) or magnetic beads (88802, Thermo Scientific). This mixture was added to 500 μg sample and incubated overnight at 4 °C while gently rocking. Samples were centrifuged at 1000 x g for 5 minutes at 4°C and supernatant was discarded. The

pellet containing the agarose beads was resuspended in TCNB buffer and was added onto a Ultra-free MC filtertop (UFC30GV00, Millipore) in an eppendorf tube to specifically isolate the beads. Next, the samples were centrifuged at 1000 g for 2 minutes at 4°C and the fluid in the eppendorf tube was discarded. The filtertop was turned upside down and 100 μl assay buffer (50 mM Tris, 10 mM $CaCl_2$, 200 mM NaCl, 20 mM $ZnSO_4$, 0.05 % Brij-35, pH 6.5) was added before centrifugation (1000 g for 2 minutes at 4°C). When performing immunoprecipitation using the magnetic beads, the antibody-bead complex was pulled down with a magnet and supernatans was discarded. Additional washing steps were performed with TCNB buffer and in the final step assay buffer was added. For both the agarose and magnetic beads procedure, all samples were incubated with the FRET peptide in a 96-well plate at 37 °C with gentle rocking. Every well contained a pool of three mice samples of the same condition and every well was made in duplicate. Fluorescence was measured every hour at 37 °C with 485ex/538em using a Flexstation II microplate reader (Molecular Devices) every hour for eight hours. A substrate control was added and this fluorescent value was subtracted from the fluorescent values of the samples to obtain relative fluorescence units (RFU). To examine the effect of beads on the fluorescent signal we included a control with agarose beads or magnetic beads and FRET substrate in assay buffer.

4.2.5 Gelatin zymography

Samples (n = 4 / condition) were collected and processed identically to the samples for the MMP-3 activity assay with the TCNB buffer put to pH 7.6. Samples of the medial monocular visual cortex of each mouse of the same condition were pooled together to perform a pilot study and 90μg of each pooled sample was first prepurified by gelatin-Sepharose affinity chromatography (described in detail in [73]). Next, the proteins were separated in 7.5% polyacrylamide gels to which 0.1% gelatin (Sigma-Aldrich, St Louis, MO, USA) was added and copolymerized. After electrophoresis, the gels were washed with Triton-X 100 to remove sodium dodecyl sulfate and incubated for the development of zymolytic bands. The gels were stained with Coomassie brilliant blue R-250 (Sigma-Aldrich, St Louis, MO, USA). For this pilot study we included

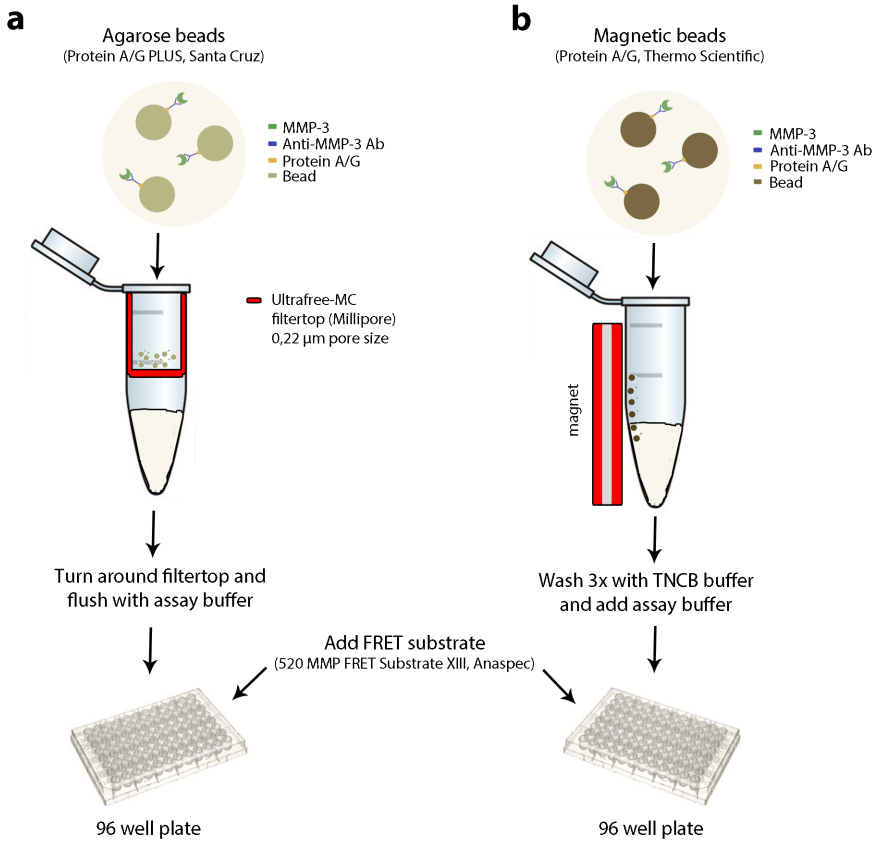

Figure 4.1: Schematic overview of the MMP-3 enzymatic activity assay.
Brain samples were either incubated with protein A/G agarose (a) or magnetic (b) beads coupled to anti-MMP-3. A filtertop was used to purify the agarose beads whereas the magnetic beads were pulled down using a magnet. The beads were then transferred to a 96-well plate and a FRET substrate was added to quantify the proteolytic activity of MMP-3.

recombinant MMP-9 and pools of the following conditions: P45 and P120 mice one, three and seven weeks post-ME. The zymography procedure was conducted by the lab of Prof. dr. G. Opdenakker (KU Leuven).

4.2.6 Statistics

All Western blot data are presented as mean ± SEM. A normal distribution was verified using the Kolmogorov–Smirnov test and parallel equal variance between groups was tested. If the test requirements were fulfilled, an unpaired Student's t-test for pairwise comparison was used (*P $<$ 0.05, **P $<$ 0.01, ***P $<$ 0.001). When criteria for this parametrical test were not fulfilled, a Mann-Whitney U rank sum test for pairwise comparison of independent samples was applied (*P $<$ 0.05, **P $<$ 0.01, ***P $<$ 0.001). Statistical analyses were performed using SigmaStat 3.1 (SYSTAT software).

4.3 Results

4.3.1 Age-dependent effect of monoculear enucleation on MMP-3 expression levels

To differentiate between MMP-3 expression involved in ME-induced cross-modal plasticity and open-eye potentiation, we analyzed the medial monocular zone (Mmz) and the binocular zone (Bz) of the visual cortex respectively, using Western analysis in P45 and P120 mice. Expression levels of MMP-3 showed significant differences across post-ME survival times and age (figure 4.2). In the Mmz of P45 control mice proMMP-3 was significantly higher expressed compared with P120 controls ($P = 0.004$, figure 4.2a), indicating that age itself has an influence on the total amount of proMMP-3 present in the visual cortex. In P45 mice one week post-ME proMMP-3 is downregulated ($P = 0.017$) and returns to control levels following three ($P = 0.119$) and seven weeks ($P = 0.969$) ME. Interestingly, in the Mmz of P120 mice no fluctuations in proMMP-3 expression levels was observed in relation to post-ME survival time (figure 4.2a). In the Bz the proform of MMP-3 remains downregulated up to seven weeks post-ME compared to control (3wME: $P = 0.010$; 7wME: $P = 0.004$) in P45 mice whereas in P120 mice the expression level is significantly higher at seven weeks post-ME compared with three weeks ($P = 0.009$) (figure 4.2b). Taken together, proMMP-3 levels in both the Mmz and Bz are differentially regulated post-ME in an age-dependent manner with the largest modulation observed in P45 mice. This suggests that MMP-3 may contribute to limiting the potential for cross-modal plasticity in the visual cortex. Importantly, we did not detect the active form of MMP-3 in our samples.

4.3.2 Optimization of an enzymatic activity assay for MMP-3

Since only the proform of MMP-3 was detected using Western analysis, efforts were taken to optimize a fluorescent activity assay to measure the net MMP-3 activity in P45 and P120 ME samples. We therefore adapted an existing protocol from Candelario-Jalil et al. (2011) [39] to optimize it for measuring MMP-3

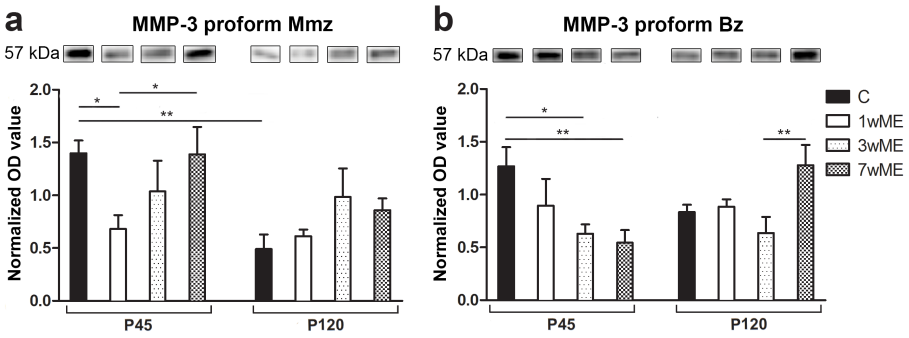

Figure 4.2: Age-dependent expression levels of MMP-3 in the medial monocular and binocular zone after enculeation.

ProMMP-3 expression levels differ in function of age and post-ME survival time, both in the medial monocular zone (Mmz) (a) and binocular zone (Bz) (b) with *P $<$ 0.05, **P $<$ 0.01, ***P $<$ 0.001. Above each graph representative bands and their corresponding molecular weight are shown. Values in a-b represent mean ± SEM. Abbreviations: C, control; ME, monocular enucleation; OD, optical density; w, week.

in brain tissue. We incubated the MMP-3 antibody with the protein A/G beads before applying this complex to the homogenized sample (figure 4.1). In addition, two different approaches to immunocapture MMP-3 from homogenized visual cortex samples were tested to reassure the specificity of measuring MMP-3 proteolytic activity with a FRET peptide. One approach utilized protein A/G agarose beads and the other encompassed the use of protein A/G magnetic beads to bind an MMP-3 antibody to capture the enzyme in the samples (figure 4.1). Since the agarose beads resuspend easily after centrifugation, we opted for the use of a filtertop as described in figure 4.1. We first tested which type of beads resulted in the best signal to noise ratio in the proposed assay. When comparing the baseline fluorescence of the FRET substrate incubated with and without antibody-bearing beads, only incubation with magnetic beads resulted in a decreased signal (figure 4.3a). In addition, samples immunoprecipitated with either agarose or magnetic protein A/G beads resulted in a higher signal in agarose beads than the magnetic beads condition (figure 4.3b). These results clearly indicate that using magnetic beads influences the readout of the assay and therefore we continued to only use the agarose beads for immunocapturing MMP-3 (figure 4.1a).

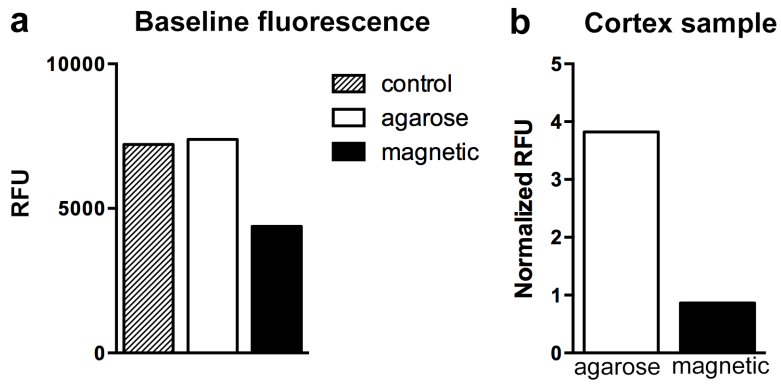

Figure 4.3: Optimization of MMP-3 immunoprecipitation from mouse brain samples. Baseline fluorescence was measured after 4h incubation in a control containing only assay buffer and FRET substrate, a condition with agarose beads and substrate and a condition with magnetic beads and substrate (a). MMP-3 from visual cortex samples was immunoprecipitated with either agarose or magnetic beads and the concomitant RFU was normalized to a substrate control (b). Both graphs (a-b) show a decrease in fluorescent signal when using magnetic beads, indicating that these beads influence the fluorescent readout of the assay. Abbreviations: RFU, relative fluorescence units.

To assess the age-dependent effect of ME on the proteolytic activity of MMP-3 in the visual cortex we compared samples of P45 and P120 old mice seven weeks (w) post-ME including age-matched controls (AMC) and P45 and P120 MMP-3$^{-/-}$ controls. The MMP-3$^{-/-}$ samples served as an age-dependent baseline for MMP activity, since the immunoprecipitation of MMP-3 was never expected to be 100% pure and small traces of other proteases in the sample would be detected with this sensitive assay. However, the RFU values of the MMP-3$^{-/-}$ control samples were in the same range as the C57Bl/6J samples, indicating that this assay was not able to obtain representative MMP-3 activity levels in the tested brain samples.

4.3.3 MMP-2 expression and gelatinolytic activity in the visual cortex after monocular enucleation

In addition to MMP-3, we wanted to focus on MMP-2 and MMP-9 since these MMPs are the most widely studied and the function of MMP-9 in synaptic plasticity is well established. To study the gelatinases we used a combination of Western analysis and the gelatin zymography for the detection of gelatinase activity. In the Western analysis for MMP-2 none of the conditions revealed differences in expression level (figure 4.4a-d). This indicates that MMP-2 protein expression does not alter in an age-dependent manner after monocular enucleation and suggest that this enzyme does not actively mediate age-dependent cortical plasticity. Of note, no suitable antibody for MMP-9 to perform Western analysis was available.

To assess differences in age-dependent ME-induced gelatinolytic activity, we conducted a pilot study on samples of the Mmz and pooled the mice for each condition. In none of the conditions tested we were able to detect any amount of MMP-9 activity, whereas MMP-2 activity was clearly visible (figure 4.5). No apparent differences in MMP-2 activity levels were observed between P45 and P120 samples or the examined post-ME survival times, similar to what was found in the Western analysis.

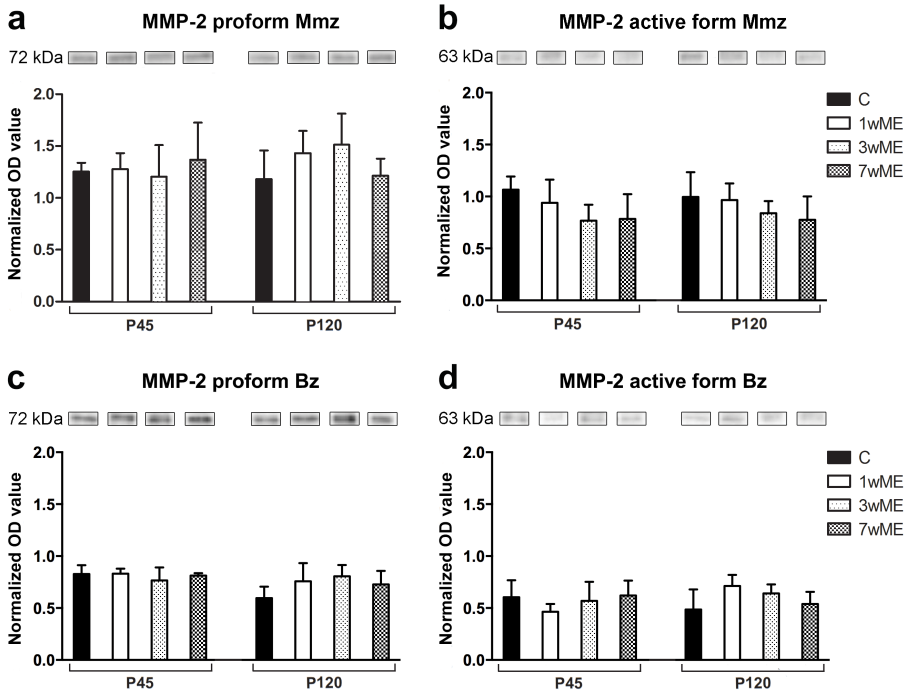

Figure 4.4: Age-dependent expression levels of MMP-2 in the medial monocular and binocular zone after enculeation.

Both the expression levels of the proform and active form in the medial monocular zone (Mmz) (a-b) did not differ significantly after enucleation in P45 and P120 mice. This was also the case in the binocular zone (Bz) (c-d), together indicating that MMP-2 may not play a role in age-dependent ME-induced cortical plasticity. Above each graph representative bands and their corresponding molecular weight are shown. Values in a-d represent mean ± SEM. Abbreviations: C, control; ME, monocular enucleation; OD, optical density.

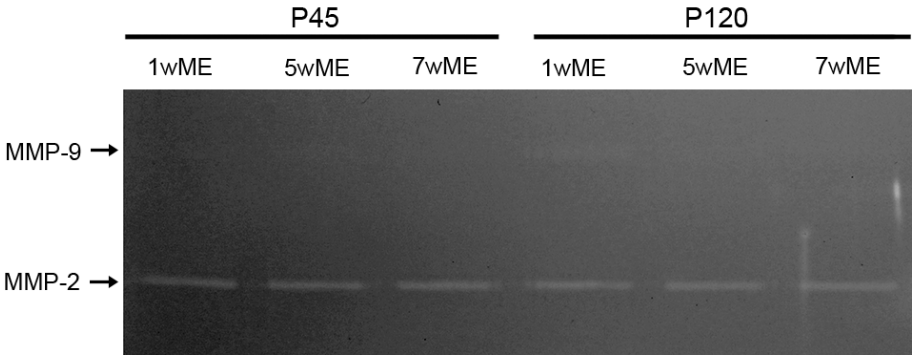

Figure 4.5: Zymogram with MMP-2 and MMP-9 activity in pooled samples of medial monocular visual cortex after enucleation.

No apparent differences in zymolytic activity corresponding to MMP-2 is detected between different post-ME survival times in P45 and P120 mice. No distinct bands corresponding to MMP-9 activity are discernible, suggesting that proteolytic activity of MMP-9 in the medial monocular zone of visual cortex is below the detectable threshold. Abbreviations: ME, monocular enucleation; w, week.

4.4 Discussion

4.4.1 Optimization of a fluorescent assay for measuring MMP-3 activity

In this study we tested a protocol to measure the activity of MMP-3 in mouse visual cortex samples. To accomplish this we modified an existing protocol from Candelario-Jalil et al. (2011) [39]. In this original protocol, the researchers incubated the samples with MMP-3 antibody before adding protein A/G beads. However, MMP-3 is capable of cleaving the Fc-fragment of human and mouse immunoglobulin G (IgG) antibody isotypes [117] rendering the anti-MMP-3 antibody unable to bind to the protein A/G beads. The MMP-3 antibody used in this study is a rabbit IgG which contains a similar MMP-3 cleavage site. In an attempt to prevent cleavage of the antibody prior to binding protein A/G beads, we therefore incubated the antibody with the beads before immunocapturing the enzyme in the samples. To ensure proper purification of the MMP-3 bearing antibody-coupled beads we tested both agarose and magnetic protein A/G beads (figure 4.1). We consistently observed lower RFU values when measuring MMP-3 proteolytic activity using the magnetic beads (figure 4.3). One reason could be that there is a difference in IgG binding capacity between the two types of beads resulting in a different amount of enzyme being immunoprecipitated. However, the magnetic beads have a binding capacity of 55 μg to 85 μg IgG per mg beads which is in the range of high capacity agarose beads and therefore a difference in binding capacity can not account for the consistent lower RFU values measured when using magnetic beads. A possible explanation for the observed difference in RFU values is that magnetic beads consist partially of magnetite which is able to absorb light with a wavelength around 485 nm, used to excite the FRET substrate [321]. A solution to this problem would be to use a near-infrared (NIR) FRET substrate to minimize the light absorption of the magnetite-containing magnetic beads. Several studies report the development of NIR FRET substrates for MMPs [119, 242] but to our knowledge no such substrate specifically targeting MMP-3 is commercially available. Therefore we opted to use agarose protein A/G beads combined with filtertops to specifically isolate the beads from the sample (figure 4.1a). Applying this strategy to measure the

MMP-3 activity in the visual cortex of P45 and P120 mice after monocular enucleation (ME) revealed a considerable amount of proteolytic activity in the included MMP-3$^{-/-}$ control samples, indicating that the assay is not specific for MMP-3. This could be the result of aspecific binding of proteins, including other MMPs or proteases to antibody and/or beads, sometimes referred to as the *bead proteome* [329]. One way to resolve this is to pre-clean the samples by first introducing beads coupled to a non-target antibody to remove all proteins that bind aspecifically to the antibody-bead complex. Finally, the FRET substrate used in this study has only been tested against MMP-1, -2, -3 and -9 and is herein specific for MMP-3 [244]. However, it is still possible that other MMPs or proteases in the bead proteome can cleave this substrate, resulting in the observed signal in the MMP-3$^{-/-}$ control mice.

4.4.2 MMP expression profiles are differentially regulated upon ME

To assess whether MMPs are involved in regulating ME-induced age-dependent cortical plasticity we examined the levels of MMP-2 and MMP-3 using Western analysis and performed gel zymography to assess the activity potential of MMP-2 and MMP-9. Expression levels of proMMP-3 did fluctuate significantly according to age and post-ME survival time, especially in P45 mice and both in the Mmz and Bz (figure 4.2a-b), suggesting that this enzyme is potentially involved in ME-induced cortical plasticity. Western analysis revealed no differences in expression level of pro- and active MMP-2 in all conditions tested (figure 4.4a-d) and this was also apparent in the gelatin zymography study (figure 4.5). Finally, we were not able to detect levels of MMP-9 using gelatin zymography (figure 4.5).

ME-induced cortical plasticity is thought to rely on axonal sprouting and structural and functional changes in synaptic contacts, rather than inducing gross changes to dendritic arbors. As a similar type of sensory manipulation, removal of whiskers in adult mice induced axonal sprouting and an increase in spine density on layer V pyramidal neurons in the spared barrel concomitant with a reduction in spine density in layer II/III pyramids in the deprived barrel [181].

In that regard, MMPs are known to regulate cytoskeletal dynamics underlying neurite growth and spine dynamics and several intracellular substrates of MMPs constitute cytoskeletal proteins [224, 338, 40]. Moreover, a recent study by Spolidoro et al. (2012) revealed that broad-spectrum inhibition of MMPs in the binocular zone of juvenile rats specifically prevents the open-eye potentiation and the increase in filopodia-like spines on basal dendrites of layer II/III pyramidal neurons after seven days of MD [309]. Together with a large body of evidence obtained in the hippocampus, MMPs have an established role as modulators of the structural and functional properties of dendritic spines [224, 247, 102, 361, 252, 325, 26] which makes them ideal candidates to modulate the ME-induced open-eye potentiation and cortico-cortical networks for cross-modal plasticity.

Accumulating evidence suggests that recalibration of the excitation-inhibition balance is responsible for regulating plasticity in the visual cortex [130, 136, 22, 100, 165, 140, 139, 212]. Interestingly, recent work in our lab revealed that 7wME of both P45 and P120 mice induced an upregulation of inhibitory markers such as GAD65/67 but only P45 mice displayed an additional increase in $GABA_AR\alpha1$ levels in the medial monocular zone (Nys et al., submitted). Recent immunohistochemical analysis of MMP-3 in the barrel cortex displayed a punctate pattern with puncta primarily located at the cell soma of pyramidal neurons, suggesting that MMP-3 is possibly associated with GABAergic synapses (personal communication with dr. G. Wiera, lab of prof. J. W. Mozrzymas). Perisomatic inhibition of pyramidal neurons is carried out by parvalbumin-positive fast-spiking interneurons which are surrounded by perineuronal nets (PNN) (figure 4.6) [7, 139]. Main components of PNN are the chondroitin sulphate proteoglycans which are known substrates of several MMPs, especially MMP-3 [239, 237]. Although we do not have information about the expression of active MMP-3, the age-dependent differences in proMMP-3 expression levels could represent changes in PNN structure which in turn modulates inhibitory transmission in cortico-cortical networks involved in ME-induced cross-modal plasticity. In that regard it would be interesting to assess the structure of PNN in both control and enucleated P45 and P120 mice. Furthermore, a high degree of structural plasticity reflected by dendritic branch tip remodeling

and spine dynamics of GABAergic interneurons in the visual cortex has been shown to occur across the lifespan and contributes to adult plasticity following sensory deprivation [189, 47, 169]. MMPs could in this case also modulate GABAergic signaling through modulation of the cytoskeleton or regulation of GABA receptor clustering.

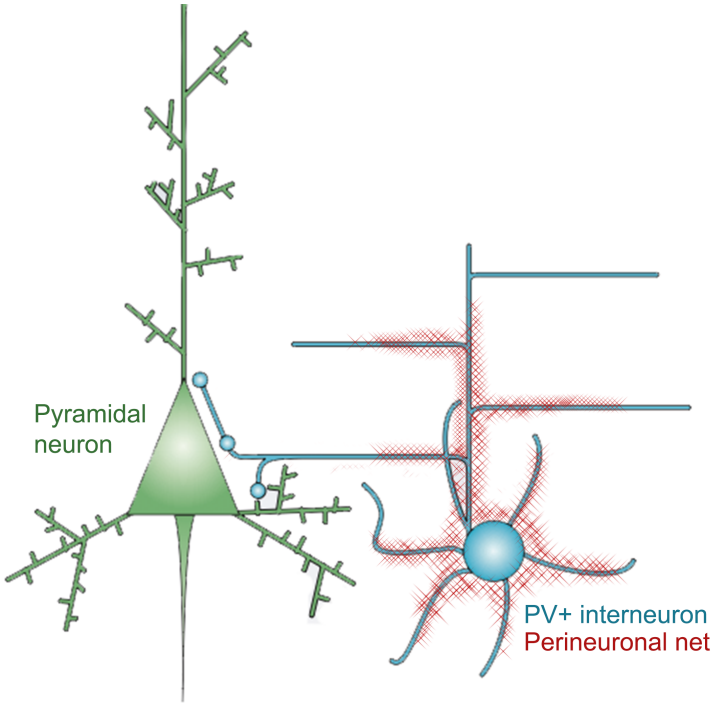

Figure 4.6: Schematic representation of perisomatic inhibtion by parvalbumin-positive interneurons.

Fast-spiking, parvalbumin-immunoreactive interneurons regulate perisomatic inhibition on pyramidal neurons and are ensheated by lattice-like structures called perineuronal nets. Perineuronal nets ensure the proper functioning of inhibitory interneurons and limit structural and functional plasticity in the visual cortex. Adapted from [139].

In this study we did not find any differences in expression levels or zymolytic activity of MMP-2 after ME in the visual cortex of both P45 and P120, suggesting that MMP-2 is not involved in regulating ME-induced cortical plasticity. The present evidence for the involvement of MMP-2 in synaptic

plasticity is circumstantial. This gelatinase cleaves similar substrates as MMP-9 involved in synaptic plasticty and spine morphology, for example ICAM-5, β-dystroglycan and several actin-related proteins [40, 344]. Moreover, MMP-2 deficient mice are impaired in their short-term working memory [228], but in contrast to MMP-9, direct functional evidence for MMP-2 in plasticity is still lacking [344]. In contrast to our study, MMP-9 was readily detectable using gelatin zymography in the barrel cortex of adult mice. One week after removal of the whiskers, MMP-2 and MMP-9 zymolytic activity was increased [163]. In the developing and adult rat visual cortex MMP-2 and MMP-9 were detectable using both in situ and gel zymography [317]. A possible explanation for the lack of MMP-9 zymolytic activity in this study is the sample preparation. During sectioning of the tissue, the brain sections inevitably have to thaw before storage at -80 °C which could influence enzyme stability. In addition, to collect all brains and sections, samples were stored for two to three months at -80 °C before proceeding with the lysis. Plasma samples stored for three months at -80 °C show a 40% reduction in MMP-9 activity [297] which could partly explain why we are not able to detect any zymolytic bands in our analysis. However, it is possible that ME does not induce upregulation of MMP-9 activity above the detection threshold because the subset of MMPs that alter their expression after injury depends on the nature of the injury itself [377]. Because we did not include control samples in the pilot study, it is also possible that MMP-9 is downregulated upon ME. In addition, the peak of MMP-9 activity could also be achieved before the first measured time point of 1wME or between 1wME and 5wME and analyzing zymolytic activity at earlier and intermediate time points could resolve this issue. Of note, other MMPs could also play a role. For example, MMP-7 is able to alter the structural and functional properties of dendritic spines [26, 319].

Based on the changes observed in the levels of MMP-3, which mainly occur in P45 mice, it could be that MMP-3 is necessary to inhibit the cortico-cortical processes that govern cross-modal plasticity. However, it is very difficult to interpret the obtained results for MMP-3 to unravel a possible function of this enzyme in age-dependent ME-induced cortical plasticity, for two reasons: 1) we could only detect the proform of MMP-3 which makes assumptions about

MMP-3 activity unreliable and 2) we did not include age-matched controls in the Western analyses. Age-matched controls are necessary to correctly interpret the ME-induced changes in MMP expression level and to distinguish these changes from normal age-dependent fluctuations in MMP expression [86, 19, 332]. The latter is partly reflected in the higher proMMP-3 expression in P45 compared with P120 control mice. Important to note is that we did not provide a causal link between MMP expression and regulation of ME-induced cross-modal plasticity. However, these results could serve as a basis for future experiments wherein MMPs can be activated or inhibited at key time-points to modulate the outcome of these age-dependent cross-modal plasticity processes in the visual cortex.

4.4.3 Conclusions

This study illustrates that the levels of proMMP-3 in the visual cortex are significantly altered upon ME in an age-dependent manner whereas MMP-2 expression does not differ and MMP-9 is seemingly undetectable. However, measuring in vivo levels of MMP activity remains challenging as proven by the attempted optimization of a fluorescent MMP-3 activity assay which did not meet the expected reproducibility. The obtained results could serve as a guide for future experiments focused on the targeted inhibition and/or activation of MMPs in the visual cortex to uncover a causal relationship between MMP activity and age-dependent ME-induced cortical plasticity.

Chapter 5

General discussion and future perspectives

5.1 Concluding remarks on the study of MMP-3 deficient mice

Chapter 2 and 3 of this manuscript revealed a striking cortical phenotype of MMP-3 deficient (MMP-$3^{-/-}$) mice which is characterized by a truncated dendritic architecture of layer V pyramidal neurons in the visual cortex. A reduced length of the apical dendrite was accompanied by a reduced length of dendritic spines on the apical shaft. Moreover, the number of apical obliques was comparable to that of wildtype (WT) mice meaning that, in combination with the reduced length of the apical dendrite, layer V pyramidal neurons of MMP-$3^{-/-}$ mice appeared to be more branched. On a molecular level the visual cortex of MMP-$3^{-/-}$ mice was characterized by an upregulation of different neurofilament protein subunits, collapsin response mediator protein-5 (CRMP-5) and the phosphatidylethanolamine-conjugated form of microtubule-associated protein 1 light chain 3 (LC3-II) which together suggest alterations in cytoskeletal dynamics, mitochondrial dynamics and autophagy.

An important remark to interpret the results described in this dissertation is that studying a gene-knockout mouse in the adult stage primarily informs one about the response of a complex organism to the loss of a gene product, rather than answering questions about the acute in vivo function of that gene product. This is especially true for multi-functional proteolytic enzymes such as MMPs, since the loss of one MMP generates gross changes in a complex degradome which can alter numerous individual and interconnected pathways known as the protease web [81, 295]. MMPs are key nodal components in this protease web which renders the interpretation of MMP gene-knockout mice very difficult [295]. Unraveling a structural, functional and molecular phenotype of MMP deficient mice can provide valuable insights into specific mechanistic properties of the protease web. Indeed, the extreme structural phenotype in the visual cortex of MMP-3$^{-/-}$ enables us to learn more about pyramidal neuron morphology in relation to cortical processing and plasticity.

5.2 Effects of MMP-3 deficiency: from molecules to cortical processing

5.2.1 CRMP-5 and autophagosome dysregulation at the origin of the dendritic phenotype?

To unite the molecular findings and the structural abnormalities in the cortex of MMP-3$^{-/-}$ mice, a hypothetical molecular framework is summarized in figure 5.1. The framework can be divided in two alternative pathways based on the yet unknown interpretation of the elevation in LC3-II levels: an increase in autophagy (1) or a perturbed autophagosome clearance (2) (decreased autophagy). As discussed in chapter 3 this can be resolved by determining the autophagic flux [229]. For the time being, both possible outcomes can explain certain aspects of the observed phenotype. The autophagy-dependent pathway (1) has largely been described in chapter 3 and is based on the fact that CRMP-5 upregulation in primary cortical neurons inhibits dendrite outgrowth through the upregulation of LC3-II and initiation of subsequent mitophagy [35]. In

addition, CRMP-5 is known to inhibit microtubule polymerization [36] through which it can affect organelle transport and docking [201]. Together, this would result in a decrease in the number of mitochondria in the apical dendrite and spines which explains the observed reduction in apical dendritic length and spine length of layer V pyramidal neurons in the visual cortex of MMP-3$^{-/-}$ mice (figure 5.1).

Important to note is that the function of CRMPs is mainly determined by their phosphorylation state, for example CRMP-2 can only bind to tubulin to promote tubulin polymerization when it is dephosphorylated [372, 37], whereas CRMP-5 needs to be phosphorylated to properly bind to tubulin to inhibit polymerization [37]. In this way, phophorylation by enzymes such as GSK3β, Cdk5 and Rho/ROCK-kinase can elegantly regulate the function of different CRMPs in one location [37, 44, 372]. In this study we did not differentiate between the phosphorylation state of CRMPs and therefore it is possible that the observed upregulation of CRMP-5 does not result in an elevated inhibition of microtubule polymerization. In addition, Western analysis revealed no differences in the total level of the other CRMPs but a shift in phosphorylation state can change their function. This line of reasoning also can also explain why CRMP-2 and CRMP-3 are differentially expressed in the 2-D DIGE study and do not differ in expression levels when measured through Western analysis. Finally, it is known that CRMPs form hetero-oligomers which alters their function [352, 113, 273] and therefore an upregulation of CRMP-5 can impact the function of other CRMPs. CRMP-5 preferentially forms oligmers with CRMP-2, -3 and -4 and only weakly interacts with CRMP-1 [113].

Another explanation for the observed MMP-3$^{-/-}$ phenotype is a defective autophagic flux caused by for example improper fusion between autophagosomes and lysosomes or impaired lysosomal activity (figure 5.1, pathway 2) [229, 176]. Defective autophagosome clearance could explain the accumulation of NF protein subunits since NF turnover is partially regulated by autophagy [129]. In addition, the observed upregulation of NF subunits could contribute to the local decline in mitochondrial numbers because NF are necessary for proper docking and distribution of mitochondria in dendrites [350, 118]. A reduction in autophagosomal clearance of mitochondria can impact mitochondrial health

by the inevitable increase of damaged mitochondria which in turn increases oxidative stress [187]. Oxidative stress is inseparably linked to mitochondrial dysfunction because mitochondria both generate and are targeted by reactive oxygen species [241]. Indications of oxidative stress and reduced ATP levels in MMP-3$^{-/-}$ mice were revealed in a proteomic screening of WT and MMP-3$^{-/-}$ medial visual cortex (mitochondrial proteins involved are marked with an asterisk in appendix table A.1). In turn, mitochondrial dysfunction can induce autophagy in neurons. For example in NGF-deprived cultured neurons it has been shown that mitochondrial ATP depletion causes an upregulation of LC3-II and subsequent autophagy [384]. To conclude, both pathways described in figure 5.1 can link the molecular data to the observed dendritic phenotype, with mitochondrial dynamics as a potential central player. One important remark is that we measured the levels of NF content with Western analysis of visual cortex homogenates and thus the source of NF upregulation remains elusive and could also come from changes in axon diameter, pyramidal neurons in other layers and non-pyramidal neurons. This remark also holds true for the presumptions made about CRMPs and autopaghic effects since we do not have cell-specific information about CRMP and LC3-II levels..

Future experiments to further dissect the proposed pathways in MMP-3$^{-/-}$ mice include the determination of the autophagic flux to distinguish between pathway 1 and 2; co-localization studies of CRMP-5 with mitochondrial markers and lysosomal markers to establish evidence for CRMP-5 mediated mitophagy; assess the number, shape and dynamics of mitochondria with live cell imaging in cultured primary cortical neurons; and analyze potential oxidative stress using for example a combination of a commercial ROS assay, measurement of antioxidant activity and DNA damage.

The upregulation and hyperphosphorylation of NF proteins and the presumptive increase in autophagosmes observed in MMP-3$^{-/-}$ mice are reminiscent of the molecular distortions observed in neurodegenerative disorders such as Parkinson's disease, Alzheimer's disease and amyotrophic lateral sclerosis (ALS) [195, 286, 196, 384]. Indeed, increased accumulation of autophagosomes has been observed in Parkinson's and Alzeimer's disease, either due to a decrease in autophagosome clearance or an overproduction of autophagosomes [288].

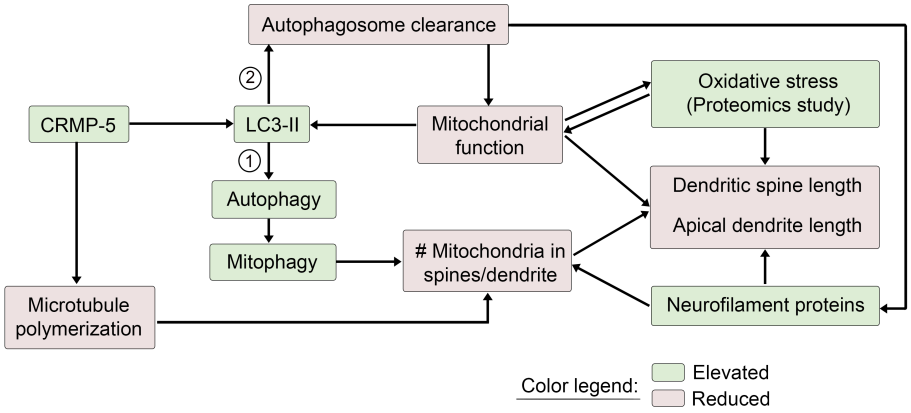

Figure 5.1: Hypothetical molecular framework underlying the MMP-3 deficient cortical phenotype.

The observed upregulation of CRMP-5 can lead to increased levels of LC3-II, which is indicative for increased autophagy (1) or a reduction in autophagosome clearance (2). The first pathway (1), in combination with the known function of CRMP-5 in inhibiting microtubule polymerization, has effect on the number of mitochondria present in the dendrite which can explain the reduction in dendritic spine length and apical dendritic length. The observed elevation in neurofilament protein levels hints towards an altered stoichiometry which can influence the distribution and docking of mitochondria. The second pathway (2) can account for the upregulation of neurofilament proteins since the turnover is determined by autophagy. An impaired autophagosome clearance accumulates dysfunctional mitochondria and produces oxidative stress, both of which can impact the structural integrity of neurons. A reduced mitochondrial function in turn stimulates autophagy onset which completes the cycle. Impairments in CRMP-mediated Ca^{2+} signaling can additionally modulate various components in this schematic (see text for details). Abbreviations: LC3-II, phosphatidylethanolamine-conjugated microtubule-associated protein 1 light chain 3.

In addition, abnormal phosphorylation of NF proteins which aggregate in Lewy bodies and neuro-fibrillary tangles (NFT), are a hallmark of Parkinson's and Alzheimer's disease respectively [196]. Alterations in NF proteins have been postulated to be an early, preclinical event in the disease progression of Alzheimer's and specifically neurons containing NF proteins, such as neocortical pyramidal cells are especially vulnerable to NFT formation [348, 78]. Interestingly, CRMPs are also involved in the pathophysiology of Alzheimer's disease [231]. Hyperphosphorylation of CRMP-2 inhibits neurite elongation and impairs microtubule-related cargo transport which contributes to the neurodegenerative process [274, 231]. A key protein in the pathophysiology of Parkinsons disease, α-synuclein, interacts with the mitochondrial inner membrane where it aggregates, causing mitochondrial dysfunction [187]. Moreover, α-synuclein is a known substrate of MMP-3 [40] which substantiates a possible link between loss of MMP-3 and an aberrant mitochondrial function. In mitochondrial-induced dopaminergic cell stress MMP-3 modulates the function of DJ-1, a peroxidase that protects the neuron against oxidative, proteasomal and mitochondrial stress [173]. Furthermore, α-synuclein promotes neurite outgrowth by stimulating microtubule polymerization in cultured primary cortical neurons [194]. However, MMP-3 is upregulated in both Parkinson's and Alzheimer's disease and MMP-3 deficient mice display a reduced dopaminergic cell death in a PD model [173, 357]. Still this provides a general link between MMP functionality, oxidative stress, neurofilament dysregulation and mitochondrial dynamics.

ALS is also characterized by an upregulation, hyperphosphorylation and aggregation of NF subunits and a defective autophagsome clearance in motor neurons [48, 67, 179]. Hyperphosphorylation of NF in ALS causes them to detach from kinesin motors which results in a decrease in transport speed and eventually leads to cytosolic accumulations [67, 371]. In our model however, immunohistochemical analysis of NF-H did not reveal any NF aggregations in the soma of layer V pyramidal neurons (supplementary figure A.2). In accordance with our data, upregulation of NF-L prevents aggregation of other overexpressed NF subunits [179]. In a specific mouse model of ALS, an increase in LC3-labeled vacuoles were observed but it is not clear whether this is a result

of an increased autophagic induction or impairment in autophagic flux [48].

The neurodegenerative diseases discussed here are all characterized by cell death that is catalyzed by protein aggregation, oxidative stress and cytoskeletal disruption. However, during disease progression it has been suggested that reduction in mitochondrial activity is an early event that precedes cell death [288]. Therefore it is conceivable that in MMP-3 deficient mice, a reduction in mitochondrial function, for example by the actions of CRMP-5, causes the observed neuronal architecture without apparent cell death.

Mitochondria serve as a Ca^{2+} buffer in dendritic spines and mitochondrial dysfunction increases cytosolic Ca^{2+} [211, 201]. Constitutive high levels of Ca^{2+}, mainly imported through NMDA receptors and voltage-dependent Ca^{2+} channels (VDCC), reduce spine length [98]. Therefore, reduced mitochondrial health by an impairment in autophagy or a lack of proper mitochondrial docking to energy-demanding dendritic spines caused by alterations in neurofilament composition, could cause a reduction in dendritic spine length in the visual cortex of MMP-$3^{-/-}$ mice. These mice are characterized by an impaired VDCC-dependent LTP in the hippocampus (personal communication with dr. G. Wiera, lab of Prof. dr. J. W. Mozrzymas) and interestingly CRMPs are known to bind to and modulate the transmission and distribution of VDCCs [358, 34]. Moreover, it has been established that a persistent or aberrant Ca^{2+} influx can trigger autophagy [384]. Aberrant Ca^{2+} has also been linked to a decrease in calpain acitivity, a protease responsible for NF degradation, which in turn results in the increase of LC3-related proteins that are calpain substrates [370, 14]. Taken together, the observed upregulation of CRMP-5 can therefore modulate CRMP-mediated VDCC Ca^{2+} influx to initiate changes in autophagosome formation and neurofilament turnover. To conclude, an aberrant Ca^{2+} signaling provides an attractive additional mechanism that can be superimposed on the pathways displayed in figure 5.1.

5.2.2 Truncated pyramidal neurons compromise cortical processing

Pyramidal neurons can be considered as the main computational unit of the neocortex, integrating information from various sources to give an appropriate output [198, 125]. Therefore, a probable consequence of the reduced apical dendritic length is that the information processing in V1 is disturbed. Considering both the traditional model for cortical processing [324] and the bistratified model of Constantinople and Bruno [57] (figure 1.2), the sensory information coming from the dLGN can not be properly processed in this case. Since structure and function are bidirectionally related you would expect severe functional abnormalities. For example, on a cellular level the length of the apical dendrite is inherently critical for proper dendritic computation because the travel-time of a dendritic signal tends to attenuate accross the apical dendrite up to the soma and therefore the length passively regulates the output signal similar to an electrical cable with insulation [198].

Although we could not make the distinction between tall-tufted, tall-simple and short pyramidal neurons [186, 185] due to the nature of the Golgi-Cox stain, we observed a considerable reduction in apical dendritic length across all examined neurons. A more detailed assessment of the different functionality of the distinct pyramidal neuron populations could be made with single unit electrophysiological recordings. A subset of pyramidal neurons (mostly tall-tufted) are intrinsically bursting and typically project to subcortical areas such as the superior colliculus and the pons to guide behavioral feedback [324, 125]. Therefore it would be interesting to assess the eye and head movements of MMP-3$^{-/-}$ mice in an optomotor system to assess superior colliculus-dependent behavior [281]. Other layer V pyramidal neurons are regular spiking and are involved in cortico-cortical signaling [183]. These pyramidal neurons in V1 receive long-range feedback connections from and serve feedforward connections to higher order visual areas [103, 186, 125]. An altered dendritic architecture could therefore have a major impact on the integration of descending pathways and top-down processing of visual information and influence the feedforward processing in the dorsal and ventral stream [103, 8]. Conclusively, it is highly

expected that the observed dendritic phenotype has a detrimental effect on the feedforward and feedback communication between V1 and extrastriate areas, which in turn can impact the dorsal and ventral stream [8, 355]. In that regard it would be very informative to functionally assess cortical processing using a combination of voltage-sensitive dye optical imaging to map the information flow between V1 and extrastriate areas and electrophysiological current source density analyses [345] to map the interlaminar temporal processing in MMP-3$^{-/-}$ mice.

Various behavioral experiments indicated that MMP-3$^{-/-}$ mice have impaired motor skills which were correlated with developmental impairments in neuronal migration and reduced Purkinje cell dendritogenesis in the cerebellum [339]. In that regard, the dendritic phenotype of the visual cortex as described in this manuscript and the concomitant abnormal visual information processing can contribute to the impaired motor behavior. Indeed, direct functional connections between V1 and motor cortex are present in rodents [289, 389, 226] and regular spiking layer V pyramidal neurons project to the striatum, which is directly involved in controlling motor behavior [324, 289].

The observed reduction in spine length on the apical shaft of the pyramidal neurons can be correlated with synaptic strength. Spine length determines the biochemical isolation of the spine and influences the electrical signaling and generally, the shorter the neck of the spine, the less electrically isolated it is from the parent dendrite [385, 386, 330]. In the case of MMP-3$^{-/-}$ mice, shorter spines could therefore be characterized by a reduced biochemical and electrical isolation which can influence dendritic computation [385, 330]. Spine length is inversely correlated with synaptic strength but the latter is additionally determined by spine head shape. The larger the head, the more current it can inject into the dendrite. Therefore, in addition to spine length, spine head shape is an important parameter in determining synaptic strength [385]. To this end, spines are often categorized in different classes according to their morphology: thin, stubby and mushroom spines [272, 31, 154]. Yet this discrete categorization has been challenged and a morphological continuum of spines has been proposed [385]. To better understand the effect of MMP-3 deficiency on circuit dynamics in the cortex, it would be useful to include parameters such as

spine head width [292] or study spine morphology in detail in MMP-3$^{-/-}$ mice using for example 3D electron microscopic reconstructions of individual spines [31, 224, 385].

5.3 MMPs and ME-induced cortical plasticity: where we are and where to go

Chapter 4 described the optimization of a fluorescent assay to measure the in vivo activity of MMP-3. Several attempts to specifically immunoprecipitate MMP-3 and detect the enzymatic activity failed since MMP-3$^{-/-}$ samples revealed considerable enzymatic activity in the performed assay. To circumvent these problems we opted for the use of Western analysis and combined this technique with gelatin zymography to additionally assess the expression levels of MMP-2 and MMP-9. Only MMP-3 expression levels were significantly affected by ME in an age-dependent manner. No differences in MMP-2 levels were found both in the Western analysis and zymography. Surprisingly, MMP-9 was not detectable using gelatin zymography in visual cortex samples.

The function and activity of MMPs in the visual cortex is still a largely unknown territory. However, unraveling the precise function of these enzymes in the visual cortex is of vital importance to comprehend cortical plasticity processes and the role of the protease web herein. To this date, the techniques to study the function of a specific MMP in a complex environment such as the brain are still lacking specificity. Nevertheless, progress is being made in the development of specific inhibitors [99, 267], the use of innovative techniques to accurately measure MMP actvity [46, 133, 171, 342] and in gaining insight in the complex degradome to identify novel MMP substrates and functions [82, 68, 295, 38].

5.3.1 Reliable assessment of MMP activity

In chapter 4 we measured MMP expression using Western analysis and we could discern the active form of MMP-2 based on molecular weight. Although

it provides us with an easy tool to demonstrate a potential link between MMP expression levels and visual cortex plasticity, Western analysis of MMP expression does not give accurate information concerning in vivo enzymatic activity levels. For example, MMP-2 activity is also determined by the levels of TIMP-2 present in the tissue and during the Western blot procedure the MMP-2/TIMP-2 complex is partly dissociated. This is also the case when using gel zymography to study MMP activity because also here the in vivo MMP/TIMP complexes are dissociated during the electrophoresis procedure [342]. Therefore it is important to note that the Western analysis and gel zymography results presented in chapter 4 do not represent actual in vivo active levels of MMP since we do not know how much MMP is bound to TIMP in vivo. These analyses rather show the maximum level of potentially active MMP and therefore this technique is valuable to uncover relative differences in experimental conditions. In addition, MMP activity can be underestimated when measuring active MMPs based on molecular weight since proMMPs can be activated by for example oxidative stress without complete proteolytic cleavage of the prodomain [259, 346]. To substantiate the net MMP activity in samples a combination of gel zymography and other complementary techniques, such as in situ zymography and fluorescent activity assays similar to the one described in Chapter 4 can be used. In situ zymography involves the sectioning of the tissue and subsequent application of a quenched fluorescently-labeled substrate to detect in vivo MMP activity [375]. This technique provides a 2D visualization of in vivo MMP activity that can be combined with IHC and even allows for a 3D representation through serial section analysis [342, 375]. However, proper controls such as selective MMP inhibitors or knockout samples have to be incorporated to deduce the specificity of substrate proteolysis. Sectioning of the tissue can also artificially mix MMPs and TIMPs which constrains the interpretation of in vivo MMP activity [342]. In that regard, in vivo zymography (IVZ) which relies on the infusion of a quenched fluorescently labeled substrate in an intact organism, provides a valuable tool to study true in vivo MMP activity [59, 171, 342]. To this date, IVZ has only been reported in transparent species and small embryos [59, 171]. Recent development of near-infrared (NIR) probes, characterized by low tissue absorption and reduced scattering coupled to MMP specific hydroxamate inhibitors holds great promise for use in non-

transparent, larger animals [172, 342], although this approach is still limited by the specificity of current available MMP substrates and inhibitors.

Another method to study MMP activity in complex sample is to assess the cleavage of endogenous MMP substrates. For example, the cleavage of the synaptic plasma membrane protein β-dystroglycan has been used as a marker for MMP-9 activity in the rodent hippocampus [222, 12]. However, caution must be taken to ensure the substrate under study is spatiotemporally specific for a certain MMP and approaches to unravel the in vivo protease web are essential in this case [81, 68].

In this dissertation we provided preliminary data that highlights the importance of MMP-3 over the gelatinases in potentially modulating plasticity in the visual cortex. Therefore, a reliable measurement of in vivo MMP-3 activity in the mouse visual cortex is essential to substantiate these results. One popular way of detecting MMP-3 activity is casein zymography [147, 93, 275, 217]. However, casein is readily cleaved by serine proteases such as tissue plasminogen activator and urokinase-type plasminogen activator with the latter having a similar molecular weight as MMP-3 [238]. This makes interpretation of MMP-3 zymolytic activity prone to error. In this case, 2D casein zymography might be useful to separate proteases with similar molecular weights and to ameliorate subsequent identification with mass spectrometry, ensuring the accurate detection of MMP-3 [342]. As argumented above, zymography provides useful but limited information as it does not reflect the in vivo activity of the enzyme. Even the activity assay described in chapter 4 only measures the net activity in a sample because of the mixture of MMPs and TIMPs during tissue homogenization. However, the net activity in a sample would provide more accurate information about the state of MMP activity in the organism compared with the potential activity measured with zymography. Of note, a similar activity assay has recently been successfully used to study the net activity of MMP-9 in the rat brain [133]. Mass spectrometry-based approaches such as the PSP-STEP method which incorporates standard MMP-derived peptides to quantify the absolute enzymatic activity for a specific MMP in a sample have been successfully performed but these techniques are also subject to the dissociation of MMP/TIMP complexes [81]. The ultimate goal is to measure the

true in vivo MMP activity in a spatiotemporal manner and in vivo zymography provides a way to accomplish this. To measure the in vivo MMP-3 activity in the visual cortex, a specific FRET or quenched NIR substrate can be injected in the cortex and allow for real-time in vivo imaging of fluorescent signals using multi-photon microscopy [137, 133]. Repeating this procedure at different time-points post-ME could provide valuable data concerning ME-induced MMP activity changes. However, this method would still be limited by the availability of specific MMP-3 substrates and possibly their pharmacokinetics in brain tissue. A combination of different approaches would yield the most accurate information.

5.3.2 Towards a causal link between MMP function and ME-induced cortical plasticity

In this dissertation we provided evidence for a modulation of proMMP-3 levels in the visual cortex according to post-ME survival times in an age-dependent manner. One logical experiment to establish a causal link between MMP activity and ME-induced cortical plasticity would be to infuse a specific MMP inhibitor intracortically in ME mice and evaluate the age-dependent reactivation in the visual cortex. Several questions accompany such an experiment: 1) what is the proper time window for inhibitor infusion? 2) can we link the observations to a specific MMP with the chosen inhibitor? and 3) if the reactivation is not modulated by infusion of an inhibitor, does this mean that MMPs do not have a function in ME-induced cortical plasticity?

The first question can be answered with a similar approach as described in chapter 4: assessment of the MMP activity in the visual cortex at different post-ME survival times. However, reliable assessment of the in vivo MMP activity is not very straightforward (see previous section). Purely on the basis of the data described in chapter 4 we can prudently conclude that inhibition of MMP-3 would be most relevant in P45 mice, specifically in the medial monocular zone where MMP-3 levels are the highest. However, higher proMMP-3 levels could reflect lower MMP-3 activity which would make this assumption incorrect.

Therefore, a more accurate measurement of MMP-3 activity in the visual cortex is necessary.

The second question deals with an established problem in the world of MMP biology: the development of specific inhibitors and the use of MMPs as therapeutic targets. Due to the large similarities of the catalytic cleft of different MMPs, inhibitor design was not that straightforward as initially thought. Since the discovery of MMPs in 1962, more than 70 pharmaceutical and biotech companies strived to get MMP inhibitors (MMPI) on the market and extensive phase III clinical trials were undertaken, without success [38, 390, 296]. Failure of these MMPIs in clinical trials was attributed to poor selectivity with inhibition of anti-targets, inadequate spatiotemporal dosing and poor knowledge of the involved pathways and substrate repertoires [58, 267, 266]. An ideal inhibitor for effective therapeutics must be selective against a validated MMP target and spare MMP anti-targets that would otherwise counterbalance the desired effects of inhibition [265]. In the past, hydroxamate-based MMPI were classically chosen because of the strong binding of hydroxamate to the Zn^{2+} in the active site [265]. However, other non-MMP metalloenzymes were also inhibited by this type of MMPIs and one example is the often used GM6001 broad spectrum MMPI [298]. Other Zn^{2+}-binding moieties have been incorporated in MMPIs to increase their specificity but highly specific inhibitors are still lacking [4, 284]. Classic MMP inhibitor design relied heavily on static structure-activity relationship analysis, which has proven to be very useful but does not take into account that specific subsites of the catalytic domain are highly flexible [60, 235, 266]. Moreover, the conformational heterogeneity and flexibility of the catalytic domain is the rule rather than an exception for MMPs [24]. Together this dramatically limits the accurate modeling of MMP-inhibitor complexes in silico. However, recent advances in the design of so-called "shape shifter" allosteric inhibitors that perturb the substrate binding properties of the catalytic site by binding to exosites holds great promise for increasing specificity of novel MMPIs [304, 265]. This approach already led to the development of highly selective MMP-13 inhibitors [248]. Using allosteric inhibitor design strategies, an inhibitory peptide against MMP-9 was synthesized that specifically targets the hemopexin domain without affecting the proteolytic activity and as a

result this peptide interferes with the integrin-binding capacity of the enzyme [28, 304]. This type of approach paves the way for highly selective inhibition of MMP activities in a biological context where only a very specific protein-protein interaction needs to be targeted. The specificity of an inhibitor may be improved by combining both interactions with the catalytic domain and exosites specific to an individual MMP [304]. However, this approach only met with limited success, likely because of the high independent mobility of different MMP domains [158]. Another possible avenue for inhibitor design is to use functional blocking antibodies due to their ability to selectively bind close-related antigens. Selective functional blocking antibodies were discovered this way for MMP-9 and MMP-14 [208, 76]. In some cases more broad-spectrum inhibitors have the advantage over specific ones for example when MMP redundancy is under study or when a physiological process is regulated by the simultaneous activity of several MMPs with low abundance anti-targets [266]. However, this still requires prior knowledge of individual MMP function. To conclude, every effort made towards synthesis of novel inhibitors to increase specificity for a certain MMP or set of MMPs is essential to progress the study of MMP function in a complex biological environment and provide the opportunity to establish a causal link between MMP function and manipulation.

Finally, the third question of the proposed experiment considers the fact that the enzymatic activity of MMPs is not always the mechanism of operation by which they regulate a physiological process. For example, MMP-9 can influence signal transduction by binding to surface receptors with its hemopexin domain [276, 287]. Therefore it is possible that infusion of a specific inhibitor that blocks MMP acitvity would not modulate ME-induced cortical plasticity. In that case it would be suitable to use an inhibitor specifically directed towards the domain that serves the interaction, e.g. the hemopexin domain (see previous paragraph).

5.4 Concluding remarks

Knockout studies can provide valuable details about the mechanistics behind the functioning of a protease web and future work on characterizing the MMP-$3^{-/-}$ phenotype can contribute to this field. Nevertheless, to unambiguously determine the activity and function of MMP-3 in the visual cortex, the techniques available today are not straightforward enough and at least a combination of different approaches should be used. All efforts to improve the synthesis of specific inhibitors and improve the techniques available to study in vivo activity of this enzyme would greatly advance the understanding of the complex MMP biology and would eventually lead to successful therapeutic applications.

Post scriptum

Recently it was brought to our attention that the MMP-3$^{-/-}$ mice used in this study harbor an inactivating mutation in the caspase-11 gene. A recent publication by Kyagaki et al. (2011) revealed that the 129 mouse strain is deficient for the caspase-11 gene located on chromosome 9 [167]. A follow-up study in 2012 by Kenneth et al. revealed that when 129 cells are used to target genes closely linked to caspase-11, the resulting mice might also carry the caspase-11 deficiency as a passenger mutation, despite extensive backcrossing to a C57Bl/6 background [170]. MMP-3 is located on chromosome 9 in close proximity to caspase-11 and the MMP-3$^{-/-}$ mice used in this study are derived from the 129 strain (The Jackson Laboratory). Indeed, genetic screening of the MMP-3$^{-/-}$ mice revealed the inactivating mutation in the caspase-11 gene, rendering these mice deficient for both genes. To exclude possible interference of caspase-11 concerning the findings presented in this manuscript and to guide future experiments, comparative studies using caspase-11$^{-/-}$ mice are needed.

Summary

The brain is able to change its functional and anatomical organization in response to environmental changes and this ability is termed neuroplasticity. The visual cortex, the area in the brain that receives visual input, is undoubtedly one of the best and most studied areas of the brain for understanding cortical plasticity and development. However, the molecular mechanisms governing cortical plasticity are still elusive. Matrix metalloproteinases (MMPs) are Zn^{2+}-dependent endopeptidases considered to be essential for normal brain development and neuroplasticity by modulating extracellular matrix proteins, receptors, adhesion molecules, growth factors and cytoskeletal proteins. Specifically, MMP-3 has recently been implicated in synaptic plasticity, hippocampus-dependent learning and neuronal development and migration in the cerebellum. However, the function of this enzyme in the neocortex is understudied. Therefore, we explored the phenotypical characteristics of the neuronal architecture and the capacity for experience-dependent cortical plasticity in the visual cortex of adult MMP-3-deficient (MMP-$3^{-/-}$) mice. Golgi–Cox stainings revealed a significant reduction in apical dendritic length, spine length and an increased number of apical obliques for layer V pyramidal neurons in the visual cortex of adult MMP-$3^{-/-}$ mice compared to wildtype (WT) animals. To assess the effect of MMP-3 deficiency on cortical plasticity, we monocularly enucleated (ME) adult MMP-$3^{-/-}$ mice and analyzed the reactivation of the contralateral visual cortex seven weeks post-ME. In contrast to previous results in C57Bl/6J adult mice, activity remained confined to the binocular zone and did not expand into the monocular regions indicative for an aberrant open-eye potentiation. Permanent hypoactivity in the monocular cortex lateral and medial to V1 also

indicated a lack of cross-modal plasticity. These observations demonstrate that genetic inactivation of MMP-3 has profound effects on the structural integrity and plasticity response of the visual cortex of adult mice. To further assess the molecular changes governing the MMP-3$^{-/-}$ cortical phenotype, we performed Western analysis on different neurofilament protein (NF) subunits and collapsin response mediator proteins (CRMP). The former are markers for a healthy cytoskeleton and determine the shape and architecture of neurons whereas CRMPs are mainly involved in regulating neurite outgrowth through microtubule polymerization. A significant upregulation of both phosphorylated and non-phosphorylated NF-high, phosphorylated NF-medium, NF-low and α-internexin was detected in the visual cortex of MMP-3$^{-/-}$ mice compared with WT. These results suggest that an altered stoichiometry of NF subunits is related to the truncated neuronal architecture observed in MMP-3$^{-/-}$ mice. In addition, the expression level of CRMP-5 was significantly elevated in MMP-3$^{-/-}$ samples whereas the levels of CRMP-1, -2, -3 and -4 did not differ compared with WT mice. Recent literature indicates that overexpression of CRMP-5 negatively regulates dendritic outgrowth by reducing the number of mitochondria through increased autophagy and mitophagy. Therefore, we assesed the expression level of a marker for autophagy, the microtubule-associated protein 1 light chain 3 (LC3-II) and found a significant increase in MMP-3$^{-/-}$ samples. The expression levels of mitochondrial fusion protein mitofusin-2 (Mfn-2) and dynamin-related protein 1 (Drp1), a mitochondrial fission protein, did not differ, indicating that the mitochondrial fusion and fission balance is not altered in the visual cortex of MMP-3$^{-/-}$ mice. Taken together, an altered NF composition, overexpression of CRMP-5 and a possible upregulation of autophagy underlie the structural phenotype in the visual cortex of MMP-3$^{-/-}$ mice.

To assess the acute role of MMPs in ME-induced visual cortex plasticity we performed Western analysis for MMP-3 to reveal fluctuations in MMP-3 expression level associated with post-ME survival time in P45 and P120 mice. This approach revealed significant differences in proMMP-3 expression especially in P45 mice both in the medial monocular and binocular zone whereas in P120 mice, enucleation did not induce large effects on proMMP-3 expression. This suggests that MMP-3 is potentially necessary to inhibit cross-modal plasticity

as normally seen in P45 mice. However, no active form of MMP-3 was visible using Western analysis and therefore we tried to optimize a fluorescent activity assay to study MMP-3 proteolysis in visual cortex samples. However, when performing this assay on samples of MMP-3$^{-/-}$ mice, a fluorescent signal in the same range as P45 and P120 ME C57Bl/6J samples was measured, rendering this technique unreliable. To extend the analysis of ME-induced cortical plasticity to other MMPs, we focused on the gelatinases (MMP-2 and MMP-9) because their function in synaptic plasticity is well established. Using a combination of Western analysis and gelatin zymography we revealed no significant differences in MMP-2 expression in all conditions studied, suggesting that this enzyme does not play a major role in ME-induced open-eye potentiation or cross-modal plasticity. No suitable antibodies for MMP-9 were available and gelatin zymography did not reveal detectable levels of MMP-9 proteolytic activity, possibly due to sample preparation issues. To conclude, further research is needed to evaluate the activity of different MMPs in the mouse visual cortex and this will provide a basis for future experiments for pharmacological intervention to establish a causal relationship between MMP function and ME-induced cortical plasticity.

Samenvatting

Onze hersenen zijn in staat om zichzelf functioneel en structureel aan te passen aan omgevingsveranderingen en dit fenomeen wordt hersenplasticiteit genoemd. De visuele cortex of het deel van de hersenen dat visuele informatie ontvangt, is ongetwijfeld de meest bestudeerde hersenregio met betrekking tot hersenplasticiteit en hersenontwikkeling. De moleculaire mechanismen die hersenplasticiteit reguleren zijn echter nog steeds grotendeels ongekend. Matrix metalloproteïnases (MMPs) zijn Zn^{2+}-afhankelijke endopeptidases die een essentïele functie hebben in normale hersenontwikkeling en neuroplasticiteit, ondermeer door het moduleren van extracellulaire matrix proteïnen, receptoren, adhesiemoleculen, groeifactoren en cytoskeletale proteïnen. Recent onderzoek heeft aangetoond dat MMP-3 betrokken is bij synaptische plasticiteit, hippocampaal-afhankelijk leren, en neuronale ontwikkeling en migratie in het cerebellum. De functie van dit enzyme in de neocortex is echter weinig onderzocht. Daarom hebben we een fenotypische karakterisatie ondernomen van de neuronale architectuur en de capaciteit voor ervaringsafhankelijke corticale plasticiteit in de visuele cortex van volwassen MMP-3-deficiënte (MMP-$3^{-/-}$) muizen. Golgi-Cox kleuringen toonden een significante reductie in de lengte van apicale dendrieten, dendritische spines en een verhoogd aantal apicale vertakkingen in laag V pyramidale neuronen in de visuele cortex van volwassen MMP-$3^{-/-}$ muizen in vergelijking met wildtype (WT) dieren. Om het effect van MMP-3 deficïentie op corticale plasticiteit na te gaan werden volwassen MMP-$3^{-/-}$ muizen monoculair geënucleëerd (ME) en de reactivatie van de contralaterale visuele cortex werd geanalyseerd zeven weken na ME. In tegenstelling tot resultaten in volwassen C57Bl/6J muizen bleef de neurale activiteit beperkt

tot de binoculaire zone en breidde niet uit tot de monoculaire zones, wat een verstoorde open-oog potentiatie doet vermoeden. Permanente hypoactiviteit in de monoculaire cortex lateraal en mediaal van V1 suggereerde eveneens een gebrek aan crossmodale plasticiteit. Deze observaties tonen aan dat genetische inactivatie van MMP-3 grote gevolgen heeft voor de structurele integriteit en de plasticiteitsrespons van de visuele cortex in volwassen muizen. Om de moleculaire veranderingen achter dit MMP-3$^{-/-}$ fenotype verder te achterhalen werd een Western analyse uitgevoerd op verschillende neurofilament proteïne (NF) subeenheden alsook op collapsine respons mediator proteïnes (CRMP). NF zijn merkers voor een gezond cytoskelet en bepalen de vorm en architectuur van neuronen terwijl CRMPs vooral betrokken zijn bij neuriet uitgroei door het moduleren van microtubule polymerisatie. Een significante stijging van zowel de gefosforyleerde en niet-gefosforyleerde vorm van NF-high, gefosforyleerd NF-medium, NF-low en α-internexine werd geobserveerd in de visuele cortex van MMP-3$^{-/-}$ muizen in vergelijking met WT. Deze resultaten suggereren dat een verandering in stoichiometrie van NF subeenheden gerelateerd is aan de afwijkende neuronale architectuur dewelke MMP-3$^{-/-}$ muizen karakteriseert. Daarbovenop werd een significant verhoogde CRMP-5 expressie vastgesteld in MMP-3$^{-/-}$ stalen in tegenstelling tot de onveranderde expressie van CRMP-1, -2, -3 en -4. Recente publicaties tonen aan dat een overexpressie van CRMP-5 de uitgroei van dendrieten negatief reguleert door het aantal mitochondriën in een neuron te verminderen door processen zoals autofagie en mitofagie. Om een mogelijke bijdrage van deze processen in kaart te brengen werd de expressie van de autofagiemerker microtubule-associated protein 1 light chain 3 (LC3-II) nagegaan en we vonden een significante overexpressie van dit molecule in MMP-3$^{-/-}$ muizen. De expressie van het mitochondriaal fusieproteïne mitofusin-2 (Mfn-2) en dynamin-related proteïne 1 (Drp1), verantwoordelijk voor mitochondriale fissie, vertoonde geen verschillen in expressie en dit suggereert dat de mitochondriale fusie en fissie balans ongewijzigd is in de visuele cortex van MMP-3$^{-/-}$ muizen. Algemeen kunnen we besluiten dat een veranderde NF compositie, overexpressie van CRMP-5 en een mogelijke verhoging in autofagie aan de basis ligt van het structurele fenotype in de visuele cortex van MMP-3$^{-/-}$ muizen.

Om de acute rol van MMPs in ME-geïnduceerde visuele cortex plasitciteit na te gaan werd een Western analyse uitgevoerd voor MMP-3 om de fluctuaties in MMP-3 expressie na te gaan die geassocieerd zijn met verschillende overlevingstijden na ME in P45 en P120 oude muizen. Dit experiment toonde significante verschillen aan in proMMP-3 expressie in P45 muizen zowel in de mediaal monoculaire als de binoculaire zone terwijl bij P120 muizen de proMMP-3 expressie na enucleatie niet significant wijzigde. Dit suggereert dat MMP-3 potentiëel noodzakelijk is om, zoals het geval is in P45 muizen, crossmodale plasticiteit te verhinderen. Desalniettemin werd geen actieve vorm van MMP-3 gedetecteerd via Western analyse en daarom probeerden we een fluorescente activiteitsassay te optimaliseren om de proteolytische activiteit van MMP-3 op te meten in de visuele cortex. Echter, wanneer uitgevoerd op MMP-$3^{-/-}$ stalen, toonde deze assay een fluorescent signaal met gelijkaardige sterkte als in P45 en P120 C57Bl/6J stalen waardoor deze techniek onbetrouwbaar werd verklaard. Om de analyse van ME-geïnduceerde corticale plasticiteit uit te breiden naar andere MMPs werd vervolgens aandacht besteed aan de gelatinases (MMP-2 en MMP-9) aangezien hun functie in synaptische plasticiteit welgekend is. Gebruikmakend van een combinatie van Western analyse en gelatine zymografie werden geen significante verschillen in MMP-2 expressie gevonden in alle geteste condities. Voor MMP-9 was geen geschikt antilichaam beschikbaar en gelatine zymografie toonde geen detecteerbare proteolytische activiteit van MMP-9 wat mogelijks te verklaren valt door problemen met staalvoorbereiding. Algemeen kunnen we besluiten dat meer onderzoek nodig is omtrent de evaluatie van MMP activiteit in de visuele cortex van de muis. Een duidelijke meting van specifieke MMP activiteit zal de basis leggen voor nieuwe farmacologische experimenten met oog op het aantonen van een causaal verband tussen MMP functie en ME-geïnduceerde corticale plasticiteit.

Appendix A

Appendix

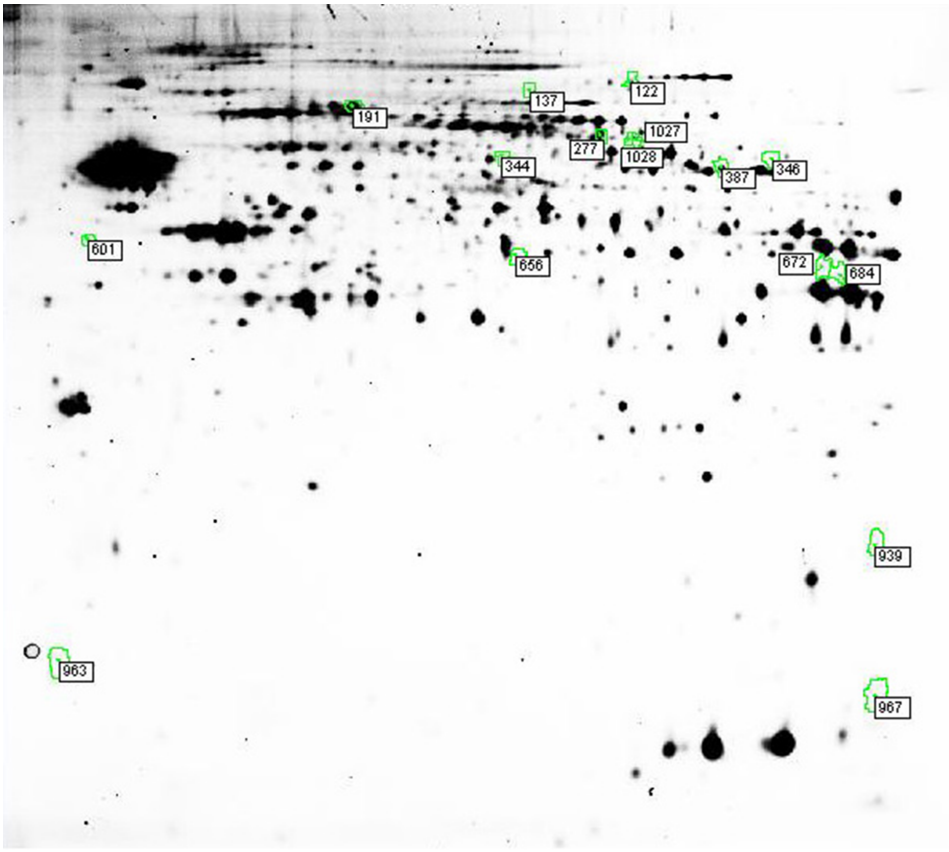

Figure A.1: Total number of differential spots between the visual cortex of WT and MMP-3$^{-/-}$ mice.

A 2-D DIGE study was performed on the medial monocular cortex of WT (n=4/condition) and MMP-3$^{-/-}$ (n=4/condition). Procedures dealing with 2-D DIGE experiments have been described in detail elsewhere [335, 55, 146]. In brief, 50 μg protein of each visual cortex sample was randomly labeled with either propyl-Cy3 or methyl-Cy5. Equal fractions of all samples were pooled and 50 μg of this pool was labeled with Cy2 to serve as an internal standard. Gels were scanned with the Ettan DIGE Imager (software 1.0; GE Healthcare) and generated gel image triplets (Cy2, Cy3, and Cy5). Spot detection and matching was performed automatically with the DeCyder Batch processor and checked manually. Statistical analysis between the two conditions was accomplished by the independent Student's t-test. Here, a total of 16 differential spots with $P < 0.01$ and $0.01 > P < 0.05$ with a ratio of 1.30 or higher are highlighted on a Cy2 image (pool sample). Each spot is delineated in green and is assigned a number for subsequent MS/MS identification.

Spot #	Identification	Average Ratio (-/- / WT)	p-value	Mascot score	# peptide matches
122	*Aconitate hydratase, mitochondrial precursor	1,34	0,0046	406	25
137	*Dynamin 1-like protein	-1,36	0,0370	193	19
191	Serum albumin precursor	1,52	0,0180	727	36
277	T-complex protein 1 (TCP1) subunit zeta	-2,08	0,0024	288	23
	Collapsin response mediator protein 3 (CRMP-3)			285	24
344	Collapsin response mediator protein 2 (CRMP-2)	-1,31	0,0491	471	30
	Glucose-6-phosphate dehydrogenase (G6PDH)			246	27
346	T-complex protein 1 (TCP1) subunit delta	-1,41	0,0142	144	16
	*ATP synthase, mitochondrial F1 complex, alpha subunit			143	15
387	*ATP synthase, mitochondrial F1 complex, alpha subunit	1,56	0,0265	252	16
	Tubulin T beta15			176	21
601	Ribosomal protein SA	-1,33	0,0444	491	23
656	Neuronal-specific septin-3	-1,18	0,0016	101	17
672	Heterogeneous nuclear ribonucleoprotein A3 (Hnrpa3), partial	-1,32	0,0064	241	13
	Glyceraldehyde-3-phosphate dehydrogenase (GAPDH)			141	16
684	no identification	-2,66	0,0322		
939	Actin-related protein 2/3 complex (Arp 2/3) subunit 3	1,41	0,0352	362	24
963	no identification	-1,32	0,0161		
967	*NADH dehydrogenase, subunit C2	1,37	0,0376	116	8
1027	no identification	1,44	0,0138		
1028	T-complex protein 1 (TCP1) subunit zeta	3,54	0,0001	156	22

Table A.1: List of all differential spots with identified proteins for WT versus MMP-$3^{-/-}$ samples.

This table shows the spot number, identified proteins, the ratios, p-values, the Mascot probability score and the number of matched peptides for each differential spot. If the ratio has a positive value this indicates a higher expression in the MMP-$3^{-/-}$ samples compared to WT and vice versa. Identifications were obtained by MALDI-TOF/TOF at Centre de Recherche Public, Grabriel Lippmann, Luxembourg. In several spots more than one protein was identified and some analyzed spots did not result in a reliable identification. Protein identifications related to mitochondrial function and dynamics are highlighted with an asterisk.

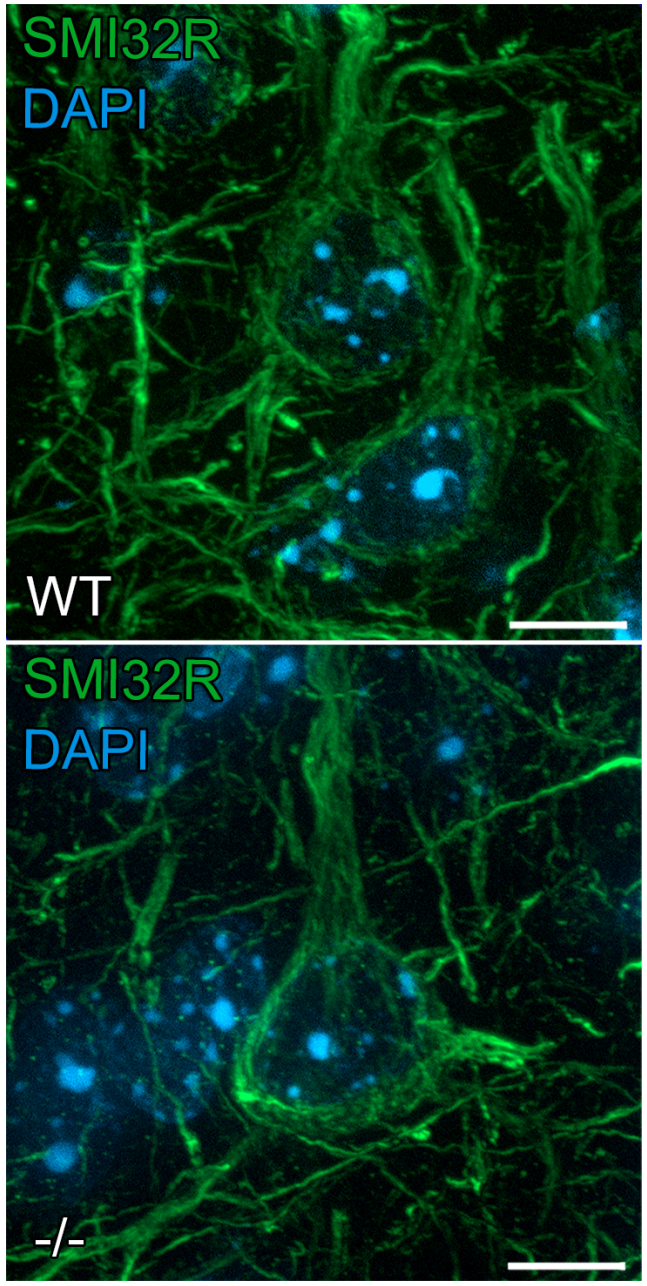

Figure A.2: Immunohistochemical detection of NF-H in pyramidal neurons in the visual cortex of WT and MMP-3$^{-/-}$ mice.

Non-phosphorylated NF-H, detected with primary antibody SMI32R (1:1000, Covance), shows no indications of neurofilament aggregation in the soma of pyramidal neurons in the visual cortex of MMP-3$^{-/-}$ mice compared with WT. Stainings were performed on 10 μm sections of paraformaldehyde-fixed tissue (secondary antibody: Alexa Fluor 488, 1:250). Scale bars: 10 μm. Abbreviations: DAPI, 4',6-diamidino-2-phenylindole (nuclear staining).

Collapsin response mediator proteins	Dihydropyrimi-dinase related proteins	Unc-33 like proteins	Toad/Ulip/Crmp family	Other names
CRMP1	DRP-1	Ulip-3	TUC-1	/
CRMP2	DRP-2	Ulip-2	TUC-2	CRMP62; TOAD-64
CRMP3	DRP-4	Ulip-4	TUC-3	/
CRMP4	DRP-3	Ulip-1	TUC-4	/
CRMP5	/	Ulip-6	/	/

Table A.2: Different names used for CRMPs in distinct species and by different laboratory groups.

Abbreviations: TOAD-64, Turned On After Division 64 kDa; Unc, Uncoordinated. Adapted from [54].

Bibliography

[1] W. C. Abraham and M. F. Bear. Metaplasticity: the plasticity of synaptic plasticity. *Trends in Neurosciences*, 19(4):126–130, 1996.

[2] J. Aerts, J. Nys, and L. Arckens. A Highly Reproducible and Straightforward Method to Perform In Vivo Ocular Enucleation in the Mouse after Eye Opening. *Journal of Visualized Experiments*, (92), 2014.

[3] J. Aerts, J. Nys, L. Moons, T.-T. Hu, and L. Arckens. Altered neuronal architecture and plasticity in the visual cortex of adult MMP-3-deficient mice. *Brain Structure and Function*, June 2014.

[4] A. Agrawal, D. Romero-Perez, J. A. Jacobsen, F. J. Villarreal, and S. M. Cohen. Zinc-Binding Groups Modulate Selective Inhibition of MMPs. *ChemMedChem*, 3(5):812–820, May 2008.

[5] S. Agrawal, L. Lau, and V. Yong. MMPs in the central nervous system: Where the good guys go bad. *Seminars in Cell & Developmental Biology*, 19(1):42–51, Feb. 2008.

[6] G. M. Aldridge, D. M. Podrebarac, W. T. Greenough, and I. J. Weiler. The use of total protein stains as loading controls: An alternative to high-abundance single-protein controls in semi-quantitative immunoblotting. *Journal of Neuroscience Methods*, 172(2):250–254, July 2008.

[7] A. Alpár, U. Gärtner, W. Härtig, and G. Brückner. Distribution of pyramidal cells associated with perineuronal nets in the neocortex of rat. *Brain Research*, 1120(1):13–22, Nov. 2006.

[8] M. L. Andermann, A. M. Kerlin, D. K. Roumis, L. L. Glickfeld, and R. C. Reid. Functional Specialization of Mouse Higher Visual Cortical Areas. *Neuron*, 72(6):1025–1039, Dec. 2011.

[9] L. Arckens, E. Van der Gucht, U. T. Eysel, G. A. Orban, and F. Vandesande. Investigation of cortical reorganization in area 17 and nine extrastriate visual areas through the detection of changes in immediate early gene expression as induced by retinal lesions. *The Journal of Comparative Neurology*, 425(4):531–544, Oct. 2000.

[10] L. Arckens, F. Zhang, W. Vanduffel, P. Mailleux, J. J. Vanderhaeghen, G. A. Orban, and F. Vandesande. Localization of the two protein kinase C beta-mRNA

subtypes in cat visual system. *Journal of Chemical Neuroanatomy*, 8(2):117–124, Feb. 1995.

[11] N. Arimura and K. Kaibuchi. Neuronal polarity: from extracellular signals to intracellular mechanisms. *Nature Publishing Group*, 8(3):194–205, Mar. 2007.

[12] M. Bajor and L. Kaczmarek. Proteolytic Remodeling of the Synaptic Cell Adhesion Molecules (CAMs) by Metzincins in Synaptic Plasticity. *Neurochemical Research*, 38(6):1113–1121, Nov. 2012.

[13] M. Bajor, P. Michaluk, P. Gulyassy, A. K. Kekesi, G. Juhasz, and L. Kaczmarek. Synaptic cell adhesion molecule-2 and collapsin response mediator protein-2 are novel members of the matrix metalloproteinase-9 degradome. *Journal of Neurochemistry*, 122(4):775–788, July 2012.

[14] D. Bano, F. Zanetti, Y. Mende, and P. Nicotera. Neurodegenerative processes in Huntington's disease. *Cell Death and Disease*, 2(11):e228–7, Nov. 2011.

[15] D. M. Barry, S. Millecamps, J.-P. Julien, and M. L. Garcia. New movements in neurofilament transport, turnover and disease. *Experimental Cell Research*, 313(10):2110–2120, June 2007.

[16] A. Bartoletti, L. Cancedda, S. W. Reid, L. Tessarollo, V. Porciatti, T. Pizzorusso, and L. Maffei. Heterozygous knock-out mice for brain-derived neurotrophic factor show a pathway-specific impairment of long-term potentiation but normal critical period for monocular deprivation. *Journal of Neuroscience*, 22(23):10072–10077, Dec. 2002.

[17] D. Bavelier and H. J. Neville. Cross-modal plasticity: where and how? *Nature Reviews Neuroscience*, 3(6):443–452, June 2002.

[18] M. F. Bear, B. W. Connors, and M. A. Paradiso. *Neuroscience*. Lippincott Williams & Wilkins, 2007.

[19] N. Bednarek, Y. Clément, V. Lelièvre, P. Olivier, G. Loron, R. Garnotel, and P. Gressens. Ontogeny of MMPs and TIMPs in the murine neocortex. *Pediatric research*, 65(3):296–300, Mar. 2009.

[20] B. F. Behabadi, A. Polsky, M. Jadi, J. Schiller, and B. W. Mel. Location-Dependent Excitatory Synaptic Interactions in Pyramidal Neuron Dendrites. *PLoS Computational Biology*, 8(7):e1002599, July 2012.

[21] R. Benavides-Piccione, I. Ballesteros-Yáñez, J. DeFelipe, and R. Yuste. Cortical area and species differences in dendritic spine morphology. *Journal of neurocytology*, 31(3-5):337–346, Mar. 2002.

[22] N. Berardi, T. Pizzorusso, and L. Maffei. Critical periods during sensory development. *Current Opinion in Neurobiology*, 10(1):138–145, Feb. 2000.

[23] N. Berardi, T. Pizzorusso, and L. Maffei. Extracellular Matrix and Visual Cortical Plasticity. *Neuron*, 44(6):905–908, Dec. 2004.

[24] I. Bertini, V. Calderone, M. Cosenza, M. Fragai, Y.-M. Lee, C. Luchinat, S. Mangani, B. Terni, and P. Turano. Conformational variability of matrix metalloproteinases: beyond a single 3D structure. *Proceedings of the National Academy of Sciences*, 102(15):5334–5339, Apr. 2005.

[25] T. V. Bilousova, L. Dansie, M. Ngo, J. Aye, J. R. Charles, D. W. Ethell, and I. M. Ethell. Minocycline promotes dendritic spine maturation and improves behavioural performance in the fragile X mouse model. *Journal of Medical Genetics*, 46(2):94–102, Nov. 2008.

[26] T. V. Bilousova, D. A. Rusakov, D. W. Ethell, and I. M. Ethell. Matrix metalloproteinase-7 disrupts dendritic spines in hippocampal neurons through NMDA receptor activation. *Journal of Neurochemistry*, 97(1):44–56, Apr. 2006.

[27] T. Birdal. Smoothing 2D contours using local regression lines. *MATLAB file exchange*.

[28] M. Bjorklund, P. Heikkila, and E. Koivunen. Peptide Inhibition of Catalytic and Noncatalytic Activities of Matrix Metalloproteinase-9 Blocks Tumor Cell Migration and Invasion. *Journal of Biological Chemistry*, 279(28):29589–29597, July 2004.

[29] T. Bonhoeffer. Neurotrophins and activity-dependent development of the neocortex. *Current Opinion in Neurobiology*, 6(1):119–126, 1996.

[30] R. Bopp, N. Maçarico da Costa, B. M. Kampa, K. A. C. Martin, and M. M. Roth. Pyramidal Cells Make Specific Connections onto Smooth (GABAergic) Neurons in Mouse Visual Cortex. *PLoS Biology*, 12(8):e1001932, Aug. 2014.

[31] J. N. Bourne and K. M. Harris. Balancing Structure and Function at Hippocampal Dendritic Spines. *Annual Review of Neuroscience*, 31(1):47–67, July 2008.

[32] S. Bretin, S. Reibel, E. Charrier, M. Maus-Moatti, N. Auvergnon, A. Thevenoux, J. Glowinski, V. r. Rogemond, J. l. Pr mont, J. r. m. Honnorat, and C. Gauchy. Differential expression of CRMP1, CRMP2A, CRMP2B, and CRMP5 in axons or dendrites of distinct neurons in the mouse brain. *The Journal of Comparative Neurology*, 486(1):1–17, 2005.

[33] C. E. Brinckerhoff and L. M. Matrisian. Matrix metalloproteinases: a tail of a frog that became a prince. *Nature Reviews Molecular Cell Biology*, 3(3):207–214, Mar. 2002.

[34] J. M. Brittain, A. D. Piekarz, Y. Wang, T. Kondo, T. R. Cummins, and R. Khanna. An Atypical Role for Collapsin Response Mediator Protein 2 (CRMP-2) in Neurotransmitter Release via Interaction with Presynaptic Voltage-gated Calcium Channels. *Journal of Biological Chemistry*, 284(45):31375–31390, Oct. 2009.

[35] S. Brot, C. Auger, R. Bentata, V. Rogemond, S. Menigoz, N. Chounlamountri, A. Girard-Egrot, J. Honnorat, and M. Moradi-Ameli. Collapsin Response Mediator Protein 5 (CRMP5) Induces Mitophagy, Thereby Regulating Mitochondrion Numbers in Dendrites. *Journal of Biological Chemistry*, 289(4):2261–2276, Dec. 2013.

[36] S. Brot, V. Rogemond, V. Perrot, N. Chounlamountri, C. Auger, J. Honnorat, and M. Moradi-Ameli. CRMP5 Interacts with Tubulin to Inhibit Neurite Outgrowth, Thereby Modulating the Function of CRMP2. *Journal of Neuroscience*, 30(32):10639–10654, Aug. 2010.

[37] S. Brot, H. Smaoune, M. Youssef-Issa, C. Malleval, C. Benetollo, R. Besançon, C. Auger, M. Moradi-Améli, and J. Honnorat. Collapsin response-mediator protein 5 (CRMP5) phosphorylation at threonine 516 regulates neurite outgrowth inhibition. *European Journal of Neuroscience*, 40(7):3010–3020, July 2014.

[38] G. S. Butler and C. M. Overall. Updated Biological Roles for Matrix Metalloproteinases and New "Intracellular" Substrates Revealed by Degradomics. *Biochemistry*, 48(46):10830–10845, Nov. 2009.

[39] E. Candelario-Jalil, J. Thompson, S. Taheri, M. Grossetete, J. C. Adair, E. Edmonds, J. Prestopnik, J. Wills, and G. A. Rosenberg. Matrix Metalloproteinases Are Associated With Increased Blood-Brain Barrier Opening in Vascular Cognitive Impairment. *Stroke*, 42(5):1345–1350, Apr. 2011.

[40] B. Cauwe and G. Opdenakker. Intracellular substrate cleavage: a novel dimension in the biochemistry, biology and pathology of matrix metalloproteinases. *Critical Reviews in Biochemistry and Molecular Biology*, 45(5):351–423, Oct. 2010.

[41] L. M. Chalupa and R. W. Williams. *Eye, Retina, and Visual System of the Mouse*. MIT Press (MA), 2008.

[42] A. R. Chandrasekaran. Evidence for an Instructive Role of Retinal Activity in Retinotopic Map Refinement in the Superior Colliculus of the Mouse. *Journal of Neuroscience*, 25(29):6929–6938, July 2005.

[43] D. T. W. Chang. Mitochondrial Trafficking to Synapses in Cultured Primary Cortical Neurons. *Journal of Neuroscience*, 26(26):7035–7045, June 2006.

[44] E. Charrier, S. Reibel, V. Rogemond, M. Aguera, N. Thomasset, and J. Honnorat. Collapsin response mediator proteins (CRMPs): involvement in nervous system development and adult neurodegenerative disorders. *Molecular Neurobiology*, 28(1):51–64, Aug. 2003.

[45] C. C. Chen. The Angiogenic Factors Cyr61 and Connective Tissue Growth Factor Induce Adhesive Signaling in Primary Human Skin Fibroblasts. *Journal of Biological Chemistry*, 276(13):10443–10452, Dec. 2000.

[46] C.-H. Chen, A. Sarkar, Y.-A. Song, M. A. Miller, S. J. Kim, L. G. Griffith, D. A. Lauffenburger, and J. Han. Enhancing Protease Activity Assay in Droplet-Based Microfluidics Using a Biomolecule Concentrator. *Journal of the American Chemical Society*, 133(27):10368–10371, July 2011.

[47] J. L. Chen, K. L. Villa, J. W. Cha, P. T. C. So, Y. Kubota, and E. Nedivi. Clustered Dynamics of Inhibitory Synapses and Dendritic Spines in the Adult Neocortex. *Neuron*, 74(2):361–373, Apr. 2012.

[48] S. Chen, X. Zhang, L. Song, and W. Le. Autophagy Dysregulation in Amyotrophic Lateral Sclerosis. *Brain Pathology*, 22(1):110–116, Dec. 2011.

[49] A. Cheng, Y. Hou, and M. P. Mattson. Mitochondria and neuroplasticity. *ASN NEURO*, 2(5):243–256, Oct. 2010.

[50] A. Citri and R. C. Malenka. Synaptic Plasticity: Multiple Forms, Functions, and Mechanisms. *Neuropsychopharmacology*, 33(1):18–41, Aug. 2007.

[51] F. Ciucci, E. Putignano, L. Baroncelli, S. Landi, N. Berardi, and L. Maffei. Insulin-Like Growth Factor 1 (IGF-1) Mediates the Effects of Enriched Environment (EE) on Visual Cortical Development. *PLoS ONE*, 2(5):e475, May 2007.

[52] S. Clavagnier, A. Falchier, and H. Kennedy. Long-distance feedback projections to area V1: implications for multisensory integration, spatial awareness, and visual consciousness. *Cognitive, affective & behavioral neuroscience*, 4(2):117–126, June 2004.

[53] R. Clay Bunn and J. L. Fowlkes. Insulin-like growth factor binding protein proteolysis. *Trends in Endocrinology & Metabolism*, 14(4):176–181, May 2003.

[54] L. Cnops. *The ups and downs of Collapsin Response Mediator Proteins 2 and 4, Dynamin I and Synaptotagmin I during development and visual deprivation-induced plasticity in the visual cortex of the cat (Felis catus)*. PhD thesis, KU Leuven, 2006.

[55] L. Cnops, T.-T. Hu, J. Vanden Broeck, K. Burnat, G. Van den Bergh, and L. Arckens. Age- and experience-dependent expression of Dynamin I and Synaptotagmin I in cat visual system. *The Journal of Comparative Neurology*, 504(3):254–264, 2007.

[56] K. Conant, Y. Wang, A. szklarczyk, A. Dudak, M. P. Mattson, and S. T. Lim. Matrix metalloproteinase-dependent shedding of intercellular adhesion molecule-5 occurs with long-term potentiation. *Neuroscience*, 166(2):508–521, Mar. 2010.

[57] C. M. Constantinople and R. M. Bruno. Deep Cortical Layers Are Activated Directly by Thalamus. *Science*, 340(6140):1591–1594, June 2013.

[58] L. M. Coussens. Matrix Metalloproteinase Inhibitors and Cancer–Trials and Tribulations. *Science*, 295(5564):2387–2392, Mar. 2002.

[59] B. D. Crawford and D. B. Pilgrim. Ontogeny and regulation of matrix metalloproteinase activity in the zebrafish embryo by in vitro and in vivo zymography. *Developmental Biology*, 286(2):405–414, Oct. 2005.

[60] P. Cuniasse, L. Devel, A. Makaritis, F. Beau, D. Georgiadis, M. Matziari, A. Yiotakis, and V. Dive. Future challenges facing the development of specific active-site-directed synthetic inhibitors of MMPs. *Biochimie*, 87(3-4):393–402, Mar. 2005.

[61] A. Cybulska-Klosowicz, M. Liguz-Lecznar, D. Nowicka, M. Ziemka-Nalecz, M. Kossut, and J. Skangiel-Kramska. Matrix metalloproteinase inhibition counteracts impairment of cortical experience-dependent plasticity after photothrombotic stroke. *European Journal of Neuroscience*, 33(12):2238–2246, May 2011.

[62] J. D' Errico. Interparc. *MATLAB file exchange*.

[63] J. M. Dale and M. L. Garcia. Neurofilament Phosphorylation during Development and Disease: Which Came First, the Phosphorylation or the Accumulation? *Journal of Amino Acids*, 2012(4):1–10, 2012.

[64] A. Datwani, M. J. McConnell, P. O. Kanold, K. D. Micheva, B. Busse, M. Shamloo, S. J. Smith, and C. J. Shatz. Classical MHCI Molecules Regulate Retinogeniculate Refinement and Limit Ocular Dominance Plasticity. *Neuron*, 64(4):463–470, Nov. 2009.

[65] J. A. Day and S. M. Cohen. Investigating the Selectivity of Metalloenzyme Inhibitors. *Journal of Medicinal Chemistry*, page 130927144712002, Sept. 2013.

[66] L. de Vivo, S. Landi, M. Panniello, L. Baroncelli, S. Chierzi, L. Mariotti, M. Spolidoro, T. Pizzorusso, L. Maffei, and G. M. Ratto. Extracellular matrix inhibits structural and functional plasticity of dendritic spines in the adult visual cortex. *Nature Communications*, 4:1484, Feb. 2013.

[67] K. J. De Vos, A. J. Grierson, S. Ackerley, and C. C. J. Miller. Role of Axonal Transport in Neurodegenerative Diseases*. *Annual Review of Neuroscience*, 31(1):151–173, July 2008.

[68] R. A. Dean and C. M. Overall. Proteomics discovery of metalloproteinase substrates in the cellular context by iTRAQ™ labeling reveals a diverse MMP-2 substrate degradome. *Molecular & Cellular Proteomics*, 6(4):611–623, 2007.

[69] E. W. Dent. Netrin-1 and Semaphorin 3A Promote or Inhibit Cortical Axon Branching, Respectively, by Reorganization of the Cytoskeleton. *Journal of Neuroscience*, 24(12):3002–3012, Mar. 2004.

[70] V. Deretic. Autophagosome and phagosome. *Methods in molecular biology (Clifton, N.J.)*, 445:1–10, 2008.

[71] E. Deryugina. MT1-MMP Initiates Activation of pro-MMP-2 and Integrin $\alpha v\beta 3$ Promotes Maturation of MMP-2 in Breast Carcinoma Cells. *Experimental Cell Research*, 263(2):209–223, Feb. 2001.

[72] N. S. Desai, R. H. Cudmore, S. B. Nelson, and G. G. Turrigiano. Critical periods for experience-dependent synaptic scaling in visual cortex. *Nature Neuroscience*, 5(8):783–789, Aug. 2002.

[73] F. J. Descamps, E. Martens, and G. Opdenakker. Analysis of Gelatinases in Complex Biological Fluids and Tissue Extracts. *Laboratory Investigation*, 82(11):1607–1608, Nov. 2002.

[74] S. A. Detmer and D. C. Chan. Functions and dysfunctions of mitochondrial dynamics. *Nature Reviews Molecular Cell Biology*, 8(11):870–879, Nov. 2007.

[75] L. Devy and D. T. Dransfield. New Strategies for the Next Generation of Matrix-Metalloproteinase Inhibitors: Selectively Targeting Membrane-Anchored MMPs with Therapeutic Antibodies. *Biochemistry Research International*, 2011(7):1–11, 2011.

[76] L. Devy, L. Huang, L. Naa, N. Yanamandra, H. Pieters, N. Frans, E. Chang, Q. Tao, M. Vanhove, A. Lejeune, R. van Gool, D. J. Sexton, G. Kuang, D. Rank, S. Hogan, C. Pazmany, Y. L. Ma, S. Schoonbroodt, A. E. Nixon, R. C. Ladner, R. Hoet, P. Henderikx, C. TenHoor, S. A. Rabbani, M. L. Valentino, C. R. Wood, and D. T. Dransfield. Selective Inhibition of Matrix Metalloproteinase-14 Blocks Tumor Growth, Invasion, and Angiogenesis. *Cancer Research*, 69(4):1517–1526, Feb. 2009.

[77] G. Di Cristo, B. Chattopadhyaya, S. J. Kuhlman, Y. Fu, M.-C. Bélanger, C. Z. Wu, U. Rutishauser, L. Maffei, and Z. J. Huang. Activity-dependent PSA expression regulates inhibitory maturation and onset of critical period plasticity. *Nature Neuroscience*, 10(12):1569–1577, Nov. 2007.

[78] T. C. Dickson, J. A. Chuckowree, M. Inn Chuah, A. K. West, and J. C. Vickers. alpha-Internexin immunoreactivity reflects variable neuronal vulnerability in Alzheimer's disease and supports the role of the beta-amyloid plaques in inducing neuronal injury. *Neurobiology of Disease*, 18(2):286–295, Mar. 2005.

[79] A. Dityatev and M. Schachner. Extracellular matrix molecules and synaptic plasticity. *Nature Reviews Neuroscience*, 4(6):456–468, June 2003.

[80] A. Dityatev, M. Schachner, and P. Sonderegger. The dual role of the extracellular matrix in synaptic plasticity and homeostasis. *Nature Reviews Neuroscience*, 11(11):735–746, Oct. 2010.

[81] A. Doucet and C. M. Overall. Protease proteomics: revealing protease in vivo functions using systems biology approaches. *Molecular aspects of medicine*, 29(5):339–358, Oct. 2008.

[82] A. Doucet and C. M. Overall. Broad coverage identification of multiple proteolytic cleavage site sequences in complex high molecular weight proteins using quantitative proteomics as a complement to edman sequencing. *Molecular & cellular proteomics*, 10(5):M110.003533, May 2011.

[83] R. J. Douglas and K. A. C. Martin. Neuronal Circuits of the Neocortex. *Annual Review of Neuroscience*, 27(1):419–451, July 2004.

[84] U. C. Dräger. Receptive fields of single cells and topography in mouse visual cortex. *The Journal of Comparative Neurology*, 160(3):269–290, Apr. 1975.

[85] A. H. Drummond, P. Beckett, P. D. Brown, E. A. Bone, A. H. Davidson, W. A. Galloway, A. J. Gearing, P. Huxley, D. Laber, M. McCourt, M. Whittaker, L. M. Wood, and A. Wright. Preclinical and clinical studies of MMP inhibitors in cancer. *Annals of the New York Academy of Sciences*, 878:228–235, June 1999.

[86] C. A. D'Souza, B. Mak, and M. A. Moscarello. The Up-regulation of Stromelysin-1 (MMP-3) in a Spontaneously Demyelinating Transgenic Mouse Precedes Onset of Disease. *Journal of Biological Chemistry*, 277(16):13589–13596, Apr. 2002.

[87] J. A. Dumin. Pro-collagenase-1 (Matrix Metalloproteinase-1) Binds the alpha 2beta 1 Integrin upon Release from Keratinocytes Migrating on Type I Collagen. *Journal of Biological Chemistry*, 276(31):29368–29374, May 2001.

[88] J. D. Durrant, C. A. F. de Oliveira, and J. A. McCammon. Pyrone-Based Inhibitors of Metalloproteinase Types 2 and 3 May Work as Conformation-Selective Inhibitors. *Chemical Biology & Drug Design*, 78(2):191–198, June 2011.

[89] M. Dziembowska, J. Milek, A. Janusz, E. Rejmak, E. Romanowska, T. Gorkiewicz, A. Tiron, C. R. Bramham, and L. Kaczmarek. Activity-Dependent Local Translation of Matrix Metalloproteinase-9. *Journal of Neuroscience*, 32(42):14538–14547, Oct. 2012.

[90] M. Dziembowska and J. Wlodarczyk. MMP9: A novel function in synaptic plasticity. *The International Journal of Biochemistry & Cell Biology*, 44(5):709–713, May 2012.

[91] Y. H. Edrey, S. Oddo, C. Cornelius, A. Caccamo, V. Calabrese, and R. Buffenstein. Oxidative damage and amyloid-β metabolism in brain regions of the longest-lived rodents. *Journal of Neuroscience Research*, 92(2):195–205, Nov. 2013.

[92] T. Eguchi, S. Kubota, K. Kawata, Y. Mukudai, J. Uehara, T. Ohgawara, S. Ibaragi, A. Sasaki, T. Kuboki, and M. Takigawa. Novel Transcription Factor-Like Function of Human Matrix Metalloproteinase 3 Regulating the CTGF/CCN2 Gene. *Molecular and Cellular Biology*, 28(7):2391–2413, Mar. 2008.

[93] S. R. Elshaw, N. Henderson, A. J. Knox, S. A. Watson, D. J. Buttle, and S. R. Johnson. Matrix metalloproteinase expression and activity in human airway smooth muscle cells. *British Journal of Pharmacology*, 142(8):1318–1324, Aug. 2004.

[94] G. N. Elston and M. G. Rosa. Pyramidal cells, patches, and cortical columns: a comparative study of infragranular neurons in TEO, TE, and the superior temporal polysensory area of the macaque monkey. *Journal of Neuroscience*, 20(24):RC117, Dec. 2000.

[95] J. Esparza, M. Kruse, J. Lee, M. Michaud, and J. A. Madri. MMP-2 null mice exhibit an early onset and severe experimental autoimmune encephalomyelitis due to an increase in MMP-9 expression and activity. *The FASEB Journal*, 18(14):1682–1691, Nov. 2004.

[96] S. Espinosa and M. P. Stryker. Development and Plasticity of the Primary Visual Cortex. *Neuron*, 75(2):230–249, July 2012.

[97] I. M. Ethell and D. W. Ethell. Matrix metalloproteinases in brain development and remodeling: Synaptic functions and targets. *Journal of Neuroscience Research*, 85(13):2813–2823, 2007.

[98] I. M. Ethell and E. B. Pasquale. Molecular mechanisms of dendritic spine development and remodeling. *Progress in Neurobiology*, 75(3):161–205, Feb. 2005.

[99] B. Fabre, A. Ramos, and B. de Pascual-Teresa. Targeting Matrix Metalloproteinases: Exploring the Dynamics of the S1' Pocket in the Design of Selective, Small Molecule Inhibitors. *Journal of Medicinal Chemistry*, page doi: 10.1021/jm500505f, Sept. 2014.

[100] M. Fagiolini, J.-M. Fritschy, K. Löw, H. Möhler, U. Rudolph, and T. K. Hensch. Specific GABAA circuits for visual cortical plasticity. *Science*, 303(5664):1681–1683, Mar. 2004.

[101] J. Faguet, B. Maranhao, S. L. Smith, and J. T. Trachtenberg. Ipsilateral Eye Cortical Maps Are Uniquely Sensitive to Binocular Plasticity. *Journal of Neurophysiology*, 101(2):855–861, Nov. 2008.

[102] M. C. Falo, H. L. Fillmore, T. M. Reeves, and L. L. Phillips. Matrix metalloproteinase-3 expression profile differentiates adaptive and maladaptive synaptic plasticity induced by traumatic brain injury. *Journal of Neuroscience Research*, 84(4):768–781, 2006.

[103] D. J. Felleman and D. C. Van Essen. Distributed hierarchical processing in the primate cerebral cortex. *Cerebral Cortex*, 1(1):1–47, Jan. 1991.

[104] V. Fenstermaker, Y. Chen, A. Ghosh, and R. Yuste. Regulation of dendritic length and branching by semaphorin 3A. *Journal of Neurobiology*, 58(3):403–412, 2004.

[105] B. Fingleton. MMPs as therapeutic targets—Still a viable option? *Seminars in Cell & Developmental Biology*, 19(1):61–68, Feb. 2008.

[106] M. Fischer, M. Fischer, K. Lüersen, M. Boll, U. Wenzel, and A. Vilcinskas. Role of matrix metalloproteinase ZMP-2 in pathogen resistance and development in Caenorhabditis elegans . *Developmental and Comparative Immunology*, 34(11):1160–1169, Nov. 2010.

[107] D. A. Fletcher and R. D. Mullins. Cell mechanics and the cytoskeleton. *Nature*, 463(7280):485–492, Jan. 2010.

[108] S. Foscarin, D. Ponchione, E. Pajaj, K. Leto, M. Gawlak, G. M. Wilczynski, F. Rossi, and D. Carulli. Experience-Dependent Plasticity and Modulation of Growth Regulatory Molecules at Central Synapses. *PLoS ONE*, 6(1):e16666, Jan. 2011.

[109] J. L. Fowlkes. Regulation of Insulin-Like Growth Factor (IGF)-I Action by Matrix Metalloproteinase-3 Involves Selective Disruption of IGF-I/IGF-Binding Protein-3 Complexes. *Endocrinology*, 145(2):620–626, Oct. 2003.

[110] K. Franklin and G. Paxinos. *The Mouse Brain in Stereotaxic Coordinates*. Elsevier, Amsterdam, 3rd edition, Apr. 2008.

[111] M. Y. Frenkel and M. F. Bear. How monocular deprivation shifts ocular dominance in visual cortex of young mice. *Neuron*, 44(6):917–923, Dec. 2004.

[112] R. Frischknecht, M. Heine, D. Perrais, C. I. Seidenbecher, D. Choquet, and E. D. Gundelfinger. Brain extracellular matrix affects AMPA receptor lateral mobility and short-term synaptic plasticity. *Nature Neuroscience*, 12(7):897–904, May 2009.

[113] M. Fukada. Molecular Characterization of CRMP5, a Novel Member of the Collapsin Response Mediator Protein Family. *Journal of Biological Chemistry*, 275(48):37957–37965, Aug. 2000.

[114] K. Ganguly, E. Rejmak, M. Mikosz, E. Nikolaev, E. Knapska, and L. Kaczmarek. Matrix Metalloproteinase (MMP)-9 transcription in mouse brain induced by fear learning. *Journal of Biological Chemistry*, May 2013.

[115] M. E. Garrett, I. Nauhaus, J. H. Marshel, and E. M. Callaway. Topography and Areal Organization of Mouse Visual Cortex. *Journal of Neuroscience*, 34(37):12587–12600, Sept. 2014.

[116] A. J. Gearing, P. Beckett, M. Christodoulou, M. Churchill, J. M. Clements, M. Crimmin, A. H. Davidson, A. H. Drummond, W. A. Galloway, and R. Gilbert. Matrix metalloproteinases and processing of pro-TNF-alpha. *Journal of Leukocyte Biology*, 57(5):774–777, May 1995.

[117] A. J. H. Gearing, S. J. Thorpe, K. Miller, M. Mangan, P. G. Varley, T. Dudgeon, G. Ward, C. Turner, and R. Thorpe. Selective cleavage of human IgG by the matrix metalloproteinases, matrilysin and stromelysin. *Immunology letters*, 81(1):41–48, Apr. 2002.

[118] B. J. Gentil, S. Minotti, M. Beange, R. H. Baloh, J. P. Julien, and H. D. Durham. Normal role of the low-molecular-weight neurofilament protein in mitochondrial dynamics and disruption in Charcot-Marie-Tooth disease. *The FASEB Journal*, 26(3):1194–1203, Feb. 2012.

[119] J. George, M. L. Teear, C. G. Norey, and D. Dougal Burns. Evaluation of an Imaging Platform during the Development of a FRET Protease Assay. *Journal of Biomolecular Screening*, 8(1):72–80, Jan. 2003.

[120] C. Gialeli, A. D. Theocharis, and N. K. Karamanos. Roles of matrix metalloproteinases in cancer progression and their pharmacological targeting. *FEBS Journal*, 278(1):16–27, Nov. 2010.

[121] L. L. Glickfeld, R. C. Reid, and M. L. Andermann. A mouse model of higher visual cortical function. *Current Opinion in Neurobiology*, 24:28–33, Feb. 2014.

[122] B. Gonthier, E. Koncina, S. Satkauskas, M. Perraut, G. Roussel, D. Aunis, J. P. Kapfhammer, and D. Bagnard. A PKC-Dependent Recruitment of MMP-2 Controls Semaphorin-3A Growth-Promoting Effect in Cortical Dendrites. *PLoS ONE*, 4(4):e5099, Apr. 2009.

[123] B. Gonthier, C. Nasarre, L. Roth, M. Perraut, N. Thomasset, G. Roussel, D. Aunis, and D. Bagnard. Functional Interaction between Matrix Metalloproteinase-3 and Semaphorin-3C during Cortical Axonal Growth and Guidance. *Cerebral Cortex*, 17(7):1712–1721, Sept. 2006.

[124] M. A. Goodale and A. D. Milner. Separate visual pathways for perception and action. *Trends in Neurosciences*, 15(1):20–25, Jan. 1992.

[125] A. Granato and A. De Giorgio. Alterations of neocortical pyramidal neurons: turning points in the genesis of mental retardation. *Frontiers in pediatrics*, 2:86, 2014.

[126] J. Gross and C. M. Lapiere. Collagenolytic activity in amphibian tissues: a tissue culture assay. *Proceedings of the National Academy of Sciences*, 48:1014–1022, June 1962.

[127] Y. Gu. Evidence That Collapsin Response Mediator Protein-2 Is Involved in the Dynamics of Microtubules. *Journal of Biological Chemistry*, 275(24):17917–17920, Apr. 2000.

[128] B. W. Guzik and L. S. Goldstein. Microtubule-dependent transport in neurons: steps towards an understanding of regulation, function and dysfunction. *Current opinion in cell biology*, 16(4):443–450, Aug. 2004.

[129] A. Hanes. *Effects of mitochondrial dysfunction on neurofilament turnover and distribution in human neuroblastoma cells.* PhD thesis, Dec. 2010.

[130] A. Harauzov, M. Spolidoro, G. DiCristo, R. De Pasquale, L. Cancedda, T. Pizzorusso, A. Viegi, N. Berardi, and L. Maffei. Reducing Intracortical Inhibition in the Adult Visual Cortex Promotes Ocular Dominance Plasticity. *Journal of Neuroscience*, 30(1):361–371, Jan. 2010.

[131] R. Hashimoto, Y. Nakamura, K. Imamura, K. Nakadate, Y. Kashiwagi, N. Matsumoto, and M. Takeda. Visual stimulation-induced phosphorylation of neurofilament-L in the visual cortex of dark-reared rats. *The European journal of neuroscience*, 14(8):1237–1245, Oct. 2001.

[132] S. Hattar. Melanopsin-Containing Retinal Ganglion Cells: Architecture, Projections, and Intrinsic Photosensitivity. *Science*, 295(5557):1065–1070, Feb. 2002.

[133] K. E. Hawkins, K. M. DeMars, C. Yang, G. A. Rosenberg, and E. Candelario-Jalil. Fluorometric immunocapture assay for the specific measurement of matrix metalloproteinase-9 activity in biological samples: application to brain and plasma from rats with ischemic stroke. *Molecular Brain*, 6(1):14, 2013.

[134] K. He, E. Petrus, N. Gammon, and H. K. Lee. Distinct Sensory Requirements for Unimodal and Cross-Modal Homeostatic Synaptic Plasticity. *Journal of Neuroscience*, 32(25):8469–8474, June 2012.

[135] J. A. Heimel, J. M. Hermans, J. P. Sommeijer, Neuro-Bsik Mouse Phenomics consortium, and C. N. Levelt. Genetic control of experience-dependent plasticity in the visual cortex. *Genes, Brain and Behavior*, 7(8):915–923, Nov. 2008.

[136] J. A. Heimel, D. van Versendaal, and C. N. Levelt. The Role of GABAergic Inhibition in Ocular Dominance Plasticity. *Neural Plasticity*, 2011(2):1–11, 2011.

[137] F. Helmchen and W. Denk. Deep tissue two-photon microscopy. *Nature Methods*, 2(12):932–940, Dec. 2005.

[138] T. K. Hensch. Local GABA Circuit Control of Experience-Dependent Plasticity in Developing Visual Cortex. *Science*, 282(5393):1504–1508, Nov. 1998.

[139] T. K. Hensch. Critical period plasticity in local cortical circuits. *Nature Reviews Neuroscience*, 6(11):877–888, Nov. 2005.

[140] T. K. Hensch, M. Fagiolini, N. Mataga, M. P. Stryker, S. Baekkeskov, and S. F. Kash. Local GABA circuit control of experience-dependent plasticity in developing visual cortex. *Science*, 282(5393):1504–1508, Nov. 1998.

[141] S. Higashi. Identification of a Region of beta -Amyloid Precursor Protein Essential for Its Gelatinase A Inhibitory Activity. *Journal of Biological Chemistry*, 278(16):14020–14028, Feb. 2003.

[142] M. J. Higley. Localized GABAergic inhibition of dendritic Ca2+ signalling. *Nature Reviews Neuroscience*, pages 1–6, Aug. 2014.

[143] C. L. Hinkle, S. Diestel, J. Lieberman, and P. F. Maness. Metalloprotease-induced ectodomain shedding of neural cell adhesion molecule (NCAM). *Journal of Neurobiology*, 66(12):1378–1395, 2006.

[144] A. Hotta, R. Inatome, J. Yuasa-Kawada, Q. Qin, H. Yamamura, and S. Yanagi. Critical role of collapsin response mediator protein-associated molecule CRAM for filopodia and growth cone development in neurons. *Molecular biology of the cell*, 16(1):32–39, 2005.

[145] P. Hotulainen and C. C. Hoogenraad. Actin in dendritic spines: connecting dynamics to function. *The Journal of Cell Biology*, 189(4):619–629, May 2010.

[146] T. T. Hu, G. Van den Bergh, L. Thorrez, K. Heylen, U. T. Eysel, and L. Arckens. Recovery from Retinal Lesions: Molecular Plasticity Mechanisms in Visual Cortex Far beyond the Deprived Zone. *Cerebral Cortex*, 21(12):2883–2892, Nov. 2011.

[147] X. Hu and C. Beeton. Detection of Functional Matrix Metalloproteinases by Zymography. *Journal of Visualized Experiments*, (45), 2010.

[148] D. H. Hubel and T. N. Wiesel. Receptive fields, binocular interaction and functional architecture in the cat's visual cortex. *The Journal of physiology*, 160(1):106, 1962.

[149] D. H. Hubel and T. N. Wiesel. Receptive fields of cells in striate cortex of very young, visually inexperienced kittens. *Journal of Neurophysiology*, 26(6):994–1002, 1963.

[150] M. Hübener. Mouse visual cortex. *Current Opinion in Neurobiology*, 13(4):413–420, Aug. 2003.

[151] A. D. Huberman and C. M. Niell. What can mice tell us about how vision works? *Trends in Neurosciences*, 34(9):464–473, Sept. 2011.

[152] G. W. Huntley. Synaptic circuit remodelling by matrix metalloproteinases in health and disease. *Nature Reviews Neuroscience*, 13:743–757, Oct. 2012.

[153] S. A. Irwin, M. Idupulapati, M. E. Gilbert, J. B. Harris, A. B. Chakravarti, E. J. Rogers, R. A. Crisostomo, B. P. Larsen, A. Mehta, C. J. Alcantara, B. Patel, R. A. Swain, I. J. Weiler, B. A. Oostra, and W. T. Greenough. Dendritic spine and dendritic field characteristics of layer V pyramidal neurons in the visual cortex of fragile-X knockout mice. *American Journal of Medical Genetics*, 111(2):140–146, July 2002.

[154] S. A. Irwin, B. Patel, M. Idupulapati, J. B. Harris, R. A. Crisostomo, B. P. Larsen, F. Kooy, P. J. Willems, P. Cras, P. B. Kozlowski, R. A. Swain, I. J. Weiler, and W. T. Greenough. Abnormal dendritic spine characteristics in the temporal and visual cortices of patients with fragile-X syndrome: a quantitative examination. *American Journal of Medical Genetics*, 98(2):161–167, Jan. 2001.

[155] G. Iurilli, D. Ghezzi, U. Olcese, G. Lassi, C. Nazzaro, R. Tonini, V. Tucci, F. Benfenati, and P. Medini. Sound-Driven Synaptic Inhibition in Primary Visual Cortex. *Neuron*, 73(4):814–828, Feb. 2012.

[156] B. C. Jackson, D. W. Nebert, and V. Vasiliou. Update of human and mouse matrix metalloproteinase families. *Human genomics*, 4(3):194–201, Feb. 2010.

[157] Y.-N. Jan and L. Y. Jan. The control of dendrite development. *Neuron*, 40(2):229–242, 2003.

[158] M. Jani, H. Tordai, M. Trexler, L. Bányai, and L. Patthy. Hydroxamate-based peptide inhibitors of matrix metalloprotease 2. *Biochimie*, 87(3-4):385–392, Mar. 2005.

[159] P. A. Janmey, J.-F. Leterrier, and H. Herrmann. Assembly and structure of neurofilaments. *Current opinion in colloid & interface science*, 8(1):40–47, 2003.

[160] J. L. Johnson, A. Dwivedi, M. Somerville, S. J. George, and A. C. Newby. Matrix Metalloproteinase (MMP)-3 Activates MMP-9 Mediated Vascular Smooth Muscle Cell Migration and Neointima Formation in Mice. *Arteriosclerosis, Thrombosis, and Vascular Biology*, 31(9):e35–e44, Aug. 2011.

[161] L. Kaczmarek and A. Chaudhuri. Sensory regulation of immediate-early gene expression in mammalian visual cortex: implications for functional mapping and neural plasticity. *Brain Research Reviews*, 23(3):237–256, Apr. 1997.

[162] V. A. Kalatsky and M. P. Stryker. New paradigm for optical imaging: temporally encoded maps of intrinsic signal. *Neuron*, 38(4):529–545, 2003.

[163] A. Kaliszewska, M. Bijata, L. Kaczmarek, and M. Kossut. Experience-Dependent Plasticity of the Barrel Cortex in Mice Observed with 2-DG Brain Mapping and c-Fos: Effects of MMP-9 KO. *Cerebral Cortex*, 22(9):2160–2170, Aug. 2012.

[164] M. Kaneko, D. Stellwagen, R. C. Malenka, and M. P. Stryker. Tumor Necrosis Factor-α Mediates One Component of Competitive, Experience-Dependent Plasticity in Developing Visual Cortex. *Neuron*, 58(5):673–680, June 2008.

[165] P. O. Kanold, Y. A. Kim, T. GrandPre, and C. J. Shatz. Co-regulation of ocular dominance plasticity and NMDA receptor subunit expression in glutamic acid decarboxylase-65 knock-out mice. *J Physiol*, 587(Pt 12):2857–2867, June 2009.

[166] M. Karetko and J. Skangiel-Kramska. Diverse functions of perineuronal nets. *Acta neurobiologiae experimentalis*, 69(4):564–577, 2009.

[167] N. Kayagaki, S. Warming, M. Lamkanfi, L. V. Walle, S. Louie, J. Dong, K. Newton, Y. Qu, J. Liu, S. Heldens, J. Zhang, W. P. Lee, M. Roose-Girma, and V. M. Dixit. Non-canonical inflammasome activation targets caspase-11. *Nature*, 479(7371):117–121, Oct. 2011.

[168] T. Keck, G. B. Keller, R. I. Jacobsen, U. T. Eysel, T. Bonhoeffer, and M. Hübener. Synaptic Scaling and Homeostatic Plasticity in the Mouse Visual Cortex In Vivo. *Neuron*, 80(2):327–334, Oct. 2013.

[169] T. Keck, V. Scheuss, R. I. Jacobsen, C. J. Wierenga, U. T. Eysel, T. Bonhoeffer, and M. Hübener. Loss of Sensory Input Causes Rapid Structural Changes of Inhibitory Neurons in Adult Mouse Visual Cortex. *Neuron*, 71(5):869–882, Sept. 2011.

[170] N. S. Kenneth, J. M. Younger, E. D. Hughes, D. Marcotte, P. A. Barker, T. L. Saunders, and C. S. Duckett. An inactivating caspase 11 passenger mutation originating from the 129 murine strain in mice targeted for c-IAP1. *Biochemical Journal*, 443(2):355–359, Mar. 2012.

[171] J. Y. Keow, K. M. Herrmann, and B. D. Crawford. Differential in vivo zymography: A method for observing matrix metalloproteinase activity in the zebrafish embryo. *Matrix Biology*, 30(3):169–177, Apr. 2011.

[172] J. Y. Keow, E. D. Pond, J. S. Cisar, B. F. Cravatt, and B. D. Crawford. Activity-Based Labeling of Matrix Metalloproteinases in Living Vertebrate Embryos. *PLoS ONE*, 7(8):e43434, Aug. 2012.

[173] E.-M. Kim and O. Hwang. Role of matrix metalloproteinase-3 in neurodegeneration. *Journal of Neurochemistry*, 116(1):22–32, Dec. 2010.

[174] S. Kim, R. Chang, C. Teunissen, Y. Gebremichael, and A. Petzold. Neurofilament stoichiometry simulations during neurodegeneration suggest a remarkable self-sufficient and stable in vivo protein structure. *Journal of the Neurological Sciences*, 307(1-2):132–138, Aug. 2011.

[175] K. T. Kishida and E. Klann. Sources and Targets of Reactive Oxygen Species in Synaptic Plasticity and Memory. *Antioxidants & Redox Signaling*, 0(0):061121054212009, Nov. 2006.

[176] D. J. Klionsky, F. C. Abdalla, H. Abeliovich, R. T. Abraham, A. Acevedo-Arozena, K. Adeli, L. Agholme, M. Agnello, et al. *Guidelines for the use and interpretation of assays for monitoring autophagy.* Apr. 2012.

[177] E. Knapska and L. Kaczmarek. A gene for neuronal plasticity in the mammalian brain: Zif268/Egr-1/NGFI-A/Krox-24/TIS8/ZENK? *Progress in Neurobiology*, 74(4):183–211, Nov. 2004.

[178] E. Knapska, V. Lioudyno, A. Kiryk, M. Mikosz, T. Gorkiewicz, P. Michaluk, M. Gawlak, M. Chaturvedi, G. Mochol, M. Balcerzyk, D. K. Wojcik, G. M. Wilczynski, and L. Kaczmarek. Reward Learning Requires Activity of Matrix Metalloproteinase-9 in the Central Amygdala. *Journal of Neuroscience*, 33(36):14591–14600, Sept. 2013.

[179] J. Kong, V. W.-Y. Tung, J. Aghajanian, and Z. Xu. Antagonistic roles of neurofilament subunits NF-H and NF-M against NF-L in shaping dendritic arborization in spinal motor neurons. *The Journal of Cell Biology*, 140(5):1167–1176, 1998.

[180] F. A. Konopacki, M. Rylski, E. Wilczek, R. Amborska, D. Detka, L. Kaczmarek, and G. M. Wilczynski. Synaptic localization of seizure-induced matrix metalloproteinase-9 mRNA. *Neuroscience*, 150(1):31–39, Nov. 2007.

[181] M. Kossut. Experience-dependent changes in function and anatomy of adult barrel cortex. *Experimental Brain Research*, 123(1-2):110–116, Nov. 1998.

[182] Y. Kovalchuk. Postsynaptic Induction of BDNF-Mediated Long-Term Potentiation. *Science*, 295(5560):1729–1734, Mar. 2002.

[183] M. E. Laramee, K. S. Rockland, S. Prince, G. Bronchti, and D. Boire. Principal Component and Cluster Analysis of Layer V Pyramidal Cells in Visual and Non-Visual Cortical Areas Projecting to the Primary Visual Cortex of the Mouse. *Cerebral Cortex*, 23(3):714–728, Feb. 2013.

[184] R. C. Lariviere and J.-P. Julien. Functions of intermediate filaments in neuronal development and disease. *Journal of Neurobiology*, 58(1):131–148, 2003.

[185] D. D. Larsen. Retrograde tracing with recombinant rabies virus reveals correlations between projection targets and dendritic architecture in

layer 5 of mouse barrel cortex. *Frontiers in neural circuits*, 1(5):doi: 10.3389/neuro.04.005.2007, 2008.

[186] D. D. Larsen and E. M. Callaway. Development of layer-specific axonal arborizations in mouse primary somatosensory cortex. *The Journal of Comparative Neurology*, 494(3):398–414, 2005.

[187] J. Lee, S. Giordano, and J. Zhang. Autophagy, mitochondria and oxidative stress: cross-talk and redox signalling. *Biochemical Journal*, 441(2):523–540, Dec. 2011.

[188] R. Lee, P. Kermani, K. K. Teng, and B. L. Hempstead. Regulation of cell survival by secreted proneurotrophins. *Science*, 294(5548):1945–1948, Nov. 2001.

[189] W.-C. A. Lee, J. L. Chen, H. Huang, J. H. Leslie, Y. Amitai, P. T. So, and E. Nedivi. A dynamic zone defines interneuron remodeling in the adult neocortex. *Proceedings of the National Academy of Sciences of the United States of America*, 105(50):19968–19973, Dec. 2008.

[190] H. Li, A. Gao, D. Feng, Y. Wang, L. Zhang, Y. Cui, B. Li, Z. Wang, and G. Chen. Evaluation of the Protective Potential of Brain Microvascular Endothelial Cell Autophagy on Blood–Brain Barrier Integrity During Experimental Cerebral Ischemia-Reperfusion Injury. *Translational Stroke Research*, 5(5):618–626, July 2014.

[191] Q. Li, H. Li, K. Roughton, X. Wang, G. Kroemer, K. Blomgren, and C. Zhu. Lithium reduces apoptosis and autophagy after neonatal hypoxia-ischemia. *Cell Death and Disease*, 1(7):e56–9, July 2010.

[192] Z. Li, K.-I. Okamoto, Y. Hayashi, and M. Sheng. The importance of dendritic mitochondria in the morphogenesis and plasticity of spines and synapses. *Cell*, 119(6):873–887, Dec. 2004.

[193] K. T. Lin, S. Sloniowski, D. W. Ethell, and I. M. Ethell. Ephrin-B2-induced Cleavage of EphB2 Receptor Is Mediated by Matrix Metalloproteinases to Trigger Cell Repulsion. *Journal of Biological Chemistry*, 283(43):28969–28979, Aug. 2008.

[194] G. Liu, P. Wang, X. Li, Y. Li, S. Xu, K. Uéda, P. Chan, and S. Yu. Alpha-synuclein promotes early neurite outgrowth in cultured primary neurons. *Journal of Neural Transmission*, 120(9):1331–1343, Feb. 2013.

[195] Q. Liu, F. Xie, A. Alvarado-Diaz, M. A. Smith, P. I. Moreira, X. Zhu, and G. Perry. Neurofilamentopathy in neurodegenerative diseases. *The open neurology journal*, 5:58, 2011.

[196] Q. Liu, F. Xie, S. L. Siedlak, A. Nunomura, K. Honda, P. I. Moreira, X. Zhua, M. A. Smith, and G. Perry. Neurofilament proteins in neurodegenerative diseases. *Cellular and Molecular Life Sciences*, 61(24):3057–3075, Dec. 2004.

[197] C. Lodovichi, N. Berardi, T. Pizzorusso, and L. Maffei. Effects of neurotrophins on cortical plasticity: same or different? *The Journal of Neuroscience*, 20(6):2155–2165, 2000.

[198] M. London and M. Häusser. Dendritic computation. *Annual Review of Neuroscience*, 28:503–532, 2005.

[199] B. Lu, G. Nagappan, X. Guan, P. J. Nathan, and P. Wren. BDNF-based synaptic repair as a disease-modifying strategy for neurodegenerative diseases. *Nature Reviews Neuroscience*, 14(6):401–16, May 2013.

[200] D. Luo. Alternative Splicing and Promoter Usage Generates an Intracellular Stromelysin 3 Isoform Directly Translated as an Active Matrix Metalloproteinase. *Journal of Biological Chemistry*, 277(28):25527–25536, May 2002.

[201] A. F. MacAskill and J. T. Kittler. Control of mitochondrial transport and localization in neurons. *Trends in Cell Biology*, 20(2):102–112, Feb. 2010.

[202] L. Maffei, N. Berardi, L. Domenici, V. Parisi, and T. Pizzorusso. Nerve growth factor (NGF) prevents the shift in ocular dominance distribution of visual cortical neurons in monocularly deprived rats. *The Journal of Neuroscience*, 12(12):4651–4662, Dec. 1992.

[203] M. Majdan and C. J. Shatz. Effects of visual experience on activity-dependent gene regulation in cortex. *Nature Neuroscience*, 9(5):650–659, Apr. 2006.

[204] S. Malanowski and C. F. Craver. The spine problem: finding a function for dendritic spines. *Frontiers in neuroanatomy*, 8:95, 2014.

[205] F. Mannello and V. Medda. Nuclear localization of Matrix metalloproteinases. *Progress in Histochemistry and Cytochemistry*, 47(1):27–58, Mar. 2012.

[206] G. Marino, P. F. Huesgen, U. Eckhard, C. M. Overall, W. P. Schröder, and C. Funk. Family-wide characterization of Matrix Metallo-proteinases from Arabidopsis thaliana reveals their distinct proteolytic activity and cleavage site specificity. *Biochemical Journal*, Oct. 2013.

[207] J. H. Marshel, M. E. Garrett, I. Nauhaus, and E. M. Callaway. Functional Specialization of Seven Mouse Visual Cortical Areas. *Neuron*, 72(6):1040–1054, Dec. 2011.

[208] E. Martens, A. Leyssen, I. Van Aelst, P. Fiten, H. Piccard, J. Hu, F. J. Descamps, P. E. Van den Steen, P. Proost, J. Van Damme, G. M. Liuzzi, P. Riccio, E. Polverini, and G. Opdenakker. A monoclonal antibody inhibits gelatinase B/MMP-9 by selective binding to part of the catalytic domain and not to the fibronectin or zinc binding domains. *Biochimica et Biophysica Acta (BBA) - General Subjects*, 1770(2):178–186, Feb. 2007.

[209] I. Massova, L. P. Kotra, R. Fridman, and S. Mobashery. Matrix metalloproteinases: structures, evolution, and diversification. *FASEB journal : official publication of the Federation of American Societies for Experimental Biology*, 12(12):1075–1095, Sept. 1998.

[210] N. Mataga, N. Nagai, and T. K. Hensch. Permissive proteolytic activity for visual cortical plasticity. *Proceedings of the National Academy of Sciences*, 99(11):7717–7721, May 2002.

[211] M. P. Mattson, M. Gleichmann, and A. Cheng. Mitochondria in Neuroplasticity and Neurological Disorders. *Neuron*, 60(5):748–766, Dec. 2008.

[212] J. F. Maya-Vetencourt, L. Baroncelli, A. Viegi, E. Tiraboschi, E. Castren, A. Cattaneo, and L. Maffei. IGF-1 Restores Visual Cortex Plasticity in Adult Life by Reducing Local GABA Levels. *Neural Plasticity*, 2012(2):1–10, 2012.

[213] A. K. McAllister, D. C. Lo, and L. C. Katz. Neurotrophins regulate dendritic growth in developing visual cortex. *Neuron*, 15(4):791–803, 1995.

[214] L. J. McCawley and L. M. Matrisian. Matrix metalloproteinases: they're not just for matrix anymore! *Current opinion in cell biology*, 13(5):534–540, 2001.

[215] S. McFarlane. Metalloproteases: carving out a role in axon guidance. *Neuron*, 37(4):559–562, Feb. 2003.

[216] S. E. Meighan, P. C. Meighan, P. Choudhury, C. J. Davis, M. L. Olson, P. A. Zornes, J. W. Wright, and J. W. Harding. Effects of extracellular matrix-degrading proteases matrix metalloproteinases 3 and 9 on spatial learning and synaptic plasticity. *Journal of Neurochemistry*, 96(5):1227–1241, Mar. 2006.

[217] J. Mercapide, R. Lopez De Cicco, J. S. Castresana, and A. J. P. Klein-Szanto. Stromelysin-1/matrix metalloproteinase-3 (MMP-3) expression accounts for invasive properties of human astrocytoma cell lines. *International Journal of Cancer*, 106(5):676–682, July 2003.

[218] M. A. Meredith and B. E. Stein. Visual, auditory, and somatosensory convergence on cells in superior colliculus results in multisensory integration. *Journal of Neurophysiology*, 56(3):640–662, Sept. 1986.

[219] E. B. Merriam, M. Millette, D. C. Lumbard, W. Saengsawang, T. Fothergill, X. Hu, L. Ferhat, and E. W. Dent. Synaptic Regulation of Microtubule Dynamics in Dendritic Spines by Calcium, F-Actin, and Drebrin. *Journal of Neuroscience*, 33(42):16471–16482, Oct. 2013.

[220] C. Métin, D. Deléglise, T. Serafini, T. E. Kennedy, and M. Tessier-Lavigne. A role for netrin-1 in the guidance of cortical efferents. *Development (Cambridge, England)*, 124(24):5063–5074, Dec. 1997.

[221] Q.-L. Miao, Q. Ye, and X.-H. Zhang. Perineuronal net, CSPG receptor and their regulation of neural plasticity. *Acta physiologica Sinica*, 66(4):387–397, Aug. 2014.

[222] P. Michaluk, L. Kolodziej, B. Mioduszewska, G. M. Wilczynski, J. Dzwonek, J. Jaworski, D. C. Gorecki, O. P. Ottersen, and L. Kaczmarek. beta-Dystroglycan as a Target for MMP-9, in Response to Enhanced Neuronal Activity. *Journal of Biological Chemistry*, 282(22):16036–16041, Mar. 2007.

[223] P. Michaluk, L. Mikasova, L. Groc, R. Frischknecht, D. Choquet, and L. Kaczmarek. Matrix Metalloproteinase-9 Controls NMDA Receptor Surface Diffusion through Integrin 1 Signaling. *Journal of Neuroscience*, 29(18):6007–6012, May 2009.

[224] P. Michaluk, M. Wawrzyniak, P. Alot, M. Szczot, P. Wyrembek, K. Mercik, N. Medvedev, E. Wilczek, M. De Roo, W. Zuschratter, D. Muller, G. M. Wilczynski, J. W. Mozrzymas, M. G. Stewart, L. Kaczmarek, and J. Wlodarczyk. Influence of matrix metalloproteinase MMP-9 on dendritic spine morphology. *Journal of Cell Science*, 124(19):3369–3380, Sept. 2011.

[225] J. P. Miller, J. Holcomb, I. Al-Ramahi, M. de Haro, J. Gafni, N. Zhang, E. Kim, M. Sanhueza, C. Torcassi, S. Kwak, J. Botas, R. E. Hughes, and L. M. Ellerby.

Matrix Metalloproteinases Are Modifiers of Huntingtin Proteolysis and Toxicity in Huntington's Disease. *Biochemistry Research International*, 2012(3):199–212, 2012.

[226] M. W. Miller and B. A. Vogt. Direct connections of rat visual cortex with sensory, motor, and association cortices. *The Journal of Comparative Neurology*, 226(2):184–202, June 1984.

[227] E. A. Milward, C. Fitzsimmons, A. szklarczyk, and K. Conant. The matrix metalloproteinases and CNS plasticity: An overview. *Journal of neuroimmunology*, 187(1-2):9–19, July 2007.

[228] H. Mizoguchi, K. Yamada, and T. Nabeshima. Matrix Metalloproteinases Contribute to Neuronal Dysfunction in Animal Models of Drug Dependence, Alzheimer's Disease, and Epilepsy. *Biochemistry Research International*, 2011(12):1–10, 2011.

[229] N. Mizushima and T. Yoshimori. How to interpret LC3 immunoblotting. *Autophagy*, 3(6):542–545, Nov. 2007.

[230] N. Mizushima, T. Yoshimori, and Y. Ohsumi. The Role of Atg Proteins in Autophagosome Formation. *Annual review of cell and developmental biology*, 27(1):107–132, Nov. 2011.

[231] S. H. Mokhtar, M. M. Bakhuraysah, D. S. Cram, and S. Petratos. The Beta-Amyloid Protein of Alzheimer's Disease: Communication Breakdown by Modifying the Neuronal Cytoskeleton. *International Journal of Alzheimer's Disease*, 2013(9):1–15, 2013.

[232] B. J. Molyneaux, P. Arlotta, J. R. L. Menezes, and J. D. Macklis. Neuronal subtype specification in the cerebral cortex. *Nature Reviews Neuroscience*, 8(6):427–437, June 2007.

[233] E. M. Y. Moresco. Integrin-Mediated Dendrite Branch Maintenance Requires Abelson (Abl) Family Kinases. *Journal of Neuroscience*, 25(26):6105–6118, June 2005.

[234] L. P. Morin and K. M. Studholme. Retinofugal Projections in the Mouse. *The Journal of Comparative Neurology*, 522(16):3733–53, May 2014.

[235] F. J. Moy, P. K. Chanda, J. Chen, S. Cosmi, W. Edris, J. I. Levin, T. S. Rush, J. Wilhelm, and R. Powers. Impact of Mobility on Structure-Based Drug Design for the MMPs. *Journal of the American Chemical Society*, 124(43):12658–12659, Oct. 2002.

[236] T. D. Mrsic-Flogel, S. B. Hofer, K. Ohki, R. C. Reid, T. Bonhoeffer, and M. Hübener. Homeostatic Regulation of Eye-Specific Responses in Visual Cortex during Ocular Dominance Plasticity. *Neuron*, 54(6):961–972, June 2007.

[237] E. M. Muir, K. H. Adcock, D. A. Morgenstern, R. Clayton, N. von Stillfried, K. Rhodes, C. Ellis, J. W. Fawcett, and J. H. Rogers. Matrix metalloproteases and their inhibitors are produced by overlapping populations of activated astrocytes. *Molecular brain research*, 100(1-2):103–117, Apr. 2002.

[238] C. M. Müller and C. B. Griesinger. Tissue plasminogen activator mediates reverse occlusion plasticity in visual cortex. *Nature Neuroscience*, 1(1):47–53, 1998.

[239] T. Murakami, T. Murakami, W. D. Su, A. Ohtsuka, K. Abe, and Y. Ninomiya. Perineuronal nets of proteoglycans in the adult mouse brain are digested by collagenase. *Archives of histology and cytology*, 62(2):199–204, 1999.

[240] G. Murphy, H. Stanton, S. Cowell, G. Butler, V. Knäuper, S. Atkinson, and J. Gavrilovic. Mechanisms for pro matrix metalloproteinase activation. *APMIS : acta pathologica, microbiologica, et immunologica Scandinavica*, 107(1):38–44, Jan. 1999.

[241] M. P. Murphy. How mitochondria produce reactive oxygen species. *Biochemical Journal*, 417(1):1, Jan. 2009.

[242] T. Myochin, K. Hanaoka, T. Komatsu, T. Terai, and T. Nagano. Design Strategy for a Near-Infrared Fluorescence Probe for Matrix Metalloproteinase Utilizing Highly Cell Permeable Boron Dipyrromethene. *Journal of the American Chemical Society*, 134(33):13730–13737, Aug. 2012.

[243] H. Nagase. Activation mechanisms of matrix metalloproteinases. *Biological chemistry*, 378(3-4):151–160, 1996.

[244] H. Nagase, C. G. Fields, and G. B. Fields. Design and characterization of a fluorogenic substrate selectively hydrolyzed by stromelysin 1 (matrix metalloproteinase-3). *Journal of Biological Chemistry*, 269(33):20952–20957, Aug. 1994.

[245] H. Nagase, R. Visse, and G. Murphy. Structure and function of matrix metalloproteinases and TIMPs. *Cardiovascular Research*, 69(3):562–573, Feb. 2006.

[246] H. Nagase and J. F. Woessner. Matrix metalloproteinases. *Journal of Biological Chemistry*, 274(31):21491–21494, 1999.

[247] V. Nagy, O. Bozdagi, A. Matynia, M. Balcerzyk, P. Okulski, J. Dzwonek, R. M. Costa, A. J. Silva, L. Kaczmarek, and G. W. Huntley. Matrix metalloproteinase-9 is required for hippocampal late-phase long-term potentiation and memory. *Journal of Neuroscience*, 26(7):1923–1934, Feb. 2006.

[248] R. Nakai, C. M. Salisbury, H. Rosen, and B. F. Cravatt. Ranking the selectivity of PubChem screening hits by activity-based protein profiling: MMP13 as a case study. *Bioorganic & Medicinal Chemistry*, 17(3):1101–1108, Feb. 2009.

[249] T. Ng, J. R. Ryu, J. H. Sohn, T. Tan, H. Song, G.-l. Ming, and E. L. K. Goh. Class 3 Semaphorin Mediates Dendrite Growth in Adult Newborn Neurons through Cdk5/FAK Pathway. *PLoS ONE*, 8(6):e65572, June 2013.

[250] H. Ni, L. Huang, N. Chen, F. Zhang, D. Liu, M. Ge, S. Guan, Y. Zhu, and J.-H. Wang. Upregulation of Barrel GABAergic Neurons Is Associated with Cross-Modal Plasticity in Olfactory Deficit. *PLoS ONE*, 5(10):e13736, Oct. 2010.

[251] M. M. Niblock, J. K. Brunso-Bechtold, and D. R. Riddle. Insulin-like growth factor I stimulates dendritic growth in primary somatosensory cortex. *Journal of Neuroscience*, 20(11):4165–4176, June 2000.

[252] M. Niedringhaus, X. Chen, R. Dzakpasu, and K. Conant. MMPs and Soluble ICAM-5 Increase Neuronal Excitability within In Vitro Networks of Hippocampal Neurons. *PLoS ONE*, 7(8):e42631, Aug. 2012.

[253] C. M. Niell. Exploring the Next Frontier of Mouse Vision. *Neuron*, 72(6):889–892, Dec. 2011.

[254] E. A. Nimchinsky, B. L. Sabatini, and K. Svoboda. Structure and function of dendritic spines. *Annual Review of Physiology*, 64(1):313–353, Mar. 2002.

[255] L. A. Nordstrom, J. Lochner, W. Yeung, and G. Ciment. The metalloproteinase stromelysin-1 (transin) mediates PC12 cell growth cone invasiveness through basal laminae. *Molecular and Cellular Neuroscience*, 6(1):56–68, 1995.

[256] J. Nys, J. Aerts, E. Ytebrouck, S. Vreysen, A. Laeremans, and L. Arckens. The cross-modal aspect of mouse visual cortex plasticity induced by monocular enucleation is age dependent. *The Journal of Comparative Neurology*, 522(4):950–970, Mar. 2014.

[257] J. Nys, I. Scheyltjens, and L. Arckens. Visual system plasticity in mammals: the story of monocular enucleation- induced vision loss. *Frontiers in systems neuroscience*, pages 1–62, Nov. submitted.

[258] Y. Ogata, J. J. Enghild, and H. Nagase. Matrix metalloproteinase 3 (stromelysin) activates the precursor for the human matrix metalloproteinase 9. *Journal of Biological Chemistry*, 267(6):3581–3584, 1992.

[259] T. Okamoto, T. Akaike, T. Sawa, Y. Miyamoto, A. van der Vliet, and H. Maeda. Activation of Matrix Metalloproteinases by Peroxynitrite-induced Protein S-Glutathiolation via Disulfide S-Oxide Formation. *Journal of Biological Chemistry*, 276(31):29596–29602, Aug. 2001.

[260] P. Okulski, T. M. Jay, J. Jaworski, K. Duniec, J. Dzwonek, F. A. Konopacki, G. M. Wilczynski, A. Sánchez-Capelo, J. Mallet, and L. Kaczmarek. TIMP-1 Abolishes MMP-9-Dependent Long-lasting Long-term Potentiation in the Prefrontal Cortex. *Biological Psychiatry*, 62(4):359–362, Aug. 2007.

[261] P. Oliveira-Silva, P. B. Jurgilas, P. Trindade, P. Campello-Costa, J. Perales, W. Savino, and C. A. Serfaty. Matrix metalloproteinase-9 is involved in the development and plasticity of retinotectal projections in rats. *Neuroimmunomodulation*, 14(3-4):144–149, 2007.

[262] M. L. Olson, P. C. Meighan, T. E. Brown, A. L. Asay, C. C. Benoist, J. W. Harding, and J. W. Wright. Hippocampal MMP-3 elevation is associated with passive avoidance conditioning. *Regulatory Peptides*, 146(1-3):19–25, Feb. 2008.

[263] S. Oray, A. Majewska, and M. Sur. Dendritic Spine Dynamics Are Regulated by Monocular Deprivation and Extracellular Matrix Degradation. *Neuron*, 44(6):1021–1030, Dec. 2004.

[264] C. M. Overall and G. S. Butler. Protease Yoga: Extreme Flexibility of a Matrix Metalloproteinase. *Structure*, 15(10):1159–1161, Oct. 2007.

[265] C. M. Overall and O. Kleifeld. Towards third generation matrix metalloproteinase inhibitors for cancer therapy. *British journal of cancer*, 94(7):941–946, Apr. 2006.

[266] C. M. Overall and O. Kleifeld. Tumour microenvironment - opinion: validating matrix metalloproteinases as drug targets and anti-targets for cancer therapy. *Nature Reviews Cancer*, 6(3):227–239, Mar. 2006.

[267] C. M. Overall and C. López-Otín. Strategies for mmp inhibition in cancer: innovations for the post-trial era. *Nature Reviews Cancer*, 2(9):657–672, Sept. 2002.

[268] T. Paperna and R. Malach. Patterns of sensory intermodality relationships in the cerebral cortex of the rat. *The Journal of Comparative Neurology*, 308(3):432–456, June 1991.

[269] W. C. Parks, C. L. Wilson, and Y. S. López-Boado. Matrix metalloproteinases as modulators of inflammation and innate immunity. *Nature Reviews Immunology*, 4(8):617–629, Aug. 2004.

[270] M. Paulussen, S. Jacobs, E. Gucht, P. R. Hof, and L. Arckens. Cytoarchitecture of the mouse neocortex revealed by the low-molecular-weight neurofilament protein subunit. *Brain Structure and Function*, 216(3):183–199, Apr. 2011.

[271] A. A. Penn and C. J. Shatz. Brain waves and brain wiring: the role of endogenous and sensory-driven neural activity in development. *Pediatric research*, 45(4 Pt 1):447–458, Apr. 1999.

[272] A. Peters and I. R. Kaiserman-Abramof. The small pyramidal neuron of the rat cerebral cortex. The perikaryon, dendrites and spines. *The American journal of anatomy*, 127(4):321–355, Apr. 1970.

[273] S. Petratos and J. Y. Lee. Stop CRMPing my style: a new competitive model of CRMP oligomerization. *Journal of Neurochemistry*, 125(6):800–802, Mar. 2013.

[274] S. Petratos, Q. X. Li, A. J. George, X. Hou, M. L. Kerr, S. E. Unabia, I. Hatzinisiriou, D. Maksel, M. I. Aguilar, and D. H. Small. The -amyloid protein of Alzheimer's disease increases neuronal CRMP-2 phosphorylation by a Rho-GTP mechanism. *Brain*, 131(1):90–108, Dec. 2007.

[275] K. Phromnoi, S. Yodkeeree, S. Anuchapreeda, and P. Limtrakul. Inhibition of MMP-3 activity and invasion of the MDA-MB-231 human invasive breast carcinoma cell line by bioflavonoids. *Nature Publishing Group*, 30(8):1169–1176, July 2009.

[276] H. Piccard, P. E. Van den Steen, and G. Opdenakker. Hemopexin domains as multifunctional liganding modules in matrix metalloproteinases and other proteins. *Journal of Leukocyte Biology*, 81(4):870–892, Jan. 2007.

[277] T. Pizzorusso. Reactivation of Ocular Dominance Plasticity in the Adult Visual Cortex. *Science*, 298(5596):1248–1251, Nov. 2002.

[278] F. Polleux, T. Morrow, and A. Ghosh. Semaphorin 3A is a chemoattractant for cortical apical dendrites. *Nature*, 404(6778):567–573, 2000.

[279] A. Polsky, B. W. Mel, and J. Schiller. Computational subunits in thin dendrites of pyramidal cells. *Nature Neuroscience*, 7(6):621–627, May 2004.

[280] V. Popov, N. I. Medvedev, H. A. Davies, and M. G. Stewart. Mitochondria form a filamentous reticular network in hippocampal dendrites but are present as discrete bodies in axons: A three-dimensional ultrastructural study. *The Journal of Comparative Neurology*, 492(1):50–65, 2005.

[281] G. T. Prusky. Rapid Quantification of Adult and Developing Mouse Spatial Vision Using a Virtual Optomotor System. *Investigative Ophthalmology & Visual Science*, 45(12):4611–4616, Dec. 2004.

[282] G. T. Prusky, P. W. West, and R. M. Douglas. Behavioral assessment of visual acuity in mice and rats. *Vision Research*, 40(16):2201–2209, 2000.

[283] M. Ptito and R. Kupers. Cross-modal plasticity in early blindness. *Journal of Integrative Neuroscience*, 4(04):479–488, 2005.

[284] D. T. Puerta, J. A. Lewis, and S. M. Cohen. New Beginnings for Matrix Metalloproteinase Inhibitors: Identification of High-Affinity Zinc-Binding Groups. *Journal of the American Chemical Society*, 126(27):8388–8389, July 2004.

[285] H.-J. Ra and W. C. Parks. Control of matrix metalloproteinase catalytic activity. *Matrix Biology*, 26(8):587–596, 2007.

[286] M. V. Rao and R. A. Nixon. Defective neurofilament transport in mouse models of amyotrophic lateral sclerosis: a review. *Neurochemical Research*, 28(7):1041–1047, July 2003.

[287] J. Redondo-MuNoz, E. Ugarte-Berzal, M. J. Terol, P. E. Van den Steen, M. H. del Cerro, M. Roderfeld, E. Roeb, G. Opdenakker, J. A. GarcIa-Marco, and A. GarcIa-Pardo. Matrix Metalloproteinase-9 Promotes Chronic Lymphocytic Leukemia B Cell Survival through Its Hemopexin Domain. *Cancer Cell*, 17(2):160–172, Feb. 2010.

[288] A. K. Reeve, K. J. Krishnan, M. R. Duchen, and D. M. Turnbull. *Mitochondrial Dysfunction in Neurodegenerative Disorders*. Springer Science & Business Media, Nov. 2011.

[289] R. Reig and G. Silberberg. Multisensory Integration in the Mouse Striatum. *Neuron*, 83(5):1200–1212, Sept. 2014.

[290] A. Remacle. Membrane type I-matrix metalloproteinase (MT1-MMP) is internalised by two different pathways and is recycled to the cell surface. *Journal of Cell Science*, 116(19):3905–3916, Oct. 2003.

[291] D. Ricard, V. Rogemond, E. Charrier, M. Aguera, D. Bagnard, M. F. Belin, N. Thomasset, and J. Honnorat. Isolation and expression pattern of human Unc-33-like phosphoprotein 6/collapsin response mediator protein 5 (Ulip6/CRMP5): coexistence with Ulip2/CRMP2 in Sema3a- sensitive oligodendrocytes. *Journal of Neuroscience*, 21(18):7203–7214, Sept. 2001.

[292] W. C. Risher, T. Ustunkaya, J. Singh Alvarado, and C. Eroglu. Rapid Golgi Analysis Method for Efficient and Unbiased Classification of Dendritic Spines. *PLoS ONE*, 9(9):e107591, Sept. 2014.

[293] S. Rivera, M. Khrestchatisky, L. Kaczmarek, G. A. Rosenberg, and D. M. Jaworski. Metzincin Proteases and Their Inhibitors: Foes or Friends in Nervous System Physiology? *Journal of Neuroscience*, 30(46):15337–15357, Nov. 2010.

[294] G. Rizzolatti and M. Matelli. Two different streams form the dorsal visual system: anatomy and functions. *Experimental Brain Research*, 153(2):146–157, Nov. 2003.

[295] D. Rodríguez, C. J. Morrison, and C. M. Overall. Matrix metalloproteinases: What do they not do? New substrates and biological roles identified by murine models and proteomics. *Biochimica et Biophysica Acta (BBA) - Molecular Cell Research*, 1803(1):39–54, Jan. 2010.

[296] M. Rothenberg, A. Nelson, and K. Hande. New Drugs on the Horizon: Matrix Metalloproteinase Inhibitors. *The oncologist*, 3(4):271–274, 1998.

[297] D. Rouy, I. Ernens, C. Jeanty, and D. R. Wagner. Plasma storage at -80 °C does not protect matrix metalloproteinase-9 from degradation. *Analytical Biochemistry*, 338(2):294–298, Mar. 2005.

[298] A. Saghatelian, N. Jessani, A. Joseph, M. Humphrey, and B. F. Cravatt. Activity-based probes for the proteomic profiling of metalloproteases. *Proceedings of the National Academy of Sciences*, 101(27):10000–10005, July 2004.

[299] A. Sale, N. Berardi, and L. Maffei. Enrich the environment to empower the brain. *Trends in Neurosciences*, 32(4):233–239, Apr. 2009.

[300] N. B. Sawtell, M. Y. Frenkel, B. D. Philpot, K. Nakazawa, S. Tonegawa, and M. F. Bear. NMDA Receptor-Dependent Ocular Dominance Plasticity in Adult Visual Cortex. *Neuron*, 38(6):977–985, June 2003.

[301] E. F. Schmidt and S. M. Strittmatter. *The CRMP Family of Proteins and Their Role in Sema3A Signaling*. Springer New York, New York, NY, 2007.

[302] S. Schuett, T. Bonhoeffer, and M. Hübener. Mapping retinotopic structure in mouse visual cortex with optical imaging. *Journal of Neuroscience*, 22(15):6549–6559, Aug. 2002.

[303] G. Schulze-Tanzil, P. de Souza, H. J. Merker, and M. Shakibaei. Co-localization of integrins and matrix metalloproteinases in the extracellular matrix of chondrocyte cultures. *Histology and Histopathology*, 16(4):1081, 2001.

[304] N. Sela-Passwell, G. Rosenblum, T. Shoham, and I. Sagi. Structural and functional bases for allosteric control of MMP activities: Can it pave the path for selective inhibition? *Biochimica et Biophysica Acta (BBA) - Molecular Cell Research*, 1803(1):29–38, Jan. 2010.

[305] D.-W. Seo, H. Li, L. Guedez, P. T. Wingfield, T. Diaz, R. Salloum, B.-y. Wei, and W. G. Stetler-Stevenson. TIMP-2 mediated inhibition of angiogenesis: an MMP-independent mechanism. *Cell*, 114(2):171–180, July 2003.

[306] S. Y. Shu, G. Ju, and L. Z. Fan. The glucose oxidase-DAB-nickel method in peroxidase histochemistry of the nervous system. *Neuroscience Letters*, 85(2):169–171, Feb. 1988.

[307] K. Si-Tayeb, A. Monvoisin, C. Mazzocco, S. Lepreux, M. Decossas, G. Cubel, D. Taras, J.-F. Blanc, D. R. Robinson, and J. Rosenbaum. Matrix Metalloproteinase 3 Is Present in the Cell Nucleus and Is Involved in Apoptosis. *The American Journal of Pathology*, 169(4):1390–1401, Oct. 2006.

[308] S. Solé, V. Petegnief, R. Gorina, A. Chamorro, and A. M. Planas. Activation of matrix metalloproteinase-3 and agrin cleavage in cerebral ischemia/reperfusion. *Journal of neuropathology and experimental neurology*, 63(4):338–349, Apr. 2004.

[309] M. Spolidoro, E. Putignano, C. Munafo, L. Maffei, and T. Pizzorusso. Inhibition of Matrix Metalloproteinases Prevents the Potentiation of Nondeprived-Eye Responses after Monocular Deprivation in Juvenile Rats. *Cerebral Cortex*, 22(3):725–734, Feb. 2012.

[310] M. Spolidoro, A. Sale, N. Berardi, and L. Maffei. Plasticity in the adult brain: lessons from the visual system. *Experimental Brain Research*, 192(3):335–341, July 2008.

[311] N. Spruston. Pyramidal neurons: dendritic structure and synaptic integration. *Nature Reviews Neuroscience*, 9(3):206–221, Mar. 2008.

[312] M. Stawarski, M. Stefaniuk, and J. Wlodarczyk. Matrix metalloproteinase-9 involvement in the structural plasticity of dendritic spines. *Frontiers in neuroanatomy*, 8:68, 2014.

[313] B. E. Stein and M. A. Meredith. Multisensory integration. Neural and behavioral solutions for dealing with stimuli from different sensory modalities. *Annals of the New York Academy of Sciences*, 608:51–65– discussion 65–70, 1990.

[314] M. D. Sternlicht and Z. Werb. How matrix metalloproteinases regulate cell behavior. *Annual review of cell and developmental biology*, 17:463–516, 2001.

[315] W. G. Stetler-Stevenson. Tissue Inhibitors of Metalloproteinases in Cell Signaling: Metalloproteinase-Independent Biological Activities. *Science Signaling*, 1(27):re6–re6, July 2008.

[316] B. G. Szaro and M. J. Strong. Post-transcriptional control of neurofilaments: New roles in development, regeneration and neurodegenerative disease. *Trends in Neurosciences*, 33(1):27–37, Jan. 2010.

[317] A. szklarczyk and L. Kaczmarek. Physiology of matrix MMPs and their tissue inhibitors in the brain . *Brain Biology*, pages 1–3, Oct. 2005.

[318] A. Szklarczyk, J. Lapinska, M. Rylski, R. D. G. McKay, and L. Kaczmarek. Matrix metalloproteinase-9 undergoes expression and activation during dendritic remodeling in adult hippocampus. *Journal of Neuroscience*, 22(3):920–930, Feb. 2002.

[319] A. Szklarczyk, G. Oyler, R. McKay, C. Gerfen, and K. Conant. Cleavage of neuronal synaptosomal-associated protein of 25 kDa by exogenous matrix metalloproteinase-7. *Journal of Neurochemistry*, 102(4):1256–1263, Aug. 2007.

[320] F. Talaei, V. M. Van Praag, M. H. Shishavan, S. W. Landheer, H. Buikema, and R. H. Henning. Increased protein aggregation in Zucker diabetic fatty rat brain: identification of key mechanistic targets and the therapeutic application of hydrogen sulfide. *BMC cell biology*, 15:1, 2014.

[321] J. Tang, M. Myers, K. A. Bosnick, and L. E. Brus. Magnetite Fe3O4 Nanocrystals: Spectroscopic Observation of Aqueous Oxidation Kinetics. *The Journal of Physical Chemistry B*, 107(30):7501–7506, July 2003.

[322] I. Tanida, N. Minematsu-Ikeguchi, T. Ueno, and E. Kominami. Lysosomal Turnover, but Not a Cellular Level, of Endogenous LC3 is a Marker for Autophagy. *Autophagy*, 1(2):84–91, 2005.

[323] J. Thevenard, L. Verzeaux, J. Devy, N. Etique, A. Jeanne, C. Schneider, C. Hachet, G. Ferracci, M. David, L. Martiny, E. Charpentier, M. Khrestchatisky, S. Rivera, S. Dedieu, and H. Emonard. Low-Density Lipoprotein Receptor-Related Protein-1 Mediates Endocytic Clearance of Tissue Inhibitor of Metalloproteinases-1 and Promotes Its Cytokine-Like Activities. *PLoS ONE*, 9(7):e103839, July 2014.

[324] A. M. Thomson and A. P. Bannister. Interlaminar connections in the neocortex. *Cerebral Cortex*, 13(1):5–14, Jan. 2003.

[325] L. Tian, M. Stefanidakis, L. Ning, P. Van Lint, H. Nyman-Huttunen, C. Libert, S. Itohara, M. Mishina, H. Rauvala, and C. G. Gahmberg. Activation of NMDA receptors promotes dendritic spine development through MMP-mediated ICAM-5 cleavage. *The Journal of Cell Biology*, 178(4):687–700, Aug. 2007.

[326] E. Tiraboschi, R. Guirado, D. Greco, P. Auvinen, J. F. Maya-Vetencourt, L. Maffei, and E. Castren. Gene Expression Patterns Underlying the Reinstatement of Plasticity in the Adult Visual System. *Neural Plasticity*, 2013(2):1–8, 2013.

[327] A. Tocchi and W. C. Parks. Functional interactions between matrix metalloproteinases and glycosaminoglycans. *FEBS Journal*, 280(10):2332–2341, Mar. 2013.

[328] L. M. Traub. Tickets to ride: selecting cargo for clathrin-regulated internalization. *Nature Reviews Molecular Cell Biology*, 10(9):583–596, Sept. 2009.

[329] L. Trinkle-Mulcahy, S. Boulon, Y. W. Lam, R. Urcia, F.-M. Boisvert, F. Vandermoere, N. A. Morrice, S. Swift, U. Rothbauer, H. Leonhardt, and A. Lamond. Identifying specific protein interaction partners using quantitative mass spectrometry and bead proteomes. *The Journal of Cell Biology*, 183(2):223–239, Oct. 2008.

[330] D. Tsay and R. Yuste. On the electrical function of dendritic spines. *Trends in Neurosciences*, 27(2):77–83, Feb. 2004.

[331] G. G. Turrigiano. The Self-Tuning Neuron: Synaptic Scaling of Excitatory Synapses. *Cell*, 135(3):422–435, Oct. 2008.

[332] R. Ulrich, I. Gerhauser, F. Seeliger, W. Baumg auml rtner, and S. Alldinger. Matrix Metalloproteinases and Their Inhibitors in the Developing Mouse Brain and Spinal Cord: A Reverse Transcription Quantitative Polymerase Chain Reaction Study. *Developmental Neuroscience*, 27(6):408–418, 2005.

[333] L. Van Brussel, A. Gerits, and L. Arckens. Identification and localization of functional subdivisions in the visual cortex of the adult mouse. *The Journal of Comparative Neurology*, 514(1):107–116, May 2009.

[334] L. Van Brussel, A. Gerits, and L. Arckens. Evidence for Cross-Modal Plasticity in Adult Mouse Visual Cortex Following Monocular Enucleation. *Cerebral Cortex*, 21(9):2133–2146, Aug. 2011.

[335] G. Van den Bergh and L. Arckens. Fluorescent two-dimensional difference gel electrophoresis unveils the potential of gel-based proteomics. *Current Opinion in Biotechnology*, 15(1):38–43, Feb. 2004.

[336] E. Van der Gucht, P. R. Hof, L. Van Brussel, K. Burnat, and L. Arckens. Neurofilament Protein and Neuronal Activity Markers Define Regional Architectonic Parcellation in the Mouse Visual Cortex. *Cerebral Cortex*, 17(12):2805–2819, Mar. 2007.

[337] S. D. Van Hooser. Similarity and Diversity in Visual Cortex: Is There a Unifying Theory of Cortical Computation? *The Neuroscientist*, 13(6):639–656, Nov. 2007.

[338] I. Van Hove, K. Lemmens, S. Van de Velde, M. Verslegers, and L. Moons. Matrix metalloproteinase-3 in the central nervous system: a look on the bright side. *Journal of Neurochemistry*, 123(2):203–216, Sept. 2012.

[339] I. Van Hove, M. Verslegers, T. Buyens, N. Delorme, K. Lemmens, S. Stroobants, I. Gantois, R. D'Hooge, and L. Moons. An Aberrant Cerebellar Development in Mice Lacking Matrix Metalloproteinase-3. *Molecular Neurobiology*, 45(1):17–29, Nov. 2011.

[340] H. E. Van Wart and H. Birkedal-Hansen. The cysteine switch: a principle of regulation of metalloproteinase activity with potential applicability to the entire matrix metalloproteinase gene family. *Proceedings of the National Academy of Sciences*, 87(14):5578–5582, July 1990.

[341] R. E. Vandenbroucke and C. Libert. Is there new hope for therapeutic matrix metalloproteinase inhibition? *Nature Reviews Drug Discovery*, pages 1–24, Nov. 2014.

[342] J. Vandooren, N. Geurts, E. Martens, P. E. Van den Steen, and G. Opdenakker. Zymography methods for visualizing hydrolytic enzymes. *Nature Methods*, 10(3):211–220, Feb. 2013.

[343] J. Vandooren, P. E. Van den Steen, and G. Opdenakker. Biochemistry and molecular biology of gelatinase B or matrix metalloproteinase-9 (MMP-9): The next decade. *Critical Reviews in Biochemistry and Molecular Biology*, 48(3):222–272, May 2013.

[344] M. Verslegers, K. Lemmens, I. Van Hove, and L. Moons. Matrix metalloproteinase-2 and -9 as promising benefactors in development, plasticity and repair of the nervous system. *Progress in Neurobiology*, 105:60–78, June 2013.

[345] R. P. Vertes and J. Robert W Stackman. *Electrophysiological Recording Techniques*. Humana Press, Nov. 2010.

[346] S. Viappiani, A. C. Nicolescu, A. Holt, G. Sawicki, B. D. Crawford, H. León, T. van Mulligen, and R. Schulz. Activation and modulation of 72kDa matrix metalloproteinase-2 by peroxynitrite and glutathione. *Biochemical Pharmacology*, 77(5):826–834, Mar. 2009.

[347] M. Vicente-Manzanares, J. Hodges, and A. R. Horwitz. Dendritic Spines: Similarities with Protrusions and Adhesions in Migrating Cells. *The open neuroscience journal*, 3:87–96, Jan. 2009.

[348] J. C. Vickers, A. Delacourte, and J. H. Morrison. Progressive transformation of the cytoskeleton associated with normal aging and Alzheimer's disease. *Brain Research*, 594(2):273–278, Oct. 1992.

[349] R. Visse and H. Nagase. Matrix Metalloproteinases and Tissue Inhibitors of Metalloproteinases: Structure, Function, and Biochemistry. *Circulation Research*, 92(8):827–839, May 2003.

[350] O. I. Wagner, J. Lifshitz, P. A. Janmey, M. Linden, T. K. McIntosh, and J. F. Leterrier. Mechanisms of mitochondria-neurofilament interactions. *Journal of Neuroscience*, 23(27):9046–9058, Oct. 2003.

[351] E. Wagor, N. J. Mangini, and A. L. Pearlman. Retinotopic organization of striate and extrastriate visual cortex in the mouse. *The Journal of Comparative Neurology*, 193(1):187–202, Sept. 1980.

[352] L. H. Wang and S. M. Strittmatter. Brain CRMP forms heterotetramers similar to liver dihydropyrimidinase. *Journal of Neurochemistry*, 69(6):2261–2269, Dec. 1997.

[353] Q. Wang and A. Burkhalter. Area map of mouse visual cortex. *The Journal of Comparative Neurology*, 502(3):339–357, 2007.

[354] Q. Wang, E. Gao, and A. Burkhalter. Gateways of Ventral and Dorsal Streams in Mouse Visual Cortex. *Journal of Neuroscience*, 31(5):1905–1918, Feb. 2011.

[355] Q. Wang, O. Sporns, and A. Burkhalter. Network Analysis of Corticocortical Connections Reveals Ventral and Dorsal Processing Streams in Mouse Visual Cortex. *Journal of Neuroscience*, 32(13):4386–4399, Mar. 2012.

[356] X.-b. Wang, O. Bozdagi, J. S. Nikitczuk, Q. Zhou, and G. W. Huntley. Extracellular proteolysis by matrix metalloproteinase-9 drives dendritic spine enlargement and long-term potentiation coordinately. *Proceedings of the National Academy of Sciences*, 105(49):19520–19525, 2008.

[357] X.-X. Wang, M.-S. Tan, J.-T. Yu, and L. Tan. Matrix Metalloproteinases and Their Multiple Roles in Alzheimer's Disease. *BioMed Research International*, 2014(2):1–8, 2014.

[358] Y. Wang, J. M. Brittain, S. M. Wilson, and R. Khanna. Emerging roles of collapsin response mediator proteins (CRMPs) as regulators of voltage-gated calcium channels and synaptic transmission. *Communicative & Integrative Biology*, 3(2):172–175, Mar. 2010.

[359] J. Westermarck and V. M. Kähäri. Regulation of matrix metalloproteinase expression in tumor invasion. *FASEB journal*, 13(8):781–792, May 1999.

[360] G. Wiera, T. Wójtowicz, K. Lebida, A. Piotrowska, D. Drulis-Fajdasz, A. Gomułkiewicz, D. Gendosz, M. Podhorska-Okołów, M. Capogna, G. Wilczyński, P. Dzięgiel, L. Kaczmarek, and J. W. Mozrzymas. Long term potentiation affects intracellular metalloproteinases activity in the mossy fiber — CA3 pathway. *Molecular and Cellular Neuroscience*, 50(2):147–159, June 2012.

[361] G. Wiera, G. Wozniak, M. Bajor, L. Kaczmarek, and J. W. Mozrzymas. Maintenance of long-term potentiation in hippocampal mossy fiber-CA3 pathway requires fine-tuned MMP-9 proteolytic activity. *Hippocampus*, 23(6):529–543, Apr. 2013.

[362] T. N. Wiesel and D. H. Hubel. Single-cell Responses in Striate Cortex Of Kittens Deprived Of Vision In One Eye. *Journal of Neurophysiology*, 26:1003–1017, Nov. 1963.

[363] T. Wilks, A. Harvey, and J. Rodger. *Seeing with Two Eyes: Integration of Binocular Retinal Projections in the Brain*. Open Access, June 2013.

[364] S. M. Wilson, A. Moutal, O. K. Melemedjian, Y. Wang, W. Ju, L. François-Moutal, M. Khanna, and R. Khanna. The functionalized amino acid (S)-Lacosamide subverts CRMP2-mediated tubulin polymerization to prevent constitutive and activity-dependent increase in neurite outgrowth. *Frontiers in cellular neuroscience*, 8:196, 2014.

[365] J.-O. Winberg, E. Berg, S. O. Kolset, and L. Uhlin-Hansen. Calcium-induced activation and truncation of promatrix metalloproteinase-9 linked to the core protein of chondroitin sulfate proteoglycans. *European Journal of Biochemistry*, 270(19):3996–4007, Sept. 2003.

[366] D. G. Woolley, A. Laeremans, I. Gantois, D. Mantini, B. Vermaercke, H. P. Op de Beeck, S. P. Swinnen, N. Wenderoth, L. Arckens, and R. D'Hooge. Homologous involvement of striatum and prefrontal cortex in rodent and human water maze learning. *Proceedings of the National Academy of Sciences of the United States of America*, 110(8):3131–3136, Feb. 2013.

[367] P. F. Worley, B. A. Christy, Y. Nakabeppu, R. V. Bhat, A. J. Cole, and J. M. Baraban. Constitutive expression of zif268 in neocortex is regulated by synaptic activity. *Proceedings of the National Academy of Sciences*, 88(12):5106–5110, 1991.

[368] J. W. Wright, T. E. Brown, and J. W. Harding. Inhibition of Hippocampal Matrix Metalloproteinase-3 and -9 Disrupts Spatial Memory. *Neural Plasticity*, 2007(2):1–8, 2007.

[369] J. W. Wright, P. C. Meighan, T. E. Brown, R. V. Wiediger, B. A. Sorg, and J. W. Harding. Habituation-induced neural plasticity in the hippocampus and prefrontal cortex mediated by MMP-3. *Behavioural Brain Research*, 203(1):27–34, Oct. 2009.

[370] H.-G. Xia, L. Zhang, G. Chen, T. Zhang, J. Liu, M. Jin, X. Ma, D. Ma, and J. Yuan. Control of basal autophagy by calpain1 mediated cleavage of ATG5. *Autophagy*, 6(1):61–66, Jan. 2010.

[371] J. T. Yabe, A. Pimenta, and T. B. Shea. Kinesin-mediated transport of neurofilament protein oligomers in growing axons. *Journal of Cell Science*, 112 (Pt 21):3799–3814, Nov. 1999.

[372] N. Yamashita and Y. Goshima. Collapsin Response Mediator Proteins Regulate Neuronal Development and Plasticity by Switching Their Phosphorylation Status. *Molecular Neurobiology*, 45(2):234–246, Feb. 2012.

[373] N. Yamashita, B. Mosinger, A. Roy, M. Miyazaki, K. Ugajin, F. Nakamura, Y. Sasaki, K. Yamaguchi, P. Kolattukudy, and Y. Goshima. CRMP5 (Collapsin Response Mediator Protein 5) Regulates Dendritic Development and Synaptic Plasticity in the Cerebellar Purkinje Cells. *Journal of Neuroscience*, 31(5):1773–1779, Feb. 2011.

[374] C. Yan and D. D. Boyd. Regulation of matrix metalloproteinase gene expression. 211(1):19–26, 2007.

[375] S. J. Yan and E. A. G. Blomme. In situ zymography: a molecular pathology technique to localize endogenous protease activity in tissue sections. *Veterinary pathology*, 40(3):227–236, May 2003.

[376] K.-I. Yasunaga, T. Kanamori, R. Morikawa, E. Suzuki, and K. Emoto. Dendrite Reshaping of Adult Drosophila Sensory Neurons Requires Matrix Metalloproteinase-Mediated Modification of the Basement Membranes. *Developmental Cell*, 18(4):621–632, Apr. 2010.

[377] V. W. Yong. Metalloproteinases: Mediators of Pathology and Regeneration in the CNS. *Nature Reviews Neuroscience*, 6(12):931–944, Nov. 2005.

[378] V. W. Yong, C. Power, P. Forsyth, and D. R. Edwards. Metalloproteinases in biology and pathology of the nervous system. *Nature Reviews Neuroscience*, 2(7):502–511, July 2001.

[379] R. J. Youle and A. M. van der Bliek. Mitochondrial Fission, Fusion, and Stress. *Science*, 337(6098):1062–1065, Aug. 2012.

[380] Q. Yu and I. Stamenkovic. Cell surface-localized matrix metalloproteinase-9 proteolytically activates TGF-beta and promotes tumor invasion and angiogenesis. *Genes & Development*, 14(2):163–176, Jan. 2000.

[381] W. H. Yu and J. F. Woessner. Heparan sulfate proteoglycans as extracellular docking molecules for matrilysin (matrix metalloproteinase 7). *Journal of Biological Chemistry*, 275(6):4183–4191, Feb. 2000.

[382] A. Yuan, M. V. Rao, T. Sasaki, Y. Chen, A. Kumar, Veeranna, R. K. H. Liem, J. Eyer, A. C. Peterson, J. P. Julien, and R. A. Nixon. Alpha-Internexin Is Structurally and Functionally Associated with the Neurofilament Triplet Proteins in the Mature CNS. *Journal of Neuroscience*, 26(39):10006–10019, Sept. 2006.

[383] A. Yuan, M. V. Rao, Veeranna, and R. A. Nixon. Neurofilaments at a glance. *Journal of Cell Science*, 125(14):3257–3263, Sept. 2012.

[384] Z. Yue and C. T. Chu. *Autophagy of the Nervous System*. Cellular Self-digestion in Neurons and Neurological Diseases. World Scientific, 2012.

[385] R. Yuste. *Dendritic Spines*. MIT Press, 2010.

[386] R. Yuste. Dendritic Spines and Distributed Circuits. *Neuron*, 71(5):772–781, Sept. 2011.

[387] S. Zangenehpour and A. Chaudhuri. Differential induction and decay curves of c-fos and zif268 revealed through dual activity maps. *Molecular brain research*, 109(1-2):221–225, Dec. 2002.

[388] X.-j. Zhang, S. Chen, K.-x. Huang, and W.-d. Le. Why should autophagic flux be assessed? *Nature Publishing Group*, 34(5):595–599, Mar. 2013.

[389] B. Zingg, H. Hintiryan, L. Gou, M. Y. Song, M. Bay, M. S. Bienkowski, N. N. Foster, S. Yamashita, I. Bowman, A. W. Toga, and H.-W. Dong. Neural Networks of the Mouse Neocortex. *Cell*, 156(5):1096–1111, Feb. 2014.

[390] S. Zucker and J. Cao. Selective matrix metalloproteinase (MMP) inhibitors in cancer therapy: ready for prime time? *Cancer biology & therapy*, 8(24):2371–2373, Dec. 2009.

[391] J. Zuo, T. A. Ferguson, Y. J. Hernandez, W. G. Stetler-Stevenson, and D. Muir. Neuronal matrix metalloproteinase-2 degrades and inactivates a neurite-inhibiting chondroitin sulfate proteoglycan. *The Journal of Neuroscience*, 18(14):5203–5211, July 1998.

List of publications

International journals

Aerts, J., Nys, J., Moons, L., Hu, TT. and Arckens, L. (2014) Altered neuronal architecture and plasticity in the visual cortex of adult MMP-3-deficient mice. *Brain Structure and Function.* DOI: 10.1007/s00429-014-0819-4.

Aerts, J.*, Nys, J.*, and Arckens, L. (2014) A highly reproducible and straightforward method to perform in vivo monocular enucleation in the mouse. *Joint first author. *Journal of Visualized Experiments.* (92), e51936, DOI: 10.3791/51936.

Aerts, J.*, Dekeyster, E.*, Valiente-Soriano, F. J., De Groef, L., Vreysen, S., Salinas-Navarro, M., Vidal-Sanz, M., Arckens, L. and Moons, L. (2014) Ocular hypertension results in retinotopic alterations in the visual cortex of adult mice. *Joint first author. *Current Eye Research.* (in press)

Nys, J., **Aerts, J.**, Ytebrouck, E., Vreysen, S., Laeremans, A., and Arckens, L. (2014) The cross-modal aspect of mouse visual cortex plasticity induced by monocular enucleation is age-dependent. *Journal of Comparative Neurology.* 522(4):950-70, DOI: 10.1002/cne.23455.,

Abstracts on international meetings

Vreysen, S., **Aerts, J.**, Van Den Boer, L., and Arckens, L. (2014) Aberrant structure and functionality of the visual cortex of MMP-3 deficient mice. *Annual Meeting of The Society for Neuroscience (SfN), Washington DC, USA, 14-19 November 2014.*

Aerts, J., Nys, J., Moons, L., Hu, T.T, and Arckens, L. (2014) MMP-3 deficient mice display an aberrant neuronal architecture and lack experience-dependent plasticity in the visual cortex. *9th FENS Forum of European Neuroscience, Milan, Italy, 5-9 July 2014.*

Aerts, J., Nys, J., Moons, L., Hu, T.T, and Arckens, L. (2014) MMP-3 deficient mice display an aberrant neuronal architecture and lack experience-dependent plasticity in the visual cortex. *Annual conference of COST action ECMNET, Volterra, Italy, 2-4 July 2014.*

Aerts, J., Nys, J., Smolders, K., Moons, L., and Arckens, L. (2013) Altered neuronal architecture and plasticity in the visual cortex of MMP-3 deficient mice. *Annual Meeting of The Society for Neuroscience (SfN), San Diego, California, USA, 8-14 November 2013.*

Smolders, K., Nys, J., **Aerts, J.**, Baggerman, G., Hu, T.T., and Arckens, L. (2013) Protein expression and cross-modal plasticity mechanisms in mouse visual cortex following monocular enucleation dier with age. *Annual Meeting of The Society for Neuroscience (SfN), San Diego, California, USA, 8-14 November 2013.*

Aerts, J., Van houcke, J., Vanlaer, R., Nys, J., Moons, L., Arckens, L. (2012) The effect of matrix metalloproteinase-3 deficiency in experience dependent cortical plasticity. *ECMNET Winter school Magdeburg, Germany, 12-18 December 2012.*

Aerts, J., Moons, L., and Arckens, L. (2012) Comparison of PNN structure, composition and distribution between MMP- 3 deficient and wild type mice. *8th FENS Forum of European Neuroscience, Barcelona, 14-18 July 2012.*

Aerts, J., Moons, L., and Arckens, L. (2012) Comparison of PNN structure,

composition and distribution between MMP- 3 deficient and wild type mice. *Second Annual Conference of COST Action ECMNET (FENS satellite event), 12-13 July 2012. Oral presentation*

Abstracts on national meetings

Aerts, J., Nys, J., Moons, L., Arckens, L. (2013) The effect of MMP-3 deficiency on neuronal architecture and plasticity in the mouse visual cortex. *Belgian Society for Neuroscience (BSN), VUB, Jette, Brussels, 31 May 2013.*

Nys, J., **Aerts, J.**, Ytebrouck, E., Vreysen, S., Laeremans, A., Arckens, L. (2013) The cross-modal aspect of mouse visual cortex plasticity induced by monocular enucleation is age-dependent. *Belgian Society for Neuroscience (BSN), VUB, Jette, Brussels, 31 May 2013*

Smolders, K., Nys, J., **Aerts, J.**, Xianyuan X., Hendrix, A., Baggerman, G., Hu, T.T., and Arckens, L. (2013) A differential screening for membrane proteins involved in age-dependent cross-modal plasticity mechanisms in mouse visual cortex. *Belgian Society for Neuroscience (BSN), VUB, Jette, Brussels, 31 May 2013.*

Dekeyster, E., **Aerts, J.**, De Groef, L., Salinas Navarro, M., Valiente-Soriano, F., Vidal-Sanz, M., Arckens, L., Moons, L. (2013) Glaucoma and the brain: the effect of monocular hypertension. *Belgian Society for Neuroscience (BSN), VUB, Jette, Brussels, 31 May 2013.*

Dekeyster, E., De Groef, L., Salinas Navarro, M., Valiente-Soriano, F., **Aerts, J.**, Vidal-Sanz, M., Arckens, L., Moons, L. (2012) Glaucoma and the brain: effects of ocular hypertension on the central visual pathway. *LIND Meeting: Neuronal function in health and disease, Mechelen, 17 December 2012.*

International training

Research stay at the lab of Prof. dr. C. Casanova: Intrinsic signal optical imaging and voltage-sensitive dye imaging in the visual cortex of the rabbit and mouse. *Lab of Visual Neuroscience, School of Optometry, Montreal, Canada, 7 August - 7 November, 2014*

ECMNET Winter school at the Leibniz Institute for Neuroscience: A Cell Biologist's View on Active Synapses and the Perisynaptic Extracellular Matrix (COST Action BM1001). *Magdeburg, Germany, 12-18 December 2012.*

FACULTY OF SCIENCE
DEPARTMENT OF BIOLOGY
Laboratory of Neuroplasticity and Neuroproteomics
Naamsestraat 59 box 2467
B-3000 LEUVEN, BELGIUM
tel. + 32 16 32 39 29
jeroen.aerts@bio.kuleuven.be